2012

A novel immunomodulatory subunit vaccine to combat the involvement of bovine respiratory coronavirus infections in shipping fever

Genevieve Elizabeth Lum
Louisiana State University and Agricultural and Mechanical College

A NOVEL IMMUNOMODULATORY SUBUNIT VACCINE TO COMBAT THE INVOLVEMENT OF BOVINE RESPIRATORY CORONAVIRUS INFECTIONS IN SHIPPING FEVER

A Dissertation

Submitted to the Graduate Faculty of the
Louisiana State University and
Agricultural and Mechanical College
in partial fulfillment of the
requirements for the degree of
Doctor of Philosophy

in

The Interdepartmental Program in
Animal and Dairy Sciences

by
Genevieve Elizabeth Lum
M.S., Louisiana State University A&M, 2008
August 2012

ACKNOWLEDGMENTS

First and foremost, there are countless people that have helped the author to get where she is today, and to thank each and every one of them individually here would be impossible. For that reason, she would like to express her thanks to these people who remain nameless, but would like for them to know that their contributions have not been forgotten.

The author would then like to start out by expressing her most sincere gratitude to her advisors, Dr. Kenneth Bondioli and Dr. Gus Kousoulas; without their generosity, support, encouragement, and, at times when it was needed, strong motivation, she would not have completed this degree. The author would like to thank them both for their willingness to "adopt" her as a graduate student and for being able to see within her a capability of which she, at times, unfortunately lost sight. Dr. Bondioli's capacity for patience is unwavering, and he could always be depended on to lend an understanding, if not mildly amused, ear. Whether he realizes it or not, Dr. Bondioli has contributed immensely to the growth and development of the author, both on a professional and personal level. The author would like to thank Dr. Kousoulas for his willingness to patiently nurture the "turtles" of the graduate student world. His inclination to believe unwaveringly in the potential of the students in his lab is a lesson the author hopes and prays that she incorporates into her life at every level, both academic as well as personal, and will always be grateful for his ability to push the opinions of all others aside and see the best in his students. For the guidance and support she has received from these men she will be eternally grateful; Her hope is that she can make them both proud to have graduated her from their programs, not just on an academic and professional level, but as a human being as well.

Obtaining a doctorate is in no way a simple undertaking, and those in pursuit of the degree will inevitably find themselves at some time or another in serious need of moral support.

That being said, the author would next like to thank her family. Without their outside support, the completion of this degree would not have been possible. Any time the author needed to vent, or celebrate, or laugh, or cry, or simply sit and be quiet, her family was there to provide whatever the moment required. The author's mother has always been there to listen and rejoice over successes in the lab and to lament over the not-so-successful outcomes, of which there have been many along the way. To her the author owes an untold number of lunches and cups of coffee. The author's father has always been there to support her on bright days and dark. The author is especially grateful for showing her what it truly means to advocate on someone's behalf and to fight for them, no matter what the cost. These two individuals have shaped the author into the person she is today, and her utmost wish is that she make them proud of what she has become in this life. To her siblings, the author would like to express her love, gratitude, and encouragement. Lauren, find what you love and pursue it with reckless abandon. Find what make you happy and brings you fulfillment. The author will be proud of you, no matter where the path leads you. Daniel, the author is impressed by your persistence, patience, tenacity, and will to succeed. She looks forward to the day she can call you "Doctor". Last but not least the author would like to thank her aunts. They have been there to support her through good times and bad, and the time they have invested in her growth and development has been tremendous. The author only fears that a lifetime of "thank yous" could never be sufficient.

The author would like to also thank her colleagues in the Kousoulas lab. This collection of graduate students and post-docs from all walks of life have gone, in four years time, from being co-workers to close friends and trusted confidants. The angst that one goes through in the pursuit of a graduate degree can only truly be understood by someone who has walked that path. The author has found strength and endless encouragement in the camaraderie she has shared with

her fellow lab mates along the way, and will be eternally grateful to them for any future successes she may have. The author asks that the lab please share in her accomplishment, for they have shared, too, in the trials and tribulations, the anxiety, and, yes, the joy, too, that have come with the pursuit of this degree. A special thanks to Dr. Vladimir Chouljenko, for teaching the author not only how to design primers, perform affinity chromatography, and develop an western immunoblot, but for also teaching her how to listen carefully, plan ahead, and execute with a purpose. Thank you, too, for the laughs and amusing translation of Ukrainian idioms. To Dr. Jason Walker, the warmest and most heartfelt gratitude for reminding the author that all graduate students go through the cycles of self-doubt, anxiety, and eventual triumph. Thank you for all of your encouragement and for patiently listening, troubleshooting, and helping to plan experiments. Thank you especially for your willingness to get dirty and "rustle cattle" alongside the author; it was fun. To Dr. Ramesh Subrumanian, Dr. Nithya Jambunathan, Dr. Anu Charles, Dr. Andrew David, Sona Chowdhury, and the rest of the BioMMed family, thank you again for your friendship and for all the help in the lab.

The author would like finally to thank Chad Fava. How does one even begin to thank the person that has been there for every late night, early morning, research related panic attack and breakdown, for every high point and low point? How does one thank someone for changing their life completely and for the better? Chad, in you I have found a true *partne*r in this life. You are my best friend, my confidant, my strength when I don't think I can continue. In short you have shown time and time again that you are my rock. Thank you for helping me to get here, for believing that I would get here, and for never doubting or allowing me to doubt. Simply, I love you, and I look forward to the life we have planned together. Thank you.

TABLE OF CONTENTS

LIST OF FIGURES

LIST OF ABBREVIATIONS

BRD……...Bovine Respiratory Disease
MDA……...Serum malondialdehyde
BRCoV…….Bovine respiratory coronavirus
BVDV……Bovine vial diarrhea virus
BHV-1…….Bovine herpes virus type 1
BRSV……...Bovine respiratory syncytial virus
PI-3……...Parainfluenza virus type 3
SARS-CoV……Sudden acute respiratory syndrome coronavirus
BCoV……..Bovine coronavirus
MLV……Modified live vaccine
TCV……...……Turkey coronavirus
IBV……Avian infectious bronchitis virus
ICTV……International Committee for the Taxonomy of Viruses
HCV……...Human coronavirus
Gp……..Glycoprotein
S……Spike
HE……...Hemagglutinin-esterase
C……..Carboxyl
N……...Nucleocapsid
RNP……..Ribonucleoprotein
TGEV……..Transmissible gastroenteritis virus
MW……Molecular weight
M……...Membrane
MHV……...Murine hepatitis virus
UTR……Untranslated region
ER…….Endoplasmic reticulum
E……..Small membrane protein E
N……..Amino
ORF……Open reading frame
HEF……..Hemagglutinin-esterase-fusion
HRT-18G……..18G clone of human rectal tumor cells
Mab……..Monoclonal antibody
FCV……..Feline coronavirus
FIPV……..Feline infectious peritonitis virus
Ns…….Nonstructural
Nsp……...Nonstructural protein
PLP……Papain-like protease
3CLpro……3C-like protease
RCoV……Rat coronavirus
APN…….Aminopeptidase N
CCoV…….Canine coronavirus
JMD…….Juxtamembrane domain
PRR……..Pattern recognition receptors

PAMP……Pathogen-associated molecular pattern
RIG-1…….Retinoic acid-inducible gene-I
RLR…….Rig-like receptor
TLR……Toll-like receptor
NOD……Nucleotide oligomerization-binding domain
IFN…….Interferon
PKR…….....Protein kinase R
MDA-5……..Melanoma differentiation-associated factor 5
LPG-2……....Laboratory of genetics and physiology-2
CARD……..Caspase recruitment domain
APC……..Antigen presenting cell
DC……Dendritic cell
TCR……T cell receptor
BCR……B cell receptor
Sopt……..Spike optimized
Sopt-CD154…….Spike optimized-CD154 fusion protein
Sol-Sopt……..Soluble Spike optimized
IFA……..Immunofluorescence assay

ABSTRACT

Bovine respiratory coronavirus (BRCoV) is a group 2a coronavirus expressing both hemagglutinin-esterase and spike (S) envelope glycoproteins. The S glycoprotein is a primary coronavirus virulence factor responsible for both receptor specificity and membrane fusion-mediated entry into host cells. In addition, the S glycoprotein serves as a major antigen targeted by both the cellular and humoral immune responses and, as such, is an important target for antibody-facilitated virus neutralization. The objective of this research was the design of a safe and effective vaccine against BRCoV using a "prime-boost" vaccination approach. This method utilized an initial DNA vaccine encoding either the soluble portion of the spike glycoprotein, or the soluble portion of the spike glycoprotein fused in-frame to bovine CD154, administered intramuscularly. The initial priming was followed 14 days later by vaccination with purified immunogenic extracellular portion of S glycoprotein alone or this portion fused in-frame to the soluble portion of the bovine CD40 ligand (CD40L; CD154). The bovine CD40L was included to enhance the immunogenicity of the S glycoprotein and elicit protective immune response against BRCoV infection. Both of the recombinant proteins were expressed in insect Sf9 cells via recombinant baculovirus expression and purified using affinity chromatography. The efficacy of these vaccine approaches in eliciting neutralizing antibody responses, preventing virus replication and spread and the onset of respiratory disease in cattle was then investigated in animal experimental infections. An ELISA was developed and utilized to screen 129 cattle for animals that did not have appreciable antibody titers to BRCoV. In addition, BRCoV-specific serum was obtained from one cow immunized with commercially available vaccine and high-titer anti BRCoV S-specific serum was obtained by immunization of rabbits with the S-CD154-fusion protein. As expected, animals responded to vaccination with the soluble portion of spike.

Furthermore, fusion of CD154 to the soluble portion of the spike glycoprotein resulted in a pronounced increase in circulating and neutralizing serum antibody specific for the BRCoV spike glycoprotein.

CHAPTER I
INTRODUCTION

Bovine respiratory disease complex

The greatest health-associated impact on beef cattle profitability is Bovine Respiratory Disease (BRD), commonly known as “shipping fever”, a disease complex typically associated with multiple etiologies (Smith, 1998). Predisposing factors commonly associated with the risk of BRD development include stress associated with fasting and transport, introduction of microbial pathogens via stressful comingling of calves, rapid environmental and weather changes, age, and sudden nutritional alterations (Callan and Garry, 2002; *reviewed by* Cusack et al., 2003). Additionally, while overall feed intake by stressed calves is low (Galyean and Hubbart, 1995; Cole, 1996), more specifically, nutritional antioxidant status has been suggested to play a role as a predisposing factor in the development of BRD (McDowell et al., 1996), although the validity of this claim has yet to be fully substantiated (Hill, 1987). Chirase et al. reported in 2004 a relationship between serum malondialdehyde (MDA) concentrations, considered a biomarker of lipid peroxidation in non-ruminants and humans, although it has not been previously established as an indicator of lipid peroxidation in ruminants, and risk of BRD. In their study, calves subjected to marketing and transport stressors showed a 3-fold increase in serum MDA concentration from pre-transit levels. In addition, calves that later died as a result of BRD complications were found to have had a 1.44-fold increase in serum MDA concentration over surviving calves before they were ever even subjected to transport stressors. Thus, it was concluded that there was, indeed, a positive correlation between pre- and post-transit antioxidant status and risk of developing BRD (Chirase et al., 2004).

The BRD complex is responsible for considerable economic losses, particularly within the feedlot industry, and is considered the most significant disease affecting young feedlot cattle after arrival to North American feedlots (Martin et al., 1998). A study performed by Snowder et al. reported that BRD was responsible for considerable economic losses to feedlots, especially when factors such as decreased weight gain and incurred treatment costs associated with BRD incidence where also factored in (2006). In fact, Snowder et al. reported that, at the time, this cost could be estimated to be approximately $13.90 per animal within a 1,000 head feedlot, excluding the costs associated with labor for increased handling of these of these animals (2006). In addition, development of BRD while in the feedlot has been reported to negatively impact carcass value at slaughter by not only decreasing weight gain of affected animals, but also be decreasing the value of carcass composition and associated yield traits (Montgomery et al., 1984; Roeber et al., 2001; Garcia et al., 2010).

Of the numerous microbial agents known to contribute to the development of BRD, one of the most consistently isolated is Bovine Respiratory Coronavirus (BRCoV; Storz et al., 1996; Storz et al., 2000). However, this virus alone is not solely responsible for development of BRD, as a number of other viruses have also been implicated in the development of the disease complex. Some of the most commonly associated viruses include Bovine viral diarrhea virus (BVDV), Bovine Herpes virus-1 (BHV-1), Bovine respiratory syncytial virus (BRSV), and Parainfluenza virus-3 (PI-3). Furthermore, previous research has strongly suggested that respiratory virus infection alone is insufficient for the development of BRD (Martin et al., 1988), although these infections are generally thought to play a pivotal role in potentiating development of the complex

(Dunn et al., 1991). Calves experimentally infected with either BHV-1 or PI-3 alone, or with both viruses simultaneously developed more conspicuous clinical disease, marked by a delayed and depressed antibody response, lower lymphocyte proliferative response, and higher increased serum cortisol levels when compared with animals infected with a single virus type (Ghram et al). The development of BRD is generally thought to follow a common progression involving viral-bacterial synergism (Jericho and Langford, 1978), starting with immune suppression due to stress or other causes and followed by exposure to respiratory viral pathogen. These viral pathogens most likely spread during the comingling of animals from different farms during shipping to feedlots (Lathrop et al., 2000). The exacerbated viral infection is thought to be followed by opportunistic overgrowth of commensal bacterial species (Lopez et al., 1976) commonly inhabiting the nasopharynx of healthy animals, some of the most commonly isolated being *Mannheimia haemolytica* and *Pasteurella multocida* (Allen et al., 1991).

Bovine respiratory disease and bovine respiratory coronavirus

Of the viruses typically thought to contribute to the development of BRD, the role of BRCoV may be one of the most controversial. This virus is an RNA virus belonging to the *Coronaviridae* family of viruses, which consists of a number of host-species specific RNA viruses, the most well known of these being the human coronavirus commonly known as the Severe Acute Respiratory Syndrome coronavirus, or SARS. Although SARS virus infection in humans results in severe respiratory distress, BRCoV infection in cattle is not generally considered to cause severe disease, with many animals actively infected and shedding virus showing no clinical indicators of disease (McNulty et al, 1982; Reynolds et al., 1984; Hasoksuz et al., 2002). The primary sites of infection are

generally the epithelial cells lining the nasal cavity and trachea, resulting in development of mild clinical symptoms, including nasal discharge, rhinitis, sneezing, and coughing, which are commonly accompanied by a mild elevation in body temperature (Reynolds et al., 1984). Lower respiratory tract involvement may also occur, resulting in the development of minor lung lesions that are subclinical in nature, although more severe lower respiratory tract involvement has been previously reported (Kapil et al., 1991). In spite of the fact that BRCoV infection does not generally result in the presentation of symptoms usually associated with the clinical representation of severe pneumonia, considerable evidence seems to support the view that infection with BRCoV serves to further the immunosuppression that was incurred as a result of the stresses of shipping by promoting infection by opportunistic flora and fauna typically associated with the respiratory tract, including the bacteria, *Mannheimia haemolytica* and *Pasteurella multocida* (Cusack et al., 2003).

Since its initial isolation from lung washes and nasopharyngeal swabs of calves involved in two pneumonic outbreaks in 1982 (Thomas et al., 1982), various strains of bovine coronavirus (BCoV) have been isolated from and implicated in cases of BRD in feedlot calves after shipping (Storz et al., 1996; Hasoksuz et al., 1999; Silva et al., 1999; Storz et al., 2000a; Storz et al., 2000b; Cho et al., 2001). Many of these same researchers suggest in their reports that BCoV infection can be considered a general indicator for increased risk of BRD development after arrival to feedlots, especially in animals actively shedding BCoV via nasal secretions (Carman and Hazlett, 1992; Storz et al., 1996; Lathrop et al., 2000), and that these animals typically show high rates of BRD-related mortality (Storz, 2000). However, findings by other researchers have challenged

this claim, reporting a failure to find any association between increase in antibody titer to BCoV after arrival to the feedlot and subsequent development of BRD (Martin et al., 1998; O' Conner et al., 2001). Previous work has shown that high antibody titers to BCoV upon arrival in the feedlot were statistically associated with decreased risk for development of BRD (Martin et al., 1998). Although O'Conner et al. report in their 2001 study that animals having higher antibody titer to BCoV upon arrival to the feedlot had significant decrease in the risk of being treated for BRD with an unconditional odds ratio of 0.3, they interpret this to mean that these animals possessed more robust immune responsiveness rather than pathogen-specific protection conferring BRD resistance via BCoV resistance, as they found that seroconversion to positive BCoV antibody titer during the time at the feedlot was not associated with increased risk of developing BRD. However, although the findings of O'Conner et al. (2001) seem to suggest differently, at present, infection with BCoV immediately following arrival to feedlot, as signified by seroconversion during time at the feedlot, continues to be considered a predisposing factor for development of BRD in feedlot cattle (Fulton et al., 2011).

Prevention of bovine respiratory disease

There is a considerable economic toll associated not only with the treatment of animals in the feedlot for BRD, but also with losses associated with decreased gains and yield scores for those animals, one estimate having been calculated as a $40.64 decrease in return per animal treated only once and as high as a $291.33 loss in return for animals treated up to three times (Fulton et al., 2002). Therefore the key to reducing or potentially eliminating BRD-associated losses may lie in development of an effective prevention strategy before animals are ever marketed, as opposed to treatment for it after animals

have arrived at the feedlot. The best means by which to achieve this would be the development of a safe and effective vaccination protocol for pre- or newly-weaned calves, and indeed a number of vaccines targeting some of the most common pathogens associated with BRD are already widely utilized in the United States. Duff and Galyean, in their discussion of management strategies for the prevention of BRD, suggest that animals undergo preconditioning programs prior to marketing to feedlots, meaning that calves have been weaned for some time, typically 30 to 45 d, vaccinated, treated for intestinal parasites, castrated, dehorned, and habituated to feed bunks and watering troughs (2007). These investigators recommend that calves be vaccinated 4 to 6 wk prior to weaning, followed by booster vaccinations at the time the animals are weaned, although, if not feasible, calves should at the very least be vaccinated at weaning followed by booster vaccination 21 d later (Duff and Galyean, 2007). Unfortunately, in addition to the non-compliance of numerous small-herd and hobby farmers to in regards to these recommendations, approximately 40% of those surveyed in 2007 (USDA, 2007), there are a number of other factors that may play a significant role in the efficacy of vaccines against the pathogens associated with BRD. Vaccine effectiveness may be considerably influenced by the nutritional status, age, immune status, and other environment factors affecting the overall health of the intended recipient (Larson and Bradley, 1996).

The general goal of a successful vaccine is the ability to induce both a humoral and cellular immune response closely mimicking that typically associated with natural infection by the pathogen against which the vaccine has been administered (Meeusen et al., 2007). An effective vaccine protocol should, then, target the most optimal antigen and

deliver it to the intended recipient at the most advantageous time and physiological location to ensure the best immune response capable of providing protection to the recipient. The term “vaccine” originates from the Latin word “vacca”, meaning “cow”, and was originally coined by Edward Jenner, responsible for discovering that humans could be protected from the deadly smallpox virus by inoculation with the closely-related but far less pathogenic cowpox virus. Although human pathogen vaccinology and animal pathogen vaccinology are closely related sciences, the criteria by which successful vaccination is judged may be vastly different, based on the ultimate goal of the vaccine itself. While development of most human and companion animal vaccines is focused primarily on the health and ultimately the well-being of the recipient, the development of most livestock vaccines is more economically driven. Considerations such as cost-to-benefit ratio must be made in the livestock industry, whereas in human and modern companion animal medicine cost-to-benefit is less of a concern, so long as the vaccine is effective and provides, preferably, safe, long-term protection. Even the exact definition of “efficacy” may differ between the two industries, with the goal of human and modern animal vaccines typically being complete protection from infection by and even eradication of a pathogen, while that of livestock vaccines is often more oriented around a vaccine’s ability to reduce the overall infection or treatment rate associated with a particular pathogen. In fact, in some cases livestock vaccine efficacy is merely associated with the ability to reduce or eliminate clinical symptoms of infection, but not to necessarily eliminate or eradicate the infectious organism itself (Martin, 1983). The end goal of the vast majority of livestock vaccines revolves around the so-called “bottom line”, that is, the ability of the vaccine to improve economic and financial return. In

addition, considerations such as ease of use as well as public perception must also be made. For instance, vaccination of livestock with every available vaccine against any and all pathogens would be financially irresponsible, as not all vaccines are equally effective or even equally applicable to a specific geographic location.

Therefore, a key aspect of BRD prevention by way of vaccination programs is determining which vaccines or combinations of vaccines produce the most beneficial protection from pathogens implicated in the development of BRD. Unfortunately, the fact of the matter is that the answer to this question is not a straightforward one. As previously discussed, bovine respiratory disease has a multi-factorial etiology, for which a number of pathogens, both viral and bacterial, have been implicated. Virus isolation and serological findings have commonly suggested that BHV-1, BVD, and PI-3 are the viral entities generally implicated in the development of BRD (Potgieter, 1977), although BRSV has also been suggested to participate in the development of the disease complex (Baker and Frey, 1985). These viruses, therefore, have been the targets of considerable effort to design effective vaccines for the prevention of BRD. In addition, development and implementation of effective bacterin-toxoid vaccines against the bacterial pathogens and their toxins most commonly associated with the development of BRD, namely *M. haemolytica* and *P. multocida*, has also been of considerable interest. The choice as to which vaccines to administer in order to optimize economic returns may vary considerably from feedlot to feedlot and depends on factors such as age class, body weight, procurement method, extent of commingling before and after arrival at the feedlot, and previous vaccination and management history, when available (Wildman et al., 2008). In addition, the geographic location of the feedlot in question my also play a

role in determining important pathogens against which cattle should be vaccinated (Hoare et al., 1994). In a 2008 study of vaccination protocols for feedlot calves upon arrival to the feedlot facility, Wildman et al. compared two vaccination strategies for their ability to decrease development of BRD in calves at high risk for development of the disease complex (2008). The first consisted of a multivalent modified-live vaccine (MLV) containing BHV-1 (for IBRV) and BVD types I and II as well as *M. haemolytica* and *P. multocida* bacterin-toxid, while the second protocol consisted of a multivalent MLV containing BHV-1, BVD type I, PI-3, and BRSV, as well as *M. haemolytica* bacterin-toxid. Wildman and colleagues reported that, surprisingly, calves vaccinated with the BHV-1/BVDV vaccine had a significantly ($p<0.05$) lower BRD treatment rate as well as a lower incidence of BRD mortality as compared with calves receiving the vaccine containing a wider range of BRD-associated pathogens. In addition, calves receiving the BHV-1/BVDV vaccine had significantly ($p<0.05$) higher average daily gain and final carcass value than did calves receiving the vaccine containing a wider range of BRD-associated pathogens. The authors concluded that on an economic basis, the BHV-1/BVDV vaccine was considerably more cost-effective than the more expensive vaccine, even though it, in theory, should confer resistance to a wider range of BRD-associate pathogens. Unfortunately, these studies underline the difficulties associated with selecting a vaccination program for implementation within cattle operations, as, at least in the latter study, contrary to what might be expected, more does not always seem to be better.

References

Allen, J. W., Viel, L., Bateman, K. G., Rosendal, S., Shewen, P. E. & Physick-Sheard, P. 1991. The microbial flora of the respiratory tract in feedlot calves: associations

between nasopharyngeal and bronchoalveolar lavage cultures. *Can. J. Vet. Res.,* 55**,** 341-346.

Baker, J. C. a. F., M.L. 1985. Bovine respiratory syncytial virus. In: Breeze, R. (ed.) *The Veterinary Clinic of North America -- Food Animal Practice.*

Callan, R. J. & Garry, F. B. 2002. Biosecurity and bovine respiratory disease. *Vet. Clin. North Am. Food Anim. Pract.,* 18**,** 57-77.

Carman, P. S. & Hazlett, M. J. 1992. Bovine coronavirus infection in Ontario, 1990-1991. *Can Vet J,* 33**,** 812-814.

Chirase, N. K., Greene, W., Purdy, C. W., Loan, R. W., Auvermann, B. W., Parke, D. B., Walborg, E. F., Stevenson, D. E., Xu, Y. & JE, J. E. K. 2004. Effect of transport stress on respiratory disease, serum antioxidant status, and serum concentrations of lipid peroxidation biomarkers in beef cattle. *Am. J. Vet. Res.,* 65**,** 860-864.

Cho, K. O., Hoet, A., Loerch, S. C., Wittum, T. E. & Saif, L. J. 2001. Evaluation of concurrent shedding of bovine coronavirus via the respiratory tract and enteric route in feedlot cattle. *Am. J. Vet. Res.,* 62**,** 1436-1441.

Cole, N. A., Phillips, W. A. & Hutcheson, D. P. 1986. The effect of pre-fast diet and transport on nitrogen metabolism in calves. *J. of Anim. Sci.,* 62**,** 1719-1731.

Cusack, P. M. V., McMeniman, N. & Lean, I. J. 2003. The medicine and epidemiology of bovine respiratory diseases in feedlots. *Austr. Vet. J.,* 81**,** 480-487.

Duff, G. C. & Galyean, M. L. 2007. BOARD-INVITED REVIEW: Recent advances in management of highly stressed, newly received feedlot cattle. *J. Anim. Sci.,* 85**,** 823-840.

Dunn, S. E., Godwin, J., Hoare, R. J. T. & Kirkland, P. D. 1991. Diseases of feedlot cattle. *Final Report to the Meat Research Corporation of Australia. (now Meat and Livestock Australia).*

Fulton, R. W., Cook, B. J., Step, D. L., Confer, A. W., Saliki, J. T., Payton, M. E., Burge, L. J., Welsh, R. D. & Blood, K. S. 2002. Evaluation of health status of calves and the impact on feedlot performance: assessment of a retained ownership program for postweaning calves. *Can. J. Vet. Res.,* 66**,** 173-180.

Fulton, R. W., Step, D. L., Wahrmund, J., Burge, L. J., Payton, M. E., Cook, B. J., Burken, D., Richards, C. J. & Confer, A. W. 2011. Bovine coronavirus (BCV) infections in transported commingled beef cattle and sole-source ranch calves. *Can. J. Vet. Res.,* 75**,** 191-199.

Galyean, M. L. & Hubbert., M. E. 1995. Effects of season, health, and management on feed intake by beef cattle. In: Owens, F. N. (ed.) *Intake by Feedlot Cattle.* Oklahoma Agric. Exp. Sta., P-942.

Garcia, M. D., Thallman, R. M., Wheeler, T. L., Shackelford, S. D. & Casas, E. 2010. Effect of bovine respiratory disease and overall pathogenic disease incidence on carcass traits. *Journal of Animal Science,* 88**,** 491-496.

Ghram A, R. P., Blecha F, Minocha HC. 1989. Effects of bovine respiratory disease viruses and isoprinosine on bovine leukocyte function in vitro. *Vet. Microbiol.,* 20**,** 307-314.

Hasoksuz, M., Lathrop, S. L., Gadfield, K. L. & Saif, L. J. 1999. Isolation of bovine respiratory coronaviruses from feedlot cattle and comparison of their biological and antigenic properties with bovine enteric coronaviruses. *Am J Vet Res,* 60**,** 1227-1233.

Hill, G. M. 1987. Vitamin E and selenium supplementation of cattle. *Proc. Georgia Nutrition Conference.* Atlanta, GA.

Jericho, K. W. F. & Langford, E. V. 1978. Pneumonia in Calves Produced with Aerosols of Bovine Herpesvirus 1 and Pasteurella haemolytica. *Can. J. Comp. Med.,* 42**,** 269-277.

Kapil, S., Pomeroy, K. A., Goyal, S. M. & Trent, A. M. 1991. Experimental infection with a virulent pneumoenteric isolate of bovine coronavirus. *J vet Diagn Invest,* 3**,** 88-89.

Larson, R. L. & Bradley, J. S. 1996. Immunologic principles and immunization strategy. *Comp. Cont. Ed. Prac. Vet.,* 18**,** 963-970.

Lathrop, S. L., Wittum, T. E., Brock, K. V. & Saif, L. J. 2000. Association between infection of the respiratory tract attributable to bovine coronavirus and health and growth performance of cattle in feedlots. *Am J Vet Res,* 61**,** 1062-1066.

Lopez, A., Thomson, R. G. & Savan, M. 1976. The pulmonary clearance of Pasteurella hemolytica in calves infected with bovine parainfluenza-3 virus. *Can J Comp Med,* 40**,** 385-391.

Martin, S. W., Darlington, G., Bateman, K. & Holt, J. 1988. Undifferentiated Bovine Respiratory Disease (Shipping Fever): Is it communicable? *Prev. Vet. Med.,* 6.

Martin, S. W., Nagy, E., Shewen, P. E. & Harland, R. J. 1998. The association of titer to bovine coronavirus with treatment for bovine respiratory disease and weight gain in feedlot calves *Can J Vet Res,* 62**,** 257-261.

McNulty, M. S., Bryson, D. G., Allan, G. M. & Logan, E. F. 1984. Coronavirus infection of the bovine respiratory tract. *Vet. Microbiol.,* 9**,** 425-434.

Meeusen, E. N. T., Walker, J., Peters, A., Pastoret, P.-P. & Jungersen, G. 2007. Current Status of Veterinary Vaccines. *Clin. Microbiol. Rev.,* 20**,** 489-510.

Montgomery, T. H., Adams, R., Cole, N. A., Hutcheson, D. P. & McLaren, J. B. 1984. Influence of feeder calf management and bovine respiratory disease on carcass traits of beef steers. *Proc. West. Sec. Am. Soc. Anim. Sci.*

O'Connor, A., Martin, S. W., Nagy, E., Menzies, P. & Harland, R. 2001. The relationship between the occurrence of undifferentiated bovine respiratory disease and titer changes to bovine coronavirus and bovine viral diarrhea virus in 3 Ontario feedlots. *Can. J. Vet. Res.,* 65**,** 137-142.

Potgieter, L. N. D. 1977. Current concepts on the role of viruses in respiratory tract diseases of cattle. *Bovine Pract.,* 10**,** 75-81.

Reynolds, D. J., Debney, T. G., Hall, G. A., Thomas, L. H. & Parsons, K. R. 1984. Studies on the relationship between coronaviruses from the intestinal and respiratory tracts of calves. *Arch Virol,* 85**,** 71-83.

Roeber, D. L., Speer, N. C., Gentry, j. G., Tatum, J. D., Smith, C. D., Whittier, J. C., Jones, G. F., Belk, K. E. & Smith, G. C. 2001. Feeder cattle health management: Effects on morbidity rates, feedlot performance, carcass characteristics, and beef palatability. *Professional Animal Scientist,* 17**,** 39-44.

Silva, M. R. d., O'Reilly, K. L., Lin, X., Stine, L. & Storz, J. 1999. Sensitivity and comparison for detection of respiratory bovine coronaviruses in nasal samples from feedlot cattle by ELISA and isolation with the G clone of HRT-18 cells. *J vet Diagn Invest,* 11.

Smith, R. A. 1998. Impact of disease on feedlot performance: a review. *J. Anim. Sci.,* 76**,** 272-274.

Snowder, G. D., Vleck, L. D. V., Cundiff, L. V. & Bennett., G. L. 2006. Bovine respiratory disease in feedlot cattle: Environmental, genetic and economic factors. *J. Anim. Sci.,* 84, 1999-2008.

Storz, J., Purdy, C. & Lin, X. B. M. 2000a. Isolation of respiratory bovine coronavirus, other cytocidal virus, and *Pasturella* spp. from cattle involved in two natural outbreaks of shipping fever. *Journal of the Veterinary Medical Association,* 216**,** 1599-1604.

Storz, j., Stine, L., Liem, A. & Anderson, G. A. 1996. Coronavirus isolation from nasal swab samples in cattle with signs of respiratory tract disease after shipping. *Journal of the Veterinary Medical Association,* 208**,** 1452-1455.

Storz, J., XiaoQing, L., Purdy, C. W., Chouljenko, V. N., Kousoulas, K. G., Enright, F. M., Gilmore, W. C., Briggs, R. E. & Loan, R. W. 2000b. Coronavirus and pasteurella infections in bovine shipping fever pneumonia and Evans criteria for causation. *Journal of Clinical Microbiology,* 38**,** 3291-3298.

System, N. A. H. M. 2000. Feedlot '99 Part II: Baseline Reference of Feedlot Health and Health Management. USDA, APHIS, National Animal Health Monitoring System.

Thomas, L. H., Gourlay, R. N., Stott, E. J., Howard, C. J. & Bridger, J. C. 1982. A search for new microorganisms in pneumonia by the inoculation of gnotobiotic calves. *Res Vet Sci,* 33**,** 170-182.

VS, U. A. April 2011. Small scale US cow-calf operations. USDA; APHIS; VS; CEAH, Fort Collins, CO.

Wildman, B. K., Perrett, T., Abutarbush, S. M., Guichon, P. T., Pittman, T. J., Booker, C. W., Schunicht, O. C., Fenton, R. K. & Jim, G. K. 2008. A comparison of 2 vaccination programs in feedlot calves at ultra-high risk of developing undifferentiated fever/bovine respiratory disease. *Can. Vet. J.,* 49**,** 463-472.

CHAPTER II
LITERATURE REVIEW

Taxonomy of coronaviruses

Coronaviruses belong to the *Coronaviridae* family of viruses (Cavanagh et al., 1994, 1995) within a relatively newly established order, *Nidovirales*, viruses producing 3' nested subgenomic RNAs. The Nidoviruses also possess additional distinguishing features that further set them apart from other positive-sense RNA viruses: expression of the replicase polyprotein by way of a unique ribosomal frameshifting technique, unique enzymatic activities among the replicase protein products, and a multi-spanning integral membrane protein. Until 1993, *Coronaviridae* was completely monogeneric, composed solely of *Coronavirus*, of which there were considered to be three antigenic groups defined primarily by monoclonal antibody analysis and nucleotide sequencing (Siddell, 1995), although, originally, the genus was divided into four antigenic groups based on serological analyses (Holmes, 1990). Refinement of the antigenic groupings was proposed based on the results of monoclonal antibody testing and nucleotide sequencing suggesting that turkey coronavirus (TCV) and BCoV were actually more closely related than originally thought (Siddell, 1995). While the members of groups I and II are closely related, not only within their respective groups, but in some respect across groups, the sole member of group III, avian infectious bronchitis virus (IBV), notably the first coronavirus to be isolated and propagated (Shalk and Hawn, 1931), is dramatically different from groups I and II, even showing a considerable amount of within-species variation. In 1993 the International Committee for the Taxonomy of Viruses (ICTV) officially included a second genus into the *Coronaviridae* family, based on previous observations that the genus *Torovirus*, which had not yet at that time officially been

included in a virus family, displayed many of the same characteristics generally associated with coronaviruses (Cavanagh et al., 1994, 1995). More recently, the ICTV once again modified the *Coronaviridae* classification, separating it into three distinct groupings, essentially divergent enough to be considered genera: the alpha-, beta-, and gammacoronaviruses, corresponding to the original groupings 1, 2, and 3, within the subfamily *Coronavirinae*, within the family *Coronaviridae* (2009). Virtually all of the group 1 and 2 coronaviruses have mammalian hosts, and the human coronaviruses are represented in each of these groups, including the newly discovered human coronaviruses (HCV) HCV-NL63 (van der Hoek et al., 2004) and HCV-HKU1 (Woo et al., 2005). A number of additional coronaviruses have also been added to groups 1 and 2, their discovery sparked by the emergence of the previously unknown SARS-CoV. These are the bat coronaviruses, three of which have been reported. Two of these belong to group 1 and the third, identified as the likely precursor to the SARS-CoV, is within group 2 (Lau et al., 2005; Li et al., 2005; Poon et al., 2005). The group 3 coronaviruses, on the other hand, have been isolated solely from avian hosts, and, much like as has occurred in groups 1 and 2, a number of new IBV-like species have been identified, including those that infect geese, ducks, and pigeons (Jonassen et al., 2005).

Coronavirus architecture

Coronaviruses are large, approximately 120 nm in diameter pleomorphic virions possessing a cell membrane-derived bi-layer lipid envelope which reflects the lipid content of the host cell membrane (Pike and Garwes, 1977). Projecting from this lipid envelope are numerous prominent, 17-20 nm petal-shaped spikes (McIntosh, 1974), glycoproteins (gp) composed of heavily glycosylated type I proteins anchored within the

lipid envelope of the virion (Fig. 2.1). These projections are easily recognizable on electron micrograph as projections with a thin base topped by a globular structure of approximately 10 nm in width at the distal extremity (Sugiyama and Amano, 1981), and it is from this “crown” of gps that coronaviruses derive their name. In addition to the large “Spike” gp (S), which is required for infection, a subset of the coronaviruses, all of those classified within the betacoronaviruses, also possess a second set of shorter, far less prominent, 5-10 nm long gps projecting from the lipid envelope (Caul and Egglestone, 1977; King and Brian, 1982; Dea and Tijssen, 1988). Unlike S, however, this type I gp, the hemagglutinin-esterase (HE) protein, is not essential for virus infectivity. An additional protein associated with the lipid envelope of the virion is the small type III membrane protein known as M or matrix protein, the integral membrane gp, formerly known as the E1 gp, and not only spans the lipid envelope three times, but is also associated at its carboxyl (C) terminus with the nucleocapsid (N) protein. The N protein is non-glycosylated and interacts with the linear viral genomic RNA in a “beads on a string” fashion (Laude and Masters, 1995) to form the 14 to 16 nm helical viral ribonucleoprotein (RNP) known as the nucleocapsid (McNaughton et al., 1978; Sturman and Holmes, 1983), located at the internal periphery of the virion, adjacent to the viral envelope as a result of its interaction with the M gp during virion assembly (Hurst et al., 2005). Interestingly, coronaviruses are generally considered to contain a helically symmetric nucleocapsid, a distinguishingly unusual characteristic for positive-sense RNA viruses but considered the norm for RNA viruses having a negative-sense genome. More recently, what was previously held as the prototypical coronavirus architecture has been challenged. Risco et al, by way of negative staining, ultra-thin sectioning, freeze-fracture,

immunogold mapping, and cryoelectron microscopy of detergent-treated transmissible gastroenteritis virus (TGEV) particles observed a previously unreported icosahedral core within the virion encompassing not only the RNP but also the M gp. Only after treatment with Triton-X did the nucleocapsid further dissociate into the expected helical arrangement (1996). However, this odd coronavirus nucleocapsid arrangement has thus far only been reported for TGEV.

Nucleocapsid protein

The nucleocapsid protein of coronavirus is a 50 to 52 kDa non-glycosylated, phosphoprotein (Calvo et al., 2005; King and Brian, 1982) capable of forming disulfide-linked trimers with an average molecular weight (MW) of 160 kDa under non-reducing conditions. The N proteins are concentrated along the internal periphery of the lipid envelope, interacting with the integral membrane protein (M). The N proteins have been reported to range anywhere from 9 to 16 nm in diameter and vary from 377 to 455 amino acids in length. These proteins are highly basic in nature and contain numerous serine residues; in fact the proteins may contain as much as 7 to 11% serine, and it is these residues that are targets for phosphorylation (Stohlman and Lai, 1979; Siddell et al., 1981). This phosphorylation is proposed to have regulatory significance, and Chen et al. have reported that, for IBV, phosphorylated N protein is better able to differentiate viral from non-viral substrates when compared with unphosphorylated N protein *in vitro* (2005). Furthermore, in studies of BRCoV N protein, researchers have reported that only a small subset of phosphorylated forms of the intracellular N protein are incorporated into virions, leading these researchers to postulate that N protein phosphorylation may be linked to virion assembly and maturation (Hogue, 1995).

In addition to its numerous serine residues, the N protein is also rich basic amino acids, which are generally concentrated in RNA-binding domains (Masters et al., 1992; Nelson and Stohlman, 1993) associated with both coronavirus and non-viral RNA binding (Robbins et al., 1986; Stohlman et al., 1988; Masters, 1992). Specifically, the murine hepatitis virus (MHV) N protein has been reported to bind to the RNA leader sequence, particularly at nucleotides 56-67, under specific binding conditions (Stohlman et al., 1988; Nelson et al., 2000; Chen et al., 2005). In addition, the N protein of IBV has been reported to bind to the 3' untranslated region (UTR) of the IBV genomic RNA *in vitro* (Zhou et al., 1996). Other proposed sites of viral genomic RNA binding include the *N* gene within the viral genome (Cologna et al., 2000) and the genomic RNA packaging signal (Molenkamp and Spaan, 1997; Cologna et al. 2000). This RNA binding ability is vital to the formation of viral particles, as N proteins interacts with the viral genomic RNA to form the viral nucleocapsid (Hurst et al., 2005); viral genomic RNA cannot be incorporated into the viral particle without this essential interaction (Bos et al., 1996; Vennema et al., 1996). Furthermore, it has been suggested that N protein may actually participate as a part of the viral RNA synthesis machinery, since it is able to both bind viral RNA and interact with the membrane (Anderson and Wong, 1993), which has been shown to be the primary site of viral RNA synthesis in infected cells (Brayton et al., 1982; Dennis and Brian, 1982). In support of this hypothesis is the report by Compton et al. in which monoclonal antibodies against the N protein added to an *in vitro* RNA synthesis effectively inhibited viral RNA replication (1987), and, more recently, it was

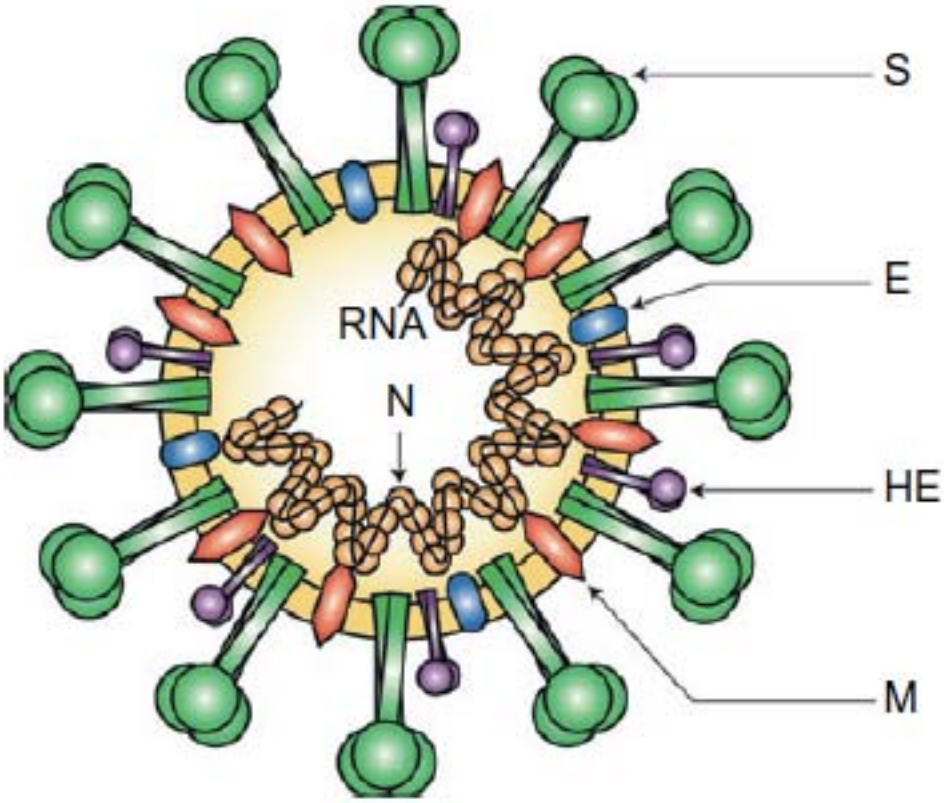

Figure 2.1. Coronavirus virion architecture. The viral ribonucleocapsid is encased within a bi-layer lipid envelope containing three viral proteins: Spike, HE, and M, from Finlay and Hancock, 2004).

demonstrated that N protein is, indeed, associated with replication-transcription complexes in infected cells (Verheije et al., 2010).

Membrane protein

The M gp of coronavirus, formerly known in the literature as gp E1, is a glycosylated, multi-spanning membrane protein that gives the viral envelope its shape. As such, it is the most abundant constituent of the virus (Sturman et al., 1980; Sturman, 1977). The protein is thought to originate as an unglycosylated polyprotein, and prior to glycosylation, the protein can be identified as a 25 to 30 kDa polypeptide, although numerous higher MW products possessing varying levels of glycosylation can be

identified by SDS-PAGE analysis (Krijnse Locker et al., 1992). The glycosidic residues are, in the vast majority of betacoronaviruses, O-linked to the polypeptide backbone, the exceptions to this being MHV-2 (Yamada et al., 2000) and the SARS coronavirus (Nal et al., 2005), both of which contain N-linked glycosidic residues. All members of the other two coronavirus groups posses M proteins with strictly N-linked glycosylation (Stern and Sefton, 1982; Jacobs et al., 1986; Cavanaugh and Davis, 1988). Interestingly, viral O-linked glycosylation had not previously been described before its discovery in the MHV-2 coronavirus (Holmes et al., 1981).

The first polytopic membrane protein to be described was the coronavirus M protein (Armstrong et al., 1984; Rottier et al., 1984), which contains a short, 5 kDa hydrophilic amino-terminal tail as its ectodomain, followed by three hydrophobic, α-helical transmembrane segments. The transmembrane domain is then followed by a large amphipathic carboxyl-terminus that makes up the majority of the molecule and which is situated within the interior of the virion (Rottier, 1995). Only the ectodomain of the M protein is glycosylated, and has been shown to be translocated to the lumen of the endoplasmic reticulum (ER) following its translation by microsomes *in vitro* (Rottier et al, 1986; Rottier et al., 1984; Cavanagh and Davis, 1988). While the ectodomain of M protein has bee shown to be particularly protease-sensitive, the C-terminus of the protein is quite resistant to proteolytic cleavage, suggesting that the endodomain is tightly associated with the surface of the viral envelope or that it has a particularly tight configuration that protects it from proteolysis (Rottier, 1995).

The M protein plays a crucial role in virion assembly and budding and has been shown to interact with each other (deHaan et al., 2000), as well as with other viral

proteins, including N protein (Kuo and Masters, 2002; Fang et al., 2005), S (deHaan et al., 1999), envelope protein (Nguyen and Hogue, 1997), and, in some betacoronaviruses, HE (Opstelten et al., 1995). In addition to these interactions, MHV N protein has also been reported to interact directly with the MHV genomic RNA packaging signal in the direction of genomic RNA packaging during virion assembly (Narayanan et al., 2003).

Small membrane protein E

The coronavirus small membrane protein, E, is a small polypeptide ranging from 8.4 to 12 kDa and makes up the smallest percentage of viral protein within the virion (Liu and Inglis, 1991; Godet et al., 1992; Yu et al., 1994; Raamsman et al., 2000). It is an integral membrane protein and, owing to its small size, one of the last coronavirus structural proteins to be discovered. The E protein was first discovered in IBV (Liu and Inglis, 1991), followed soon after in TGEV (Godet et al., 1992), and finally was reported in the MHV coronavirus (Yu et al., 1994), representing all three genre of the *Coronavirinae*. The E protein is an unusual coronaviral protein in that it is not translated from its own individual subgenomic mRNA; instead, it has been reported to be translated in a bi- or tri-cistronic manner from an open reading frame (ORF) downstream of, in the case of MHV, one (Leibowitz et al., 1988) or, in the case of IBV, two (Liu et al., 1991), ORFs that encode viral accessory genes which are also expressed from the same mRNA. Furthermore, IBV M protein is also unusual for the coronaviral proteins in that its translation from mRNA has been shown to be facilitated by an internal ribosomal entry site (IRES; Liu and Inglis, 1992). However, it is currently unknown whether or not other coronaviruses utilize this mechanism for translation of the E protein.

The E protein gene of the coronaviruses is not well conserved across the three coronavirus genre, even showing considerable variation between members within a single genre. However, in spite of this considerable divergence, the E protein maintains the same general architecture amongst all three genres, having three distinct domains: a short hydrophilic N-terminus consisting of approximately 8 to 12 amino acid residues followed by an unusually long hydrophobic region representing the transmembrane domain containing two to four cystine residues which are important for the function of the protein. This intermembrane region is followed then by a considerable hydrophilic C-terminal tail consisting of 39 to 76 amino acid residues. Additionally, the C-terminal domain of the protein has been reported to be both palmitoylated (Yu et al., 1994; Liao et al., 2006; Boscarino et al., 2008) and ubiquinated (Alvarez et al., 2010).

The topology of the E protein has only been partially elucidated. Studies of the MHV and IBV E proteins strongly suggest that the C-terminal tail of the protein is situated within the virion (Corse and Machamer, 2000; Raamsman et al., 2000), while less extensive analysis of the TGEV E protein suggested it was oriented with the C-terminus exterior to the virion, while the amino (N)-terminus was within (Godet et al., 1992). Corse and Machamer also reported that the C-terminal domain of the IBV E protein, in the absence of its membrane-bound domain, is sufficient to specify targeting to the budding compartment (2002). Elucidation of the N-terminus orientation has been less straightforward, however. While molecular dynamics simulations have previously suggested that the E protein should be a single-transit transmembrane protein (Torres et al., 2005), results of studies with MHV using an E protein expressing an N-terminus epitope tag have revealed that this domain may very well be buried within the membrane

near the cytoplasmic face, suggesting that the protein is oriented in a hairpin fashion within the viral membrane (Maeda et al., 2001). In support of this finding is the report by Raasmsman and colleagues that none of the E protein in purified MHV virions is accessible to degradation by protease treatment (2000). Furthermore, these findings together are in agreement with those predicted for SARS-CoV E protein (Arbely et al., 2004). Thus, additional work remains to be done to fully determine the orientation of this protein.

The E protein plays a vital role in virion assembly (Bos et al., 1996; Corse and Machamer, 2000), and palmitoylation of one or both of its cystine residues on the C-terminal tail has been shown to be required for this function (Alvarez et al., 2010). Additionally, complete palmitoylation of the protein has been shown to be important for protein stability (Lopez et al., 2008). Fischer et al. (1998) reported that E protein plays a significant role in the assembly of viral particles, and co-expression of the E and M proteins has previously been shown to be sufficient for assembly of virus-like particles of most of the coronaviruses that have been examined to-date (Bos et al., 1996; Baudoux et al., 1998; Corse and Machamer, 2000). However, the E protein does not appear to be absolutely essential for the assembly of all coronaviruses. In their 2003 study, Kuo and Masters constructed an E-deleted MHV mutant via targeted recombination that was shown to be viable through several passages in cell culture, in spite of the production of tiny plaques and significantly decreased viral replication. Likewise, DeDiego et al. (2007) constructed an E-deleted SARS-CoV in similar fashion, which they reported was also viable, in fact only reaching titers that were approximately 1-2 log lower than that observed for wild-type virus in culture.

Hemagglutinin-esterase

The hemagglutinin-esterase gp (HE) is an unusual viral gp protein in that it is not possessed by all coronaviruses. Rather, only a specific subset of coronaviruses, those belonging to group 2a, including HEV, MHV, HCV-OC43, BCoV, and TCV, contain the gene for expression of this membrane gp, which possesses both receptor binding (hemagglutinin) and receptor destroying (acetylesterase) activities. Even more interesting is the observation that not all of the viral strains within the group 2a coronaviruses express the HE gene, as the MHV strain A59 possesses an untranscribed HE pseudogene lacking the initiation codon in the open reading frame (orf; Lutjes et al., 1988). Other group 2a coronavirus strains have also been reported to possess truncated versions of the HE gene that also remain unexpressed (Yokomori et al., 1991). In fact, despite the fact that HE was first reported in BCoV in 1985 (King et al., 1985), it was not accepted as a true viral gp for quite some time due to the fact that MHV-A59, one of the most thoroughly-studied coronaviruses, did not possess HE.

The HE gp is an approximately 65 kDa glycoprotein that exists as a homodimer anchored by its C-terminus within the viral membrane (Caul and Egglestone, 1977; Dea and Tijssen, 1988; Zeng et al., 2008), a conformation achieved via interaction of the receptor and membrane-proximal domains of the protein (Zeng et al., 2008). It is believed that the HE of the group 2a coronaviruses was obtained as a result of a non-homologous recombination event between an ancestral coronavirus and an influenza C virus (Luytjes et al., 1988), and, indeed, the two share approximately 30% homology in the gene encoding their respective HE/hemagglutinin-esterase-fusion proteins (HEF, influenza C virus; Kienzle et al., 1990). Additionally, the putative esterase-active site, FGDS, is

conserved between the two viruses (Parker et al., 1989; Kienzle et al., 1990), as are a number of cystine residues (Zhang et al., 1991). Interestingly, the membrane proximal domain is formed from the remnant of the F1 fusion domain and the F2 domain of the closely related HA protein from influenza A and B viruses and the HEF protein of influenza C viruses (reviewed in Mesecar and Ratia, 2008). The dimerization of the HE protein of coronavirus is thus accomplished by a unique arrangement for this family of proteins, as both the HA and HEF proteins exist in their respective viruses as trimeric structures resulting from significant interaction of the entire fusion domain of these viruses, inclusive of F1, F2, and F3, as well as the membrane-proximal domain (Wilson et al., 1981; Rosenthal et al., 1998; Ha et al., 2002). The coronavirus HE, in the course of evolution, has, in contrast, lost most of its F1 domain, as well as its F2 and F3 domains in their entirety, most likely as a result of decreased selection pressure to retain these domains, as coronaviruses depend largely on the fusogenic function of the S gp for receptor binding and membrane fusion, unlike the influenza viruses, which rely on the action of the HA or HEF proteins for this function (Zeng et al., 2008).

The HE of coronaviruses possesses both hemagglutination and hemadsorption properties, the latter being the ability to adsorb erythrocytes to the membranes of infected cells (Sharpee et al., 1976; King et al., 1985; Kienzle et al, 1990; Payne and Stortz, 1990). The cellular receptor target for the HE protein is the cell membrane carbohydrate moiety 9-*O*-acetylated neuraminic acid (Vlasak et al., 1988; Schultze et al., 1991), which it is also able to hydrolyze via its neuraminate-*O*-acetylesterase activity, an enzyme activity that releases the protein from its receptor, effectively reversing hemagglutination induced by it or the S gp (Vlasak et al., 1988; Yokomori et al., 1989; Parker et al., 1990).

For this reason HE is also considered to be a receptor destroying enzyme. Interestingly, however, like the newly described orthomyxovirus, infectious salmon anemia virus (Hellbeo et al., 2004), the MHV-S strain of coronavirus has been reported to instead bind 4-*O*-acetylated neuraminic acid (Regl et al., 1999).

The functional significance of the coronavirus HE gp is not currently fully understood. It has been previously reported that HE contains multiple important neutralizing epitopes (Deregt et al., 1989) mapping primarily to one of three epitope locations on the protein (Deregt and Babiuk, 1987; Parker et al., 1989, 1990; Vautherot et al., 1990) and that antibodies directed against these epitopes were neutralizing both *in vitro* and *in vivo* (Deregt et al., 1989). This research has suggested that specific monoclonal antibodies against the HE of the enteropathic strain of BCOV are capable of inhibiting virus infectivity (Deregt and Babiuk, 1987; Deregt et al., 1989; Hussain et al., 1991), and that development of antibodies against both the S and HE gps play significant roles in clearing viral infection (Lin et al., 2000). Given this apparent antigenicity, a feature typically reserved for epitopes on pathogens mapping to highly conserved and necessary proteins, it was originally thought, at least with respect to BCoV infectivity, that HE was necessary for infectivity (Yokomori et al, 1992, 1995); however, this was disproven by Popova et al. (2002) utilizing chimeric MHV virions expressing either BCoV S or BCoV HE gps. When these chimeric viruses were used to inoculate cultures of the 18G clone of human-derived rectal tumor cells (HRT-18G), an immortalized cell line known to support infection and replication by BCoV (Thompkins et al., 1974; Storz et al., 1996), only those viruses expressing the functional BCoV S gp, and not the chimeric MHV virions expressing the functional BCoV HE gp, were able to enter HRT-

18G cells. Thus the group concluded that the BCoV S gp alone is necessary and sufficient for infection of HRT-18G cells. Alternatively, based on studies utilizing monoclonal antibody (Mab) against the MHV HE which suggested that MHV with the functional HE may have altered neuropathogenicity when compared with MHV lacking functional HE (Yokomuri et al., 1992, 1995), it was proposed that HE may allow coronaviruses bearing this protein to utilize alternative receptors independent of the S gp. However, this, too, was shown to not be the case, based on a report in which the use of Mab against the major receptor for the MHV S inhibited infection of cells by an MHV expressing the HE gp (Gagneten et al., 1995). Thus, although the coronavirus HE seems to bear some importance with respect to infectivity based on the presence of strongly neutralizing viral epitopes, the function of this protein with respect to viral infectivity and replication has yet to be fully understood.

Spike

The spike gp (S) of coronaviruses is arguably the most distinctive coronaviral protein, as it projects some 17 to 20 nm out from the surface of the viral envelope, giving the virus the appearance of a crown. Responsible for facilitating not only host receptor recognition and binding (Collins et al., 1982; Godet et a., 1994; Kubo et al., 1994), but also virus-host and host-host membrane fusion and viral entry (Gallagher et al., 1991; Qiu et al., 2006), S plays a vital role in promoting infection and has been implicated as a significant factor influencing virulence (Navas et al., 2001) as well as both tissue (Navas et al., 2001; Phillips et al., 2001; Navas and Weiss, 2003) and host tropism (Li et al, 2006). The protein exists on the virion surface as a trimer (Delmas and Laude, 1990), with the S1 subunits, the approximately N-terminal one-half of the polypeptide,

interacting to form the globular head and the S2 subunits, comprised of the approximately C-terminal one-half of the polypeptide, interacting to form the transmembrane stalk (de Groot et al., 1987; Figure 2.2).

Spike is a large gp, ranging anywhere from 1160 amino acids in the IBV S to 1452 in feline coronavirus (FCV). The protein contains an N-terminal cleaved signal sequence that directs its cotranslational insertion into the endoplasmic reticulum (Cavanagh et al., 1986) and a transmembrane sequence near the C-terminus, with the N-terminal ectodomain making up the vast majority of the protein, while the C-terminal transmembrane and ectodomains are, by comparison, significantly shorter, consisting of only 71 or fewer amino acids. The S ectodomain contains between 30 and 50 cystine residues, the positions of which have been shown to be well-conserved within each of the coronavirus groups (Abraham et al., 1990; Eickmann et al., 2003), although comprehensive mapping of resulting potential disulfide linkages has yet to be performed for any of the coronaviruses. Some of these cystine-rich domains have been shown to be critical in the expression of S gp on the surface of host cell membranes (Petit et al., 2005). The protein also contains numerous glycosylation sites, ranging in number anywhere from 21 to 35, all of which are exclusively N-linked (Holmes et al., 1981; Rottier et al., 1981). The ectodomain of the coronavirus S proteins contains an assortment of potential conserved glycosylation sites, but comprehensive mapping of these sites has yet to be reported for any coronavirus to date. However, mass spectrometric studies of the SARS-CoV have shown that at least 12 of the 23 potential sites are glycosylated in this virus (Krokhin et al., 2003. Additionally, these modifications appear to occur in a

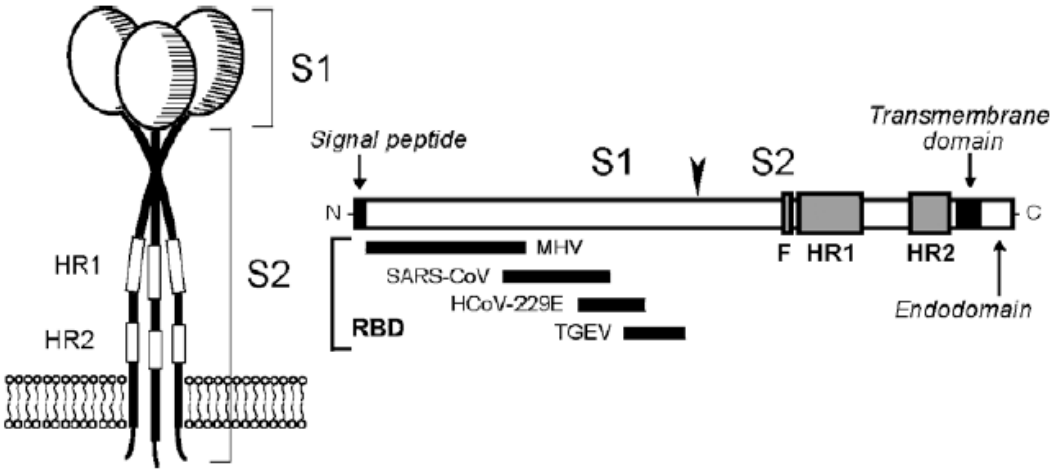

Figure 2.2. The primary structure and functional domains of the S glycoprotein, from Masters, 2006.

cotranslational manner, although it has been reported in TGEV that terminal glycosylation is in fact preceded by trimerization of the protein, an event that can also be rate-limiting in S protein maturation (Delmas and Laude, 1990). Furthermore, monomer folding may also be assisted by proper glycosylation of the TGEV S protein, as it has been reported that treatment with tunicamyacin, which inhibits high-mannose transfer, was shown to block trimerization of the S monomers (Delmas and Laude, 1990).

Spike can be divided into two approximately 90 kDa subunits, the S1 and S2 domains of the protein, which can be cleaved from one another in the presence of trypsin (Hogue and Brian, 1986), the latter of the two being acylated (Sturman et al., 1985). Most of the MHV S proteins, with the exception of those belonging to MHV-2, are cleaved postranslationally by a cellular furan-like protease into the S1 and S2, which remain bound via a non-covalent linkage (Frana et al., 1985; Sturman et al., 1985). Interestingly, trypsin treatment of MHV S proteins causes cleavage of all S gps without disruption of

the spikes (Sturman et al., 1985), but treatment with mild alkali or urea will release S1 from the virion (Cavanagh and Davis, 1986; Sturman et al., 1990; Weismiller et al., 1990). Peptide sequencing of the cleavage products for a number of coronaviruses has determined that cleavage occurs following the last residue in a highly basic motif, which varies between coronavirus species. In the IBV S protein the sequence of this motif has been shown to be RRFRR (Cavanagh et al., 1986), while in MHV-A59 it has been reported to be RRAHR (Luytjes et al., 1987), and KRRSRR in BCoV (Abraham et al., 1990). Amongst the coronaviruses as a whole, S2 is considered to be far more conserved as compared with S1 (de Groot et al., 1987), in which there is virtually no sequence conservation, even among strains and isolates within a single coronavirus species (Parker et al., 1989; Gallagher et al., 1990; Wang et al., 1994). Additionally, comparison of the S1 sequences amongst strains within a species or between species of a given group have shown that the S1 contains a number of hypervariable regions denoted by frequent deletions, mutations, or even areas of recombination (Cavanagh et al, 1988; Parker et al., 1989; banner et al., 1990; Gallagher et al., 1990).

The S gp, a class I fusion protein (Bosch et al., 2003), alone is sufficient to cause membrane fusion, an observation supported by the formation of syncytia in the presence of recombinant S (de Groot et al., 1989; Pfleiderer et al., 1990; Yoo et al., 1991; Taguchi, 1993), and posttranslational cleavage of the S gp following its synthesis in the endoplasmic reticulum has been implicated in induction of the membrane fusion process for a number of coronavirus species (Sturman et al., 1985). The binding of the MHV S S1 subunit to its cellular receptor results in a conformational change accompanied by separation of the S1 and S2 subunits, a change which may be involved in triggering

membrane fusion and that can be mimicked in the absence of a cellular receptor by exposure of the S gp to 37°C and an elevated pH of 8 (Gallagher, 1997; Holmes et al., 2001; Sturman et al., 1990). However, cleavage of the S protein is not necessary in all cases to facilitate the fusogenic activity of S, as shown via studies utilizing MHV S proteins containing mutated S1-S2 connecting peptides (Stauber et al., 1993; Taguchi, 1993, Bos et al., 1995), although the process has been shown to enhance the fusogenicity of S (Gombold et al., 1993; Taguchi, 1993). Naturally occurring MHV mutants defective in S cleavage recovered from persistently infected murine cells remain infective but have delayed fusion activity (Gombold et al., 1993). Furthermore, neither the feline infectious peritonitis virus (FIPV) (de Groot et al., 1989) nor the SARS-CoV (Simmons et al., 2011) S gp are cleaved during synthesis, but still enter host cells and result in cell-cell fusion and syncytia formation. For these cleavage-deficient viruses, it is thought that, rather than entering the host cell at the level of the cell membrane via fusion of the viral and cellular lipid membranes, the virus may employ an endosomal route of entry. In this scenario, the virus, following attachment to the cellular receptor, is taken up by into cellular endosomes, at which point cathepsin or another cellular trypsin-like protease dependent upon decreasing endosomal pH is responsible for cleavage of the S1 and S2 subunits, triggering fusion of the viral and endosomal membranes, in turn resulting in release of the viral from the endosomal compartment (Qiu et al., 2006; Simmons et al., 2011).

The S2 subunit contains two 4,3-hydrophobic heptad repeat sequences (Delmas and Laude, 1990) termed HR1 and HR2, which together form a six helix bundle structure, a motif characteristic of coiled coils. Specifically, the helices of HR1 form a homotrimeric coiled coil into the hydrophobic grooves of which are tightly packed the

coils of HR2, in an antiparallel manner, a conformation that brings the fusion peptide into close proximity with the transmembrane anchor (reviewed by Eckert and Kim, 2001). When the fusion peptide is inserted into the host cell membrane, this conformation brings the two membranes into close apposition, facilitating their fusion (Melikyan et al., 2000; Russell et al, 2001). Like many features of the S2 subunit, these HRs are highly conserved in both sequence and position across the members of the three groups of coronaviruses. A combination of predictions and observations have led to the supposition that the HR1 and HR2 motifs of the S S2 subunit are directly involved in mediating viral envelope fusion with the cell membrane. The first of these predictions is that a fusion peptide may lie near (Chambers et al., 1990) or within (Luo and Weiss, 1998) the HR1 region, and, secondly, that viruses containing mutations in the HR2 region are defective with regard to oligomerization and fusogenicity (Luo et al., 1999). In fact, mutations within HR1 or HR2 of the MHV S gp have been shown to abolish the fusogenic properties of the protein (Luo and Weiss, 1998; Luo et al., 1999). Thirdly, the JHM strain of MHV has been shown to be capable of host entry via the endosomal pathway, but does not require low pH for release from the endosomal compartment (Nash and Buchmeier, 1997); however, for those viruses utilizing the same pathway but requiring acidic endosomal pH for release, the defect has generally mapped to HR1 (Gallagher et al., 1991). Further underlining the importance of the S heptad repeats in viral-mediated membrane fusion are the observations that, 1) three site-directed mutations in or near the HR1 region were responsible for conveying the low pH requirement of some MHV-JHM mutant strains isolated from persistently infected cells (Gallagher et al., 1991), and 2) a significant reduction in cell-cell fusion exhibited by some MHV-JHM mutant strains was

attributed to two mutations in the gene encoding the S protein, one of which, again, mapped to HR1 and could be overcome by acidification (Krueger et al., 2001). Additionally, codon mutations in HR2 have also been reported to severely inhibit fusogenicity and oligomerization of the S gp, in spite of the fact that the mutations did not hinder their expression on the membrane surface (Luo et al., 1999).

The highly variable S1 subunit, on the other hand, has been implicated in receptor binding, a function that has been mapped to the N-terminal 330 amino acids for MHV (Williams et al., 1991; Taguchi, 1995). In fact, previous researchers have reported that changes in the residues located at positions 62, 212, 214, and 216 via site-directed mutagenesis were able to completely abolish the binding of S to its receptor (Suzuki and Taguchi, 1996). Receptor binding sites have also been mapped for the TGEV S gp, and reside within a 223-residue region at amino acids 506-729 of the S1 subunit (Godet et al., 1994). Perhaps interestingly, but not surprisingly, this region overlaps with and epitope for a neutralizing Mab, which was reported as capable of blocking binding by the 223 amino acid polypeptide to its receptor. A finding, however, that was somewhat surprising was that, conversely, the receptor did not in turn block binding of the Mab to the 223 amino acid polypeptide, suggesting that the epitope and receptor binding domain were, although overlapping, distinct and possibly conformation-dependent (Godet et al, 1994).

Being the primary viral protein involved in host cell binding, and, ultimately, the determinant of host cell infectivity, it is perhaps no surprise that the S gp is also the primary target of the host adaptive immune response (Collins et al. 1982; Stohlman, 1985; Williams et al., 1991; Compton et al., 1992), with antibodies developed against this protein generally associated with strong protection against viral infection (Buchmeier et

al., 1984; Nakanaga, 1986). A considerable body of work has been done in the past in an attempt to delineate both the continuous and discontinuous epitopes of the S gp associated with development of neutralizing antibodies. In a1984 study performed by Wege et al., the group characterized a set of MHV-JHM S gp-specific Mab, which were used to identify six antigenic sites, A through F. Of these, they found that two sites were associated with strong binding with neutralizing antibodies, and were noted to define discontinuous epitopes, epitopes encompassing sections of the protein only close together in the secondary structure of the protein, on the S gp. On the other hand, antigenic sites C through F were noted to be associated with continuous epitopes, not dependent on protein secondary structure for recognition (Wege et al., 1988). The discontinuous antigenic site A was found to be contained within the S1 subunit, considered to be the immunodominant B-cell determinant of the S gp (Stuhler et al., 1991), a finding supported by previous work utilizing Mab-selected neutralization-resistant MHV mutants having extensive deletions in the S1 subunit (Parker et al., 1989), suggesting that this portion of the S gp is a major target for the induction of neutralizing antibody (Gallagher et al., 1990). Additional work performed with Mab produced against the S gp of IBV also showed that strongly neutralizing antibody formation was associated primarily with the S1 subunit of S (Mockett et al., 1984), and, in fact, research utilizing IBV in which the S1 portion of the S gp had been removed via treatment with urea, while the S2 portion was retained, failed to induce production of protective antibody (Cavanagh et al., 1986). However, neutralizing antibodies mapping to the S2 subunit of the S gp have been reported (Collins et al., 1982; Taguchi and Shimazaki, 2000); these antibodies, in the case of MHV, have been mapped to domains within S2 involved in membrane fusion,

although the authors do allow that the neutralizing activity of the anti-S2 antibodies are not as strongly neutralizing as those associated with binding of the S1 subunit, especially those domains on S1 associated directly with receptor binding (Taguchi and Shimazaki, 2000). It is worth mentioning, however, that the S2 subunit of the S gp may play a vital role in the induction of a strong neutralizing antibody response unrelated to the production of anti-S2 antibody. Recent research in the development of a SARS DNA vaccine has shown that truncation of portions of the S2 subunit, namely the transmembrane domain, result in the production of only poorly virus neutralizing antibody. The authors suggest that this may be a result of the involvement of the transmembrane domain in supporting proper tertiary structure development, or that anchoring in the membrane may give rise to a more stable, physiologically relevant form of the protein, in turn preserving conformational determinants important for epitope formation (Yang et al., 2004).

Accessory proteins

In addition to the five structural proteins encoded within the coronavirus genome, there are also additional accessory proteins encoded, in some cases within their own ORF, but in many cases within or overlapping the ORFs encoding the structural proteins. Analysis of numerous coronavirus genomes has revealed the presence of at least 10 ORFs, some of these corresponding to a distinct mRNA product, but others being less conventional in the method of their processing and translation. These proteins were originally described as the nonstructural (ns) proteins, but this may turn out to be somewhat of a misnomer, since the function of some of these proteins has been elusive and remains to be described; however, description of function for some of these proteins

has been at least partially determined, although there remains some disagreement about the complete function even of many of these proteins, necessitating further research in the future.

The first polyproteins to be translated following viral entry into the host cells are encoded within ORF1a, which encodes the approximately 450 kDa pp1a, and ORF1b, encoding the approximately 750 kDa pp1ab, also known jointly as the coronavirus replicase locus, encompassing an impressive 20 kb, or almost two-thirds of the coronavirus genome. The protein product of this locus is cotranslationally processed into 16 nonstructural proteins (nsp1 through nsp16), which are thought to assemble into a cytoplasmic, membrane-associated replication complex involved in both replication of the genome and production of the 3' nested subgenomic RNAs (Snijder et al., 2003; Stadler et al., 2003). Cotranslational processing of these polyproteins is accomplished by either one or two papain-like proteases (PLP) encoded within ORF1a, the most commonly identified of these being nsp3. ORF1a has been predicted to encode at least one PLP (nsp3) and a 3C-like protease ($3CL^{pro}$) similar to those observed in picornaviruses, as well as a number of putative nsps of unknown function. ORF1b is located downstream of ORF 1a and is transcribed as a fusion protein via a -1 ribosomal frameshift (Herold and Siddell, 1993), resulting in the production of pp1ab, which includes the core RNA polymerase nsp12, a helicase domain (nsp13), and a predicted primase, nsp8. Additional nsps are also contained within this large polyprotein, including the N7-capping enzyme, an exonuclease (Minskaia et al., 2006; Chen et al., 2007) and proposed proofreading enzyme (Denison et al., 2011), nsp14, the endoribonuclease nsp15

(Bhardwaj et al., 2004; Ivanov et al., 2004; Bhardwaj et al., 2006), and a 2'-O-methyltransferase, nsp16 (Snijder et al., 2003; Decroly et al., 2008).

The proteins Nsp12 and Nsp8 are encoded within orf1b and are involved in viral genome replication. Nsp12 contains the RNA-dependent RNA polymerase core activity associated with both replication of the genomic RNA via a negative stranded RNA intermediate (te Velthuis et al., 2010) as well as transcription of the multiple nested subgenomic mRNAs, while Nsp8 has similar activity but preferentially initiates synthesis of short oligonucleotides containing fewer than six residues (*reviewed in* Weiss and Leibowitz, 2011). It has been proposed that, at least for the SARS-CoV, Nsp8 may in fact act as a primase in concert with nsp7 and be responsible for synthesizing the short oligo primers that are then utilized by Nsp12 for RNA synthesis (Imbert et al., 2006; te Velthuis et al., 2009; te Velthuis et al., 2012).

The helicase activity associated with the coronavirus replicase belongs to a 66 kDa protein known as Nsp13. This protein contains an N-terminal binuclear zinc finger structure linked to a C-terminal superfamily 1 helicase domain, unusual for positive-stranded RNA viruses but commonly seen in other nidoviruses (Gorbalenya et al., 1989; Heusipp et al., 1997; Van Dinton et al., 2000) and has been shown to, as a recombinant protein expressed via baculovirus in infected insect cells (Ivanov and Ziebuhr, 2004) and as a fusion protein expressed in *E. coli* (Ivanov et al., 2004), possess both RNA and DNA duplex 5' to 3' unwinding capabilities (Seybert et al., 2000). The directionality of this helicase has been proposed to be a result of the necessity of synthesizing multiple subgenomic coronavirus mRNAs from their templates, which have negative polarity. In addition to its helicase activity, the nsp13 of the human coronavirus, HCV-229E, has also

been shown to have nucleoside triphosphatase and RNA 5' triphosphatase activities (Heusipp et al., 1997; Ivanov and Ziebuhr, 2004).

The mature nsp14, an approximately 60 kDa protein, is cleaved from pp1ab by the CL3pro (Xu et al., 2001). Nsp14 contains within its N-terminal half a domain predicted to belong to an exonuclease family belonging to the DEDD superfamily of proteins (Snijder et al., 2003), and has been shown to be essential to RNA synthesis in MHV-A59 infected cells (Sawicki et al., 2005). The 3' to 5' exonuclease activity of nsp14 has previously been confirmed (Minskaia et al., 2006; Chen et al., 2007), and, interestingly, observations that the protein both shares considerable similarities with DNA polymerase-associated 3' to 5' exonuclease domains and prefers dsRNA substrates to ssRNA has led to the supposition that nsp14 may, in fact, act as a proofreading exonuclease during coronavirus RNA synthesis (Snijder et al., 203; Minskaia et al., 2006). Further evidence of this activity has also been reported by Denison et al. (2011), via genetic inactivation of the DEDD exonuclease active site, which resulted in viruses having 15- to 20-fold increases in mutation rates when compared with virus containing nsp14 with a functional DEDD site. If this postulate holds true, the discovery of an RNA virus encoding a proofreading enzyme will be a substantial one, as this type of enzymatic activity has never before been described for an RNA virus.

Yet another protein synthesized as the pp1ab precursor, the mature nsp15 is protealytically cleaved by the $C3L^{pro}$ into an approximately 38 kDa protein product (Xu et al., 2001) containing an NendoU (*N*idoviral *endo*nuclease specific for *U*) domain sharing considerable similarity to the *Xenopus laevis* U-specific endonuclease, XendoU, that has been implicated in small nucleolar RNA processing (Snijder et al., 2003).

Interestingly, this is another example of protein unique to viruses within the Nidovirus order, and is present not only in the coronaviruses, but also in the arteriviruses as well (Nedialkova et al., 2009). Like the *X. laevis* endonuclease (Laneve et a., 2003), nsp15 cleaves uridylate stretches in a Mn 2+ dependent manner to release 2'-3' cyclic phosphodiester products (Bhardwaj et al., 2004; Ivanov et al., 2004; Xu et al., 2006). Previous studies utilizing either site-directed mutagenesis or reverse genetic approaches have suggested that nsp15 plays a significant role in maximizing viral RNA synthesis, although, based on results of these studies, it does not appear to be essential for coronaviral replication (Ivanov et al., 2004; Posthuma et al., 2006; Ricagno et al., 2006; Kang et al., 2007). However, it is notable that induced mutations resulting in the inability of the protein to form hexameric structures, the only form of the protein that is catalytically active (Joseph et al., 2007), were lethal (Ivanov et al., 2004; Almazan et al., 2006), in turn suggesting that nsp15 may actually have an essential role in virus replication that has yet to be described.

Organization of the viral genome

The coronavirus genome consists of a single, nonsegmented RNA of positive polarity with an estimated molecular weight of 6×10^6 to 8×10^6 Da (Lomniczi and Kennedy, 1977; Lai and Stohlman, 1978) and averages on the order of 27 to 32 kb, the largest viral RNA genomes known (Lai, et al., 2001), a surprising fact given the high error rates associated with RNA-dependent RNA synthesis (Holland et al., 1982). The genome of coronaviruses is both 5' capped (Lai and Stohlman, 1981) and 3' polyadenylated (Yogo et al., 1977), and, in the manner of most RNA viruses, replicates within the cytoplasm of host cells (Masters, 2006). As a result of its positive polarity, the

naked RNA itself is infectious and can instigate infection upon transfection or entry into a permissive cell, as the genomic RNA itself serves as an initial template for translation of the viral RNA-dependent RNA polymerase and other viral proteins involved in the replication-transcription complex (Leibowitz et al., 1982; Siddell, 1983).

At least 10 ORFs have been identified in the genomic RNA of coronaviruses, some of which encode a single mRNA species, while others are polycistronic, containing multiple ORFs that may or may not overlap. The 5' UTR is comprised of approximately 200 to 500 nucleotides, the terminal 60 to 70 nucleotides of which make up the leader sequence that is transposed to the 5' end of each nested mRNA that is produced via discontinuous transcription (Lai et al., 1981; Lai et al., 1983; Spaan et al., 1983; Sawicki and Sawicki, 1990). Additionally, at each intergenic region is a small stretch of consensus sequence, termed an acceptor "hotspot", the donor sequence responsible for internal template switching (Zuniga et al., 2004; Sola et al., 2005). Comparison of multiple coronavirus genomes has revealed that the gene arrangement is surprisingly conserved, exceptions being the genes 3a and 3b and 5 for IBV, which do not have homologues in the group 1and 2 coronaviruses (Boursnell et al., 1985; Liu et al., 1991; Enjuanes et al., 2000), and TGEV, which possibly contains an additional gene at its 3' end (Kapke and Brian, 1986). In addition, many of the group 2 coronaviruses, including MHV and BCoV, contain two additional genes encoding the HE protein and a nonstructural protein, p30 (Zhang et al., 1992).

The coronavirus lifecycle

Host cell infection by the coronaviruses is initiated when a virion interacts with specific host cell receptors. This interaction is typically virus species-specific, with most

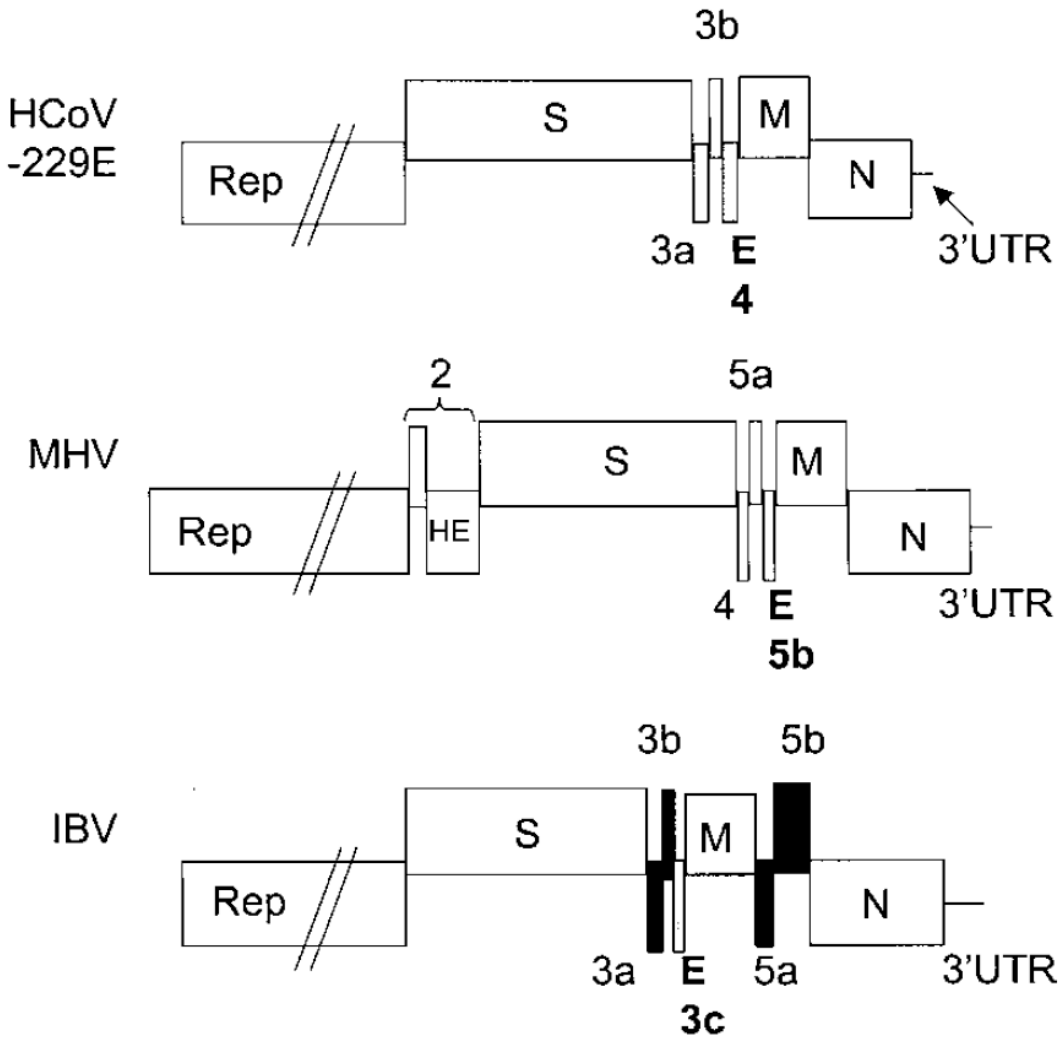

Figure 2.3. From Cavanagh et al., 2001. Comparison of Group 1, 2, and 3 coronavirus genome arrangements.

coronaviruses exhibiting a very particular and narrow host range, although, as previously discussed, there are exceptions to this rule, including BCoV (Zhang et al., 1994; Tsunemitsu et al., 1995; Erles et al., 2003; Saif, 2004) and, more recently, SARS-CoV (Holmes, 2005). In spite of this, the coronavirus S gp remains recognized as the primary, if not sole, determinant of host range and tissue tropism (Kuo et al., 2000), a phenomenon that has been demonstrated multiple times for multiple coronavirus species. For example, when a usually non-permissive cell line is made to express an identified host receptor

protein of a heterologous species, it has been shown that the cell line is then rendered permissive to the corresponding coronavirus (Delmas et al., 1992; Yeager et al., 1992; Tresnan et al., 1996; Li et al., 2003; 2004; Mossel et al., 2005). Additionally, construction of chimeric S proteins has been reported to alter host range *in vitro*. Specifically, transferring the ectodomain of the FIPV S gp to that of MHV rendered the new, chimeric virus specific to infection of normally FIPV, but not MHV, permissive cells Kuo et al., 2000). The reverse of this observation also holds true (Haijema et al., 2003). Likewise, replacement of the S gp ectodomain of MHV strain A59 with that of the highly neurotropic MHV-JHM strain rendered the otherwise hepatotropic A59 strain highly neurotropic (Philips et al., 1999).

The receptors for many group 1 and group 2 coronaviruses have been identified, including the first cellular receptor identified for any virus, that of the widely-studied MHV, the murine carcinoembryonic antigen cell adhesion molecule-1 (mCEACAM-1), a member of the carcinoembryonic family within the immunoglobulin superfamily (Williams et al., 1990; 1991; Compton et al., 1992). However, not all coronaviruses utilize the same cellular receptors for entry, as demonstrated by studies with a coronavirus infecting a very closely related species, rats. Rat coronavirus (RCoV) and Sialodacryoadenitis virus (SDAV) have both been studied for their ability to bind mCEACAM-1, as these viruses are capable of growing in some of the same cells lines as MHV. Interestingly, what researchers found when using a Mab against mCEACAM-1 capable of completely blocking infection by MHV was that infection by the rat coronaviruses was not hindered at all (Gagneten et al., 1996). This evidence of a completely separate cellular receptor for the rat coronaviruses was further supported

when BHK cells, which are non-permissive to MHV infection, were transfected with a plasmid for the expression of mCEACAM-1. While MHV was now able to infect the transfected BHK cells, the rat coronaviruses remained unable to infect this cell line (Gagneten et al., 1996). The S and HE glycoproteins of BCoV virus bind 9-*O*-acetyl sialic acid, as demonstrated by the potent ability of both glycoproteins to aggregate erythrocytes (Schultze et al., 1991), as well as by the ability to block BCoV infection of MDCK cells via pretreatment with neuraminidase or acetylesterase (Schultze and Herrler, 1992). However, there is a considerable amount of uncertainty as to whether or not the BCoV S gp has an additional, more specific, cellular receptor associated with its entry into host cells.

Interestingly, while SARS-CoV is considered to be a member of the group 2 coronaviruses, it is one of the most phylogenetically distant members of the group. Thus, it is perhaps not surprising that this virus utilizes receptors wholly unrelated to the CEACAMs. The SARS-CoV S gp recognizes as its cognate receptor the cellular metallopeptidase, angiotensin-converting enzyme-2 (ACE-2), a zinc-binding carboxypeptidase involved in the regulation of heart function. This receptor was identified as the SARS-CoV receptor via development of a SARS-CoV S1-IgG fusion protein, which was then used to immunoprecipitate cellular membrane proteins of Vero E6 cells, the cell type found to be most permissive to SARS-CoV infection. The binding of the SARS S1 fusion protein to Vero E6 cells was then found to be blocked by soluble ACE-2, but not by a closely related membrane protein, ACE-1 (Li et al., 2003), evidence yet further supported when cloned ACE-2 was expressed in cell lines otherwise non-permissive to SARS-CoV infection rendered the virus capable of producing syncytia

within the transfected cell line (Li et al., 2003; Mossel et al., 2005). Furthermore, studies into the neuronal involvement of SARS-CoV in human hosts with transgenic mice engineered to express hACE-2 showed that these mice, usually unaffected by SARS-CoV, were able to support SARS-CoV infection resulting in extensive neuronal cell death when inoculated intracranially with the virus, while non-transgenic mice did not succumb to lethal infection (Netland et al., 2008).

Finally, a discussion of CoV cellular receptors would be incomplete without a mention of the group 1 coronaviruses, many of which utilize the aminopeptidase N (APN) of their respective species to facilitate fusion (Delmas et al., 1992; Yeager et al., 1992; Tresnan et al., 1992). This protein is a membrane-bound cell surface, zinc-binding protease that participates in the proteolysis of small peptides within the respiratory and enteric epithelia. It is also located within some human neural tissues, rendering them susceptible to infection by the HCoV-229E (Lachance et al., 1998). Although it seems that a number of the group 1 coronaviruses utilize this receptor, interestingly, the receptor activities of APN homologues are generally not interchangeable across species, that is, the hAPN cannot serve as a receptor for TGEV and vice versa (Delmas et al., 1994). However, there is a curious exception to this generalization: fAPN has been shown to serve as a receptor not only for the very closely related FIPV type II, but also for canine coronavirus (CCoV), TGEV, and HCoV-229E (Tresnan et al., 1996). Furthering this curiosity is the observation that, while FIPV type II can utilize fAPN as a cellular receptor, FIPV type I seemingly cannot, since antibody to fAPN effectively blocks FIPV type II infection but not FIPV type I infection (Hohdatsu et al., 1998).

The interaction of the coronavirus S gp with its cognate cellular receptor leads then to either the pH-independent fusion of host and viral membranes (Gallagher et al., 1991; Nash and Buchmeier, 1997) or, in the case of virus lacking proper S fusion function, the uptake of virus into endocytic vesicles followed by pH-dependent uncoating of the virus (Qiu et al., 2006; Simmons et al., 2011); in both scenarios the end result of the pathways is the release of the viral nucleocapsid into the cytoplasm of the cell, where the positive sense viral genome is then available for translation by host cell ribosomes. As a class I fusion protein (Bosch et al., 2003), both virus-cell and cell-cell membrane fusion are facilitated by conformational changes of the fusion protein, in this case, the S gp, that trigger first the formation of intermediate conformations, followed by the final formation of the six-helix bundle conformation (Coleman and Lawrence, 2003; Earp et al., 2005). These conformational changes result in exposure of a hydrophobic fusion peptide, predicted to reside at the N-terminus of S2 (Sainz et al., 2005), which, when inserted into the host cell membrane, brings the two membranes into close apposition as a result of the overall changes in conformation, facilitating their fusion (Melikyan et al., 2000; Russell et al, 2001), events similar to those observed for other class I fusion peptides (Baker et al., 1999; Melikyan et al., 2000; Russell et al., 2001). The conformational changes are mediated, at least in part, by a region of the protein termed the juxtamembrane domain (JMD), an area located in the ectodomain between the previously discussed HR2 and the beginning of the transmembrane domain (Coleman and Lawrence, 2003). In addition, this JMD may also interact directly with host membranes and/or induce membrane destabilization (Guillen et al., 2005; Broer et al., 2006). In fact, several synthetic peptides derived from the SARS-CoV S gp JMD have previously been

shown to interact directly with synthetic lipid bilayers, resulting in destabilization of the liposomes, supporting the hypothesis that the JMD may interact directly with host membranes (Sainz et al., 2005; Guillen et al., 2005). Interestingly, the JMDs of other enveloped virus families, including the Lentiviruses, Filoviruses, Rhabdoviruses, Orthomyxoviruses, and Paramyxoviruses, have been shown to highly variable within family in regards to amino acid sequence; in contrast, this domain seems to be highly conserved across all three genre of Coronaviruses (Howard et al., 2008). In particular, the Coronavirus S gp JMDs contain six highly conserved aromatic amino acids that have been shown in SARS-CoV to be of critical importance to the membrane fusion activity leading both to virus-cell as well as cell-cell fusion (Howard et al., 2008). It is worth noting that, although fusion for many coronaviruses is mediated in a pH-independent manner, there are coronaviruses, primarily within group 1, that appear to rely solely on acidification within endosomal compartments for membrane fusion, including TGEV (Hansen et al., 1998) and HCoV-229E (Nomura et al., 2004). In addition, subtle changes in the amino acid residues of the S gp can also have a dramatic effect on the ability of the virus to enter host cells via membrane fusion; for instance, studies with MHV S gp have shown that changes in as few as 3 amino acids within one of the HRs within S2 were capable of rendering the virus unable to enter via membrane fusion, resulting in reliance of the virus on receptor-mediated uptake into endocytic vesicles in order to enter host cells (Gallagher et al., 1991; Nash and Buchmeier, 1997).

Following viral entry into the host cell, ORF1a and 1b are translated to produce the enormous polyproteins pp1a and pp1ab, which are co-translationally processed into the individual components of the replicase complex by one or more proteases situated *in*

syn within the developing polyprotein (Snijder, 2005). Following translation and processing, the viral replicase proteins assemble into membrane-bound replication-transcription complexes, accumulating at perinuclear regions within the cell and associating with double-membrane vesicles (DMV; Gosert et al., 2002; Brockway et al., 2003; Snijder et al., 2006). These DMVs are thought to be generated via cellular autophagy-related processes (Prentice et al., 2004) and may be derived from either late endosomal membranes (van der Meer et al., 1999) or the endoplasmic reticulum (Shi et al., 1999; Prentice et al., 2004). The assembled replication-transcription complexes then serve to synthesize the negative strand intermediates of both progeny genomes as well as a set of 3' coterminal nested subgenomic mRNAs, each of the latter possessing a 5' leader sequence derived from the 5' end of the genomic RNA template via a process of discontinuous transcription (Sawicki and Sawicki, 1995; 1998), joined to the main mRNA transcripts at regions termed transcription-regulation sequences (Zuniga et al., 2004; Sola et al., 2005). The template switch that occurs during the process of discontinuous transcription has been likened to the process of copy-choice recombination (Jarvis and Kirkegaard, 1991; Lai, 1992; Brian et al., 1997; Nagy and Simon, 1997), as it, too, occurs during RNA synthesis and typically requires the pairing of bases between the core donor and acceptor sites, the transcription-regulation sequences (Ozdarendeli et al., 2001; Alonso et al., 2002; Sola et al., 2005). This 5'-proximal genomic "acceptor hotspot" has been shown in BCoV to be a surprisingly large 65 nucleotides wide and may, in fact, actually be part of a larger yet-to-be-determined 5'-proximal multifunctional structure (Wu et al., 2006).

As translation of the viral mRNA progresses, resulting membrane-bound proteins are co-translationally inserted into the ER, from which they traverse the ER to the ER-Golgi intermediate compartment (*reviewed by* Spaan et al., 1988). Of all of the structural proteins, M was the first to be shown to play a central role in the coordination of the other structural proteins in virion assembly (Holmes et al., 1981; Rottier et al., 1981; Holmes et al., 1987), and it, too, travels the secretory pathway as far as the *trans*-golgi network (Swift and Machamer, 1991). In spite of its importance in directing virion assembly, M protein is insufficient for the assembly of viral particles, as expression of M proteins alone results in its accumulation in the *trans*-golgi compartment, from whence it is not transported to the plasma membrane (Rottier and Rose, 1987; Krijnse-Locker *et al.*, 1992). By contrast, MHV, IBV, TGEV, and FIPV have all been shown to bud into the proximal compartment, the ERGIC (Klumperman et al., 1994; Krijnse-Locker et al., 1994; Tooze et al., 1984, 1988). This was a curious observation until the role of E was better understood, as it plays the second critical part in directing virion assembly and is necessary and sufficient for the assembly of virus particles lacking both N and S proteins (Bos et al., 1996).

On the other hand, internal viral structural proteins, namely nucleocapsid protein, interact with the newly synthesized, positive strand progeny genomic RNAs, encapsidating the genomes and resulting in the assembly of the nucleocapsid (van der Most et al., 1991; Fosmire et al., 1992), which then coalesce with the membrane-bound viral components at the ERGIC (Anderson and Wong, 1993). As the nucleocapsids bud through into this compartment, they obtain a lipid envelope and intact virions are thus formed (Krijnse-Locker, 1994). In what is the last step of the infective lifecycle, progeny

virions are exported from infected cells by transport in smooth-walled vesicles, also known as Golgi sacs, to the plasma membrane, to be released into the extracellular environment. In some cases however, for those coronaviruses capable of mediating cell-cell fusion, a fraction of the processed S gp is not included in virion assembly, but eventually makes its way to the plasma membrane, where it facilitates fusion of adjacent cell membranes, resulting in the formation of large, multinucleate syncytia (Lontok et al., 2004). Curiously, a 2004 study of the IBV and other coronavirus S gps has shown that the group 1 and 3 coronavirus S gps contain within their cytoplasmic domains an intracellular retention signal, responsible for recovering S that has escaped from the ERGIC (Lontok et al., 2004). This recognition of this signal results in endocytosis of escaped S that has traversed to the plasma membrane, a finding that is in direct apposition to the idea that S gps expressed on the surface of host cells result in the formation of syncytia (Lontok et al., 2004). Conversely, the researchers report that S gps of the group 2 coronaviruses, including BCoV, lack this intracellular retention signal within their cytoplasmic domain, suggesting that these viruses may then be more adept at cellular syncytia formation, in turn allowing progeny virions to spread from cell to cell with minimal exposure to extracellular viral surveillance systems.

Recognition of viruses by the innate immune system

During the course of evolution, viral pathogens have successfully found a way to infect an incredibly diverse range of living organisms, and science has discovered viruses that infect species as simple as the single-celled amoeba to those that infect the most complex of mammalian hosts. In this context, living organisms have thus, too, evolved to protect themselves from these invading pathogens. Evolutionarily speaking, the innate

immune system is the oldest system for the detection of and protection against viral infection, and, as such, is the first line of defense against invading organisms, including viruses. This system consists of a network of germline-encoded “nonspecific” receptors called pattern recognition receptors (PRRs; Janeway, 1989) as well as phagocytes such as macrophages and dendritic cells responsible for engulfing invading organisms. These PRRs all share a few common characteristics: 1) PRRs recognize microbial components, pathogen-associated molecular patterns (PAMPs) that are typically highly conserved and essential to the lifecycle of that microbe within the host cell. This, in turn, makes it difficult for the microbes to alter these components in a effort to evade immune surveillance; 2) PRRs are germ-line encoded proteins constitutively expressed within the host and are expressed regardless of lifecycle stage; and lastly, 3) PRRs are non-clonal and expressed independent of immunologic memory. The PRRs vary with regard to the PAMPs that they detect, as not all PRRs interact with all PAMPs, and different PRRs activate different signaling pathways, giving what was originally thought to be a non-specific immune system a certain degree of specificity.

There are 3 classes of PRRs that have been described to date: the retinoic acid-inducible gene-I (RIG-I)-like receptors (RLRs), the Toll-like receptors (TLRs), and the nucleotide-binding oligomerization domain (NOD)-like receptors (NLRs). These receptors each have differing signaling pathways with varying downstream targets, although for most of those that detect viral PAMPs, the most common end result is the expression of genes encoding the type I interferons (IFN), IFN-α and -β, an essential step in the antiviral response (Medzhitov, 2007). These type I IFNs induce intracellular signaling pathways via a type-I IFN receptor, to which IFN-α and β bind, in turn

regulating the expression of the IFN-inducible genes. These genes encode antiviral products such as protein kinase R (PKR) and 2'5'-oligoadenylate synthase, responsible for eliminating viral components from infected cells, as well as eliminating infected cells themselves by inducing apoptosis. Furthermore, these products also act on uninfected cells to confer resistance to infection by viral pathogens. Additionally, expression of the very receptors responsible for inducing downstream IFN production are also, in turn, themselves induced by IFN, resulting in a positive feedback loop that creates a local cellular response (Stetson and Medzhitov, 2006). Interferon is also responsible in some ways for linking the innate and adaptive immune systems (Tough, 2005), as IFN acts to directly activate dendritic cells and natural killer cells (Theofilopoulos et al., 2006), as well as promotes the survival of T and B cells (Marrack et al., 1999; Braun et al., 2002). The NLRs, however, are slightly different in their antiviral mechanism, as these receptors are known to induce not IFN production, but instead regulate interleukin 1β (IL-1β) maturation (Kanneganti et al., 2007).

The RLRs are a class of PRRs responsible for the detection of cytosolic viruses and viral products. This family of membrane-bound receptors currently consists of three members: RIG-I (Yoneyama, et al., 2004) melanoma differentiation-associated factor 5 (MDA5; Kang et al., 2002) and laboratory of genetics and physiology-2 (LPG-2; Takeuchi et al., 2007). The RLRs RIG-I and MDA5 share considerable homology, as both contain a DExD/H box helicase domain capable of binding dsRNA and responsible for the binding of these RNAs (Kang et al., 2002; Yoneyama et al., 2004), and two N-terminal caspase recruitment (CARD) domains, which are responsible for initiating downstream signaling (Kovacsovics et al., 2002) via CARD-CARD interactions with

IFN-β promoter stimulator 1 (IPS-1) located on the outer mitochondrial membrane (Kawai et al., 2005; Xu et al., 2005; Kumar et al., 2006). In addition, both RIG-I and MDA5 also contain repressor domains within their C-terminus responsible for blocking signal transduction in the absence of bound ligand (Saito et al., 2007). The RLR LPG-2, on the other hand, contains the helicase domain, but lacks the CARD domains seen in its fellow RLR family members; thus, it is thought that LPG-2 may play a role as a negative regulator (Rothenfusser et al., 2005; Venkataraman et al., 2007).

Differences in ligand recognition by PRRs results in a certain amount of specificity for the recognition of specific viruses or virus families. Infection of cells with RNA viruses results in the production of viral products not typically found in the cytoplasm of uninfected cells. For instance, replication of RNA viral genomes, both ds and ss by RDRP within the cytoplasm results in long dsRNAs and RNAs containing 5' triphosphates; long dsRNAs are not normal constituents of the cytoplasm of healthy cells and most cytoplasmic RNAs of cellular origin are 5'-capped mRNAs. Thus, the immune system uses the discrimination of dsRNA versus ssRNA as a means by which to detect viral infection. RIG-I has been implicated in the preferential binding of ssRNAs containing homopolyuridine or homopolyriboadenine motifs (Saito et al., 2008; Kato et al., 2008; Saito et al., 2008) and phosphorylated at the 5' end (Hornung et al., 2006; Pichlmair et al., 2006), while MDA5 has been shown to recognize long dsRNAs that may or may not also have 5' phosphorylation (Gitlin et al., 2006; Kato et al., 2006, 2008). The recognition of viral products by these PRRs results in a downstream signaling cascade via the adaptor IPS-1 that eventually results in the production of type 1 IFN. In addition, the expression of proinflammatory genes is also activated by this pathway, as another

downstream target of RLR signaling is the nuclear transcription factor NF-κB (Takahashi et al., 2006).

In addition to the RLR family of PRRs, the TLRs are vital participants in antiviral surveillance and signaling by the innate immune system. These proteins are membrane-bound and contain luminal leucine-rich repeats responsible for detection of PAMPs, as well as a cytoplasmic domain designated the Toll/IL-1 receptor homology (TIR) domain, responsible for signaling through downstream adaptors (Akira et al., 2006). While RLRs are solely intracytoplasmic viral product detectors, the TLRs are capable of detecting viral components both outside of cells as well as within cytoplasmic vacuoles following phagocytosis or endocytosis (Iwasaki and Medzhitov, 2004). All TLRs, with the notable exception of TLR3, activate a common signaling pathway responsible for the production of both pro-inflammatory cytokines as well as type I IFN via the signaling adaptor protein myeloid differentiation factor 88 (MyD88; Medzhitov et al., 1998).

There are currently 10 members of the TLR family that have been identified in humans, and 13 that have been identified in mice, although not all of these receptors are involved in detection of viral components. Specifically, the TLRs 3, 7, 8, and 9 are localized on the luminal membranes of cytoplasmic vesicles such as endosomes and within the ER, and are involved in detection of various viral components within cellular endosomal compartments (Iwasaki et al., 2004). On the other hand, TLR2, which is known to detect a variety of bacterial lipoproteins as well as yeast-associated zymosan, and TLR4, traditionally known as a sensor of LPS, are situated on the extracellular surface of the plasma membrane and have been implicated in the detection of viral envelope proteins expressed on the outer plasma membrane of infected cells (Morrison,

2004; Zhang et al., 2007). The TLRs 3, 7, and 8 have been shown to be important in the detection of viruses containing genomic RNA: TLR3 recognizes dsRNA (Alexopoulou et al., 2001), while TLR7 and 8 are responsible for the detection of ssRNA and imidazolequinilone compounds (Diebold et al., 2004; Heil et al., 2004; Lund et al., 2004; Beignon et al., 2005). TLR9, on the other hand, is implicated in detection of DNA viruses, as it recognizes unmethylated CpG-containing DNA, a common component of DNA virus genomes (Bauer et al., 2001).

Linking the innate and adaptive immune systems

Although the innate immune system has and continues to serve as an effective method of surveillance for would-be pathogenic intruders, its lack of true specificity and, arguably more importantly, immunological memory, has necessitated the need for a more robust system for recognition of pathogens that have previously been encountered. This is especially true in the context of pathogenic microorganisms that provide an almost constant onslaught of attack, including the ubiquitous viral pathogens to which exposure occurs on virtually a daily basis. Thus, over the course of evolution, more highly evolved life forms, namely mammals and cartilaginous fishes, have evolved an immunological system capable of, in some cases, extreme specificity as well as memory, conveying the ability to very quickly recognize and respond to pathogenic organisms, especially those that have already been eliminated once by the immune system some time in the past (*reviewed by* Cooper and Alder, 2006).

Although it seems clear that this “adaptive immune system” evolved independently of the ancient innate immune system, the adaptive system relies heavily on instruction from the innate system for identification of invading microorganisms as well

as activation of adaptive responses (Janeway, 1989). One essential link between these two systems is the antigen presenting cell (APC), including macrophages and especially dendritic cells (DC), the professional APCs of the immune system (Banchereau and Steinman, 1998). The uniquely shaped DCs are responsible for "sampling" the extracellular milieu via receptor-mediated endocytosis, macropinocytosis, and even uptake of apoptotic cell bodies (Sallusto and Lanzavaecchia, 1994; Sallusto et al., 1995), actively differentiating self from non-self via a variety of PRRs (Fearon et al., 1996; Medzhitov and Janeway, 1997; Muzio et al., 1998).

First observed in 1868 as Langerhans cells present in the epidermis, DC make up a heterogeneous family of leukocytes capable of integrating innate information and effectively conveying it to lymphocytes of the adaptive immune system. These cells encompass multiple subsets, including Langerhans cells, interstitial DCs, and plasmacytoid DCs; it is thought that these subsets may have distinct biological functions within the immune system (Ibrahim et al., 1995; Fearon et al., 1996; Banchereau et al., 1998). For this reason, DC are commonly delineated by their stage of maturation: precursor DC patrol the blood and lymphatics, while immature DC reside in the tissues where they survey the interstitial spaces for both self and non-self peptide antigens. Finally, mature DC can be found within the lymphoid organs where they interact with B and T lymphocytes to direct the maturation of these cells (*reviewed by* Palucka and Banchereau, 1999). Tissue resident immature DC are exceptional at capturing antigen, which is then directed towards MHC class II-rich late endosomal compartments within the cell. Here antigen is loaded onto MHC class II molecules, which subsequently relocalize to the cell surface to be displayed for T cell receptor (TCR) recognition. These

cell surface complexes can remain stable for days, helping to ensure that CD4+ T cells bearing cognate TCRs will come into contact with the DC (Cella et al., 1997; Pierre et al., 1997; Pierre et al., 1998). While presentation of antigen to CD4+ T cells is vital to eventual development of a B cell-mediated antibody response, CD8+ cytotoxic T cells are also important in eliminating virus-infected cells. In order to "communicate" with CD8+ T cells, however, antigen must be presented by DCs in the context of MHC class I (Watts, 1997). This may occur via two potential routes: 1) the DC itself may be infected with the virus, in which case viral peptides may be processed in the DC proteosome and translocated to the ER, where they are loaded via TAP onto MHC class I molecules for presentation at the cell surface (Watts, 1997), or, conversely, 2) viral peptides may become available to the DC when they take up apoptotic cell bodies and process the resulting self and non-self peptides in a poorly-understood process commonly referred to as "cross-priming" (Bhardwaj et al., 1994; Albert et al., 1998; Ridge et al., 1998).

T lymphocyte priming and activation

One of the primary and essential functions of DCs is the priming and activation of T cells within lymphoid tissues. After the uptake of antigen, DCs undergo migration to the lymph nodes under the direction of homing signals, the receptors for which are upregulated in DCs that have taken up antigen (Tang et al., 1993; Roake et al., 1995; Sozzani et al., 1995; Rubbert et al., 1998; Dieu et al., 1998). While en route to the lymph nodes, DCs undergo further maturation from immature antigen-capture cells to cells fully capable of antigen presentation and activation of alloreactive T cells (*reviewed by* Bell et al., 1998). This maturation process includes the upregulation of a number of co-stimulatory molecules required for formation of an effective immunological synapse

between the DC and its alloreactive T cell, including adhesion molecules such as the β1 and 2 integrins, as well as several members of the immunoglobulin superfamily. In addition, several receptors, present only in low number on the surface of immature DCs, undergo intense upregulation. Amongst these are CD80/86 and CD40, a 50 kDa integral membrane protein and member of the TNF-receptor family (Stamenkovic et al., 1989) also present on the surface of macrophages (Alderson et al., 1993), and B cells (Stamenkovic et al., 1989), as well as on the surface of endothelial cells (Karmann et al., 1995), the thymic epithelium (Ruggerio et al., 1996), and fibroblasts (Yellin et al., 1995). These molecules act as the "second signal" following MHC class II-TCR interaction, signals required to avoid induction of T cell anergy following TCR recognition of peptide in the context of MHC class II (Caux et al., 1994; Fanslow et al., 1994; Inaba et al., 1994, 1995). The interaction of the B7 and CD40 co-stimulatory molecules found on mature DCs with CD28 and CD154, respectively, found on the surface of T cells, results in the activation of the T cell. This in turn induces the upregulation of these receptors on the surface of both cell types in a positive feedback loop, an important occurrence, as the strength of the immune response is dependent on the density and duration of the immunological synapse (Pinchuk et al., 1996). In fact, previous research has shown that a minimum of ten peptide-MHC interactions are required in order for an immunological synapse to form, and *in vivo* induction of T cell proliferation has been shown to require DCs with at least 2×10^4 peptide-MHC complexes (Henrickson et al., 2008). In addition to the activation of T cells that occurs when these cells interact with DCs presenting alloantigen, the DCs themselves also undergo further activation, primarily thorough signaling resulting from the interaction of CD40 on the surface of the DC with CD154 on

the surface of the T cell. The ligation of CD40 on the DC results in further upregulation in the expression of CD80, CD83, and CD86 on the surface of the DC, as well as in the production and release of cytokines, including IL-1, tumor necrosis factor (TNF), IL-12, and various chemokines. The upregulation of these genes results in DCs with even further improved ability to interact with, prime, and activate additional alloreactive T cells (Bell et al., 1998; Banchereau and Steinman, 1998).

B lymphocyte regulation and activation

Dendritic cells are indirectly responsible for influencing the activation of B cell effector functions by activating the CD4+ T cells responsible for providing the T cell help that eventually leads to B cell activation and class switching (Banchereau and Steinman, 1998). In fact, the activation and differentiation of both B *and* T cells is dependent on the cognate interaction of these two lymphocyte classes, with the specificity of the interaction determined via interaction of the TCR/CD3 complex on the surface of the T cell (Weissman et al., 1989; Cleavers et al., 1998) with peptide presented by B cells in the context of MHC class II (Allen, 1987). This is because B cells are capable of acting, in some capacity, as APCs, binding specific soluble antigen with high affinity via their B cell receptor (BCR), a membrane-bound Ig molecule, and taking it into the cell via either pinocytosis or BCR-mediated endocytosis. In fact, B cell antigen affinity has been shown to be directly related to the ability of the B cell to effectively present antigen to CD4+ T cells (Batista and Neuberger, 1998). However, much like the activation of naïve T cells by DC ligand binding, activation of B and T cells as a result of their interaction requires the involvement of additional co-receptors, although resting B cells circulating in the blood or localized within the lymph nodes do not express the co-stimulatory molecules

necessary to accomplish this. The activation required for B cell expression of co-stimulatory molecules is initiated by signaling as a result of two distinct events: binding by the BCR of cognate antigen and ligation of CD40 on the B cell surface by its cognate T cell receptor, CD154, expressed on the surface of activated T cells (*reviewed by* Rodriguez-Pinto, 2005). Unlike T cells, in which the ligation of co-stimulatory molecules acts primarily to regulate activation of the antigen receptor complex, the BCR and B cell co-stimulatory molecules serve, to a greater extent, to help maintain viability of the mature and activated B cell. Recognition and binding of antigen by the BCR results in extensive crosslinking of neighboring BCRs, required for the initiation of B cell activation. This crosslinking induces growth and proliferation of the B cell and ensures its survival; in addition, signals resulting from the crosslinking of numerous BCRs also result in the expression of a vital co-stimulatory molecule, CD86, important for naïve T cell activation (Lenschow et al., 1994; Nashar and Drake, 2005). The ligation of CD40 is vital for sustaining B cell activation as well as for promoting enhancement of B cell antigen processing (Faassen et al., 1995), upregulation of the expression of MHC class II molecules, increased expression of CD86, and induction of the expression of yet another co-stimulatory molecule, CD80 (Ranheim and Kipps, 1983; Kennedy et al., 1994; Roy et al., 1995; Wu et al., 1995; Mackey et al., 1998; Evans et al., 2000). Thus, although B cells are capable of antigen presentation, they require interaction with previously activated CD4+ T cells, both in order to engage in this role as well as to become activated themselves, further underlining the importance of DCs in the activation of T cells.

B lymphocyte and humoral immunity: Affinity maturation and class switching

Although mature B lymphocytes are capable of binding and presenting antigen, in the naïve state they are only capable of doing so with relatively low affinity, binding antigen with what is commonly termed “natural IgM”, the BCR (Jerne, 1955; Boyden, 1966). The specific humoral response that follows this initial recognition of cognate antigen is not immediate, requiring a number of days to develop. Furthermore, the Ig produced from this initial response is still not of high affinity, but activation of the B cell triggers the maturation of the antibody response from relatively low affinity Ig to that of a highly specific, high affinity Ig response, maturation that occurs within a somewhat brief period of B cell development. Generally late within the humoral response following the primary exposure to antigen, the production of antigen-specific antibodies has improved dramatically, with resulting Ig not only having marked higher affinity, but also being of a different class other than the IgM involved in the initial antibody response. This increase in antigen affinity is the result of a process known as “affinity maturation”, in which specific “hotspots” within the BCR undergo hypermutation, carried out by the enzyme activation-induced cytidine deaminase (AID; Muramatsu et al., 2000).Thus, as antigen become increasingly limiting, those clones expressing BCRs with higher affinity will have a selective advantage and preferentially be selected for survival and proliferation (*reviewed by* Wabl and Steinberg, 1996). In addition to the somatic hypermutation that results in the production of B cells capable of expressing Ig receptors having high affinity, a second set of molecular modifications occur that result in the production of soluble Ig versus the membrane-bound IgM responsible for the initial antigen recognition. In the process of class switching, the segments that make up the gene

encoding the Ig itself undergo rearrangement, such that the Ig heavy chain constant region (C_H) is rearranged for expression from other C_H regions such as C_γ, C_δ, C_ε, or C_α, instead of from the C_μ, which encodes IgM (*reviewed by* Zhang et al, 1995). This results in the production of soluble, highly specific antibody that can be targeted to specific sites or biologic functions within organism.

Development of immunological memory: Memory B cells and plasma cells

While the development of a robust primary antibody response marked by affinity maturation and class switching is vital to eventual clearance of infectious pathogens, as evidenced in individuals with hyper M syndrome (Levy et al., 1997), it is the establishment of immunological memory that sets the adaptive immune response apart as an effective and efficient protector from these would be invaders. While the initial antibody response is quite slow, requiring as many as 10 to 12 d post-exposure in most cases to develop, and composed primarily of IgM having a relatively low affinity for antigen, secondary exposure to antigen results in a response that is markedly quicker and exhibits the secretion of primarily IgG antibody with a considerably increased affinity for cognate antigen. This improvement in response time is explained in part by the clonal selection theory (Burnet, 1957), which simply states that an initial exposure to antigen leads to the clonal expansion of those B cells possessing a specific cognate BCR capable of recognizing said antigen. Thus, at the time of secondary of exposure, there are simply an increased number of circulating B cells possessing the same BCR and capable of now recognizing and binding antigen. That being said, clonal selection is insufficient to fully explain the quality of the secondary antibody response, a function of the affinity maturation discussed in the previous section. A strong memory response, then, is incurred

when B cell clones not only divide and expand in response to antigen, but when the mature with respect to both the affinity for antigen of the antibodies they produce as well as the type of antibody being secreted, thus resulting their maturation to and selection as memory B cells (*reviewed by* Neuberger et al., 2000, Gass et al., 2004). Interestingly, maturation to memory B cells results in cells that do not secrete antibody (McHeyzer-Williams and Ahmed, 1999), but that are surprisingly long-lived even in the absence of antigen (Maruyama et al., 2000) and capable of undergoing rapid and massive expansion in response to secondary exposure to antigen, in some cases generating an 8- to 10-fold increase in the population (McHeyzer-Williams and Ahmed, 1999).

There is, however, a second part to this phenomenon of immunological memory: the development of a circulating population of cells with the sole responsibility of producing significant levels of high-affinity secretory antibody. These cells are known as plasma cells, and are essentially B-cells that have terminally differentiated and exist in a post-mitotic state, as these end-stage cells do not divide. Although no plasma cells are produced following a primary antigen encounter, memory B cells in the bone marrow and spleen are biased to develop into plasma cells following a secondary encounter of antigen (Arpin et al., 1997). The lifespan of these cells can vary from only a few days to numerous months, a span of time that appears to be determined in some regard by their developmental history and the ability of the spleen to support them (Sze et al., 2000). Plasma cells are essentially cellular factories whose sole purpose is high-level secretion of soluble antibody. As such, these cells have high rates of transcription and translation, supported by significantly increased cytoplasmic to nuclear ratio and a pronounced increase in the amount of ER and secretory vesicles (*reviewed by* Gass et al., 2004).

Following the secondary antigen stimulation resulting in their differentiation, plasma cells, especially those that home to the bone marrow, are capable of secreting antibody for many months, resulting in the levels of circulating antibody that may persist long after the secondary exposure event. Interestingly however, these cells do not respond to further antigenic stimulation (Slifka, 1998).

CD154 as an immunomodulator in vaccination

As discussed previously, the role of the CD40-CD154 interaction in development of the adaptive immune response has been clearly established. Present primarily on the surface of activated CD4+ T cells (Roy et al., 1993), but also found on the surface of CD8+ T cells (Hermann et al., 1995; Sad et al., 1997), eosinophils (Gauchatet al., 1995), mast cells (Gauchat et al., 1993), and natural killer (NK) cells (Carbone et al., 1997), CD154 is a 39 kDa type II integral membrane protein and a member of the TNF superfamily (*reviewed by* Grewal and Flavell, 1998; van Kooten and Banchereau, 2000). CD154 ligation with CD40 on DCs results in production of signals required for the activation and survival of both DC and T cells (Banchereau et al., 1998), while ligation of CD154 with CD40 on the surface of B cells influences the maturation of B cells, inducing the secretion of various cytokines as well as the process of class switching (Burden et al., 1996), processes vital to the induction of a robust humoral immune response. The use of CD154 as an immunomodulator, or adjuvant, in vaccine therapy has its roots in the observation that antigens linked to or administered in conjunction with molecules targeting them to APCs generally increases the response of the immune system versus administration of the antigen alone (Chaplin et al., 1999; Deliyannis et al., 2000). Examples include the use of CTLA-4 and L-selectin (Drew et al., 2001), as well as

plasmids expressing cytokines such as IL-18 (Reddy et al., 2010). The development of methods for production and expression of recombinant fusion proteins and cDNA vaccines for the expression of these proteins has paved the way for the use of CD154 fusion to a plethora of antigens as potential vaccines. The idea is that CD154 fused to the expressed recombinant protein will target the relatively small quantities of expressed antigen specifically to APCs within the tissues in which they are expressed, resulting in significantly more efficient antigen uptake and presentation, in turn eliciting a faster and potentially more robust immune response (Manoj et al., 2004). Although there have been some reports that this method for immunomodualtion is ineffective (Manoj et al., 2004; Maue et al., 2004), Zhang and colleagues reported that incorporation of human CD154 into simian immunodeficiency virus (SIV)-human immunodeficiency virus (HIV) chimeric (SHIV) virus-like particles (VLP) enhanced SHIV-VLP induced dendritic cell activation, effectively boosting immune responses against HIV (2010). Likewise, Manoj and colleagues reported that fusion of the gene encoding bovine CD154 to that encoding a truncated version of BHV-1 gD and inserted into a plasmid for use as a cDNA vaccine effectively targeted the expressed fusion protein to APCs, eliciting a significantly enhanced antibody response versus animals vaccinated with a cDNA plasmid expressing only the truncated portion of BHV-1 gD (2003). In another set of studies in the design of a vaccines for use in domestic waterfowl, immunotargeting via the duck homologue of CD154 effectively enhanced humoral immune responses to both duck hepatitis V core antigen in pekin ducks (Gares et al., 2006) as well as a cDNA vaccine against avian influenza virus using the HA subtype H5 protein (Yao et al., 2010), providing evidence that the use of CD154 as an immunomodulator is not limited to use only in mammalian

species, but may be extended to application within a wide range of species for which the gene encoding CD154 has been identified.

References

Abraham, R., Minor, P., Dunn, G., Modlin, J. F. & Ogra, P. L. 1993. Shedding of virulent poliovirus revertants during immunization with oral poliovirus vaccine after prior immunization with inactivated polio vaccine. *J. Infect. Dis.,* 168, 1105-1109.

Aiyar, A., Xiang, Y. & Leis, J. 1996a. Site-directed mutagenesis using overlap extension PCR. *Methods Mol. Biol.,* 57, 177-191.

Aiyar, A., Xiang, Y. & Leis, J. 1996b. Site-directed mutagenesis using overlap extension PCR. *Methods Mol. Biol.,* 57, 177-91.

Akira, S., Uematsu, S. & Takeuchi, O. 2006. Pathogen recogntion and innate immunity. *Cell,* 124, 783-801.

Alderson, M. R., Armitage, R. J., Tough, T. W., Strockbine, L., Fanslow, W. C. & Spriggs, M. K. 1993. CD40 expression by human monocytes: regulation by cytokines and activation of monocytes by the ligand for CD40. *J. Exp. Med.,* 178, 669-674.

Alexopoulou, L., Holt, A. C., Medzhitov, R. & Flavell, R. A. 2001. Recognition of double-stranded RNA and activation of NF-kappaB by Toll-like receptor 3. *Nature,* 413, 732-738.

Allen, J. W., Viel, L., Bateman, K. G., Rosendal, S., Shewen, P. E. & Physick-Sheard, P. 1991. The microbial flora of the respiratory tract in feedlot calves: associations between nasopharyngeal and bronchoalveolar lavage cultures. *Can. J. Vet. Res.,* 55, 341-346.

Allen, P. M. 1987. Antigen processing at the molecular level. *Immunol. Today,* 8, 270.

Álvarez, E., DeDiego, M. L., Nieto-Torres, J. L., Jiménez-Guardeño, J. M., Marcos-Villar, L. & Enjuanes, L. 2010. The envelope protein of severe acute respiratory syndrome coronavirus interacts with the non-structural protein 3 and is ubiquitinated. *Virology,* 402, 281-291.

Anderson, R. & Wong, F. 1993. Membrane and phospholipid binding by murine coronavirla nucleocapsid N protein. *Virology,* 194, 224-232.

Arbely, E., Khattari, Z., Brotons, G., Akkawi, M., Salditt, T. & Arkin, I. T. 2004. A highly unusual palindromic transmembrane helical hairpin formed by SARS coronavirus E protein. *J. Mol. Biol.,* 341, 769-779.

Armstrong, J., Niemann, H., Smeekens, S., Rottier, P. J. & Warren, G. 1984. Sequence and topology of a model intracellular membrane protein, E1 glycoprotein, from a coronavirus. *Nature (London),* 308, 751-752.

B. Sainz, J., Rausch, J. M., Gallaher, W. R., Garry, R. F. & Wimley, W. C. 2005. The aromatic domain of the coronavirus class I viral fusion protein induces membrane permeabilization: putative role during viral entry. *Biochemistry,* 44, 947-958.

Baker, J. C. a. F., M.L. 1985. Bovine respiratory syncytial virus. In: Breeze, R. (ed.) *The Veterinary Clinic of North America -- Food Animal Practice.*

Baker, K. A., Dutch, R. E., Lamb, R. A. & Jardetzky, T. S. 1999. Structural basis for paramyxovirus-mediated membrane fusion. *Mol. Cell,* 3, 309-319.

Banchereau, J. & Steinman, R. M. 1998. Dendritic cells and control of immunity. *Nature,* 392, 245-252.

Baric, R. S., Nelson, G. W., Fleming, J. O., Deans, R. J., Keck, J. G., Casteel, N. & Stohlman, S. A. 1988. Interactions between coronavirus nucleocapsid protein and viral RNAs: Implications for viral of the head of transcription. *J. Virol.,* 62, 4280-4287.

Baric, R. S., Stohlman, S. A. & Lai, M. M. 1983. Characterization of replicative intermediate RNA of mouse hepatitis virus: presence of leader RNA sequences on nascent chains. *J. Virol.,* 48, 633-640.

Baric, R. S., Stohlman, S. A., Razavi, M. K. & Lai, M. M. 1985. Characterization of leader-related small RNAs in coronavirusinfected cells: further evidence for leader-primed mechanism of transcription. *Virus Res.,* 3.

Baric, R. S. & Yount, B. 2000. Subgenomic negative-strand RNA function during mouse hepatitis virus infection. *J. Virol.,* 74, 4039-4046.

Batista, F. D. & Neuberger, M. S. 1998. Affinity dependence of the B cell response to antigen: a threshold, a ceiling, and the importance of off-rate. *Immunity,* 8, 751-759.

Baudoux, P., Carrat, C., Besnardeau, L., Charley, B. & Laude., H. 1998. Coronavirus pseudoparticles formed with recombinant M and E proteins induce alpha interferon synthesis by leukocytes. *J. Virol.,* 72, 8636-8643.

Beignon, A. S., McKenna, K., Skoberne, M., Manches, O., DaSilva, I., Kavanagh, D. G., Larsson, M., Gorelick, R. J., Lifson, J. D. & Bhardwaj, N. 2005. Endocytosis of HIV-1 activates plasmacytoid dendritic cells via Toll-like receptor– viral RNA interactions. *J. Clin. Invest.,* 115, 3265-3275.

Benfield, D. A. & Saif, L. J. 1990. Cell Culture Propagation of a Coronavirus Isolated from Cows with Winter Dysentery. *J. Clin. Microbio.,* 28, 1454-1457.

Beutler, B., Jiang, Z., Georgel, P., Crozat, K., Croker, B., Rutschmann, S., Du, X. & Hoebe, K. 2006. Genetic analysis of host resistance: Toll-like receptor signaling and immunity at large. *Annu. Rev. Immunol.,* 24, 353-389.

Boileau, M. J. & Kapil, S. 2010. Bovine coronavirus associated syndromes. *Vet Clin Food Anim,* 26, 123-146.

Bos, E. C. W., LUYTJES, W., MEULEN, H. V. D., KOERTEN, H. K. & SPAAN, W. J. M. 1996. The Production of Recombinant Infectious DI-Particles of a Murine Coronavirus in the Absence of Helper Virus. *Virology,* 218, 52-60.

Boscarino, J. A., Logan, H. L., Lacny, J. J. & Gallagher, T. M. 2008. Envelope Protein Palmitoylations Are Crucial for Murine Coronavirus Assembly. *J. Virol.,* 82, 2989-2999.

Bosch, B. J., Zee, R. v. d., Haan, C. A. M. d. & Rottier, P. J. M. 2003. The coronavirus spike protein is a class I virus fusion protein: Structural and functional characterization of the fusion core complex. *J. Virol.,* 77, 8801-8811.

Boursnell, M. E. G., Binns, M. N. & Brown, T. D. K. 1985. Sequences of th nucleocapsid genes from two strains of avian infectious bronchitis virus. *J. Gen. Virol.,* 66, 573-580.

Boyle, J. S., Brady, J. L. & Lew, A. M. 1998. Enhanced responses to a DNA vaccine encoding a fusion antigen that is directed to sites of immune induction. *Nature,* 392, 408-411.

Brakel, W. J. & Leis, R. A. 1976. Impact of social disorganization on behavior, milk yield, and body weight of dairy cows. *Journal of Dairy Science,* 59, 716-721.

Braun, D., Caramalho, I. & Demengeot, J. 2002. IFN-alpha/beta enhances BCR-dependent B cell responses. *Int. Immunol.,* 14, 411-419.

Brayton, P. R., M. M. C. Lai, D. F. Patton, D. F. & Stohlman, S. A. 1982. Characterization of two RNA polymerase activities induced by mouse hepatitis virus. *J. Virol.,* 42, 847-853.

Brennan, R. E., Corstvet, R. E. & Paulsen, D. B. 1998. Antibody responses to Pasterella haemolytica 1:A and three of its outer embrane proteins in serum, nasal secretions, and bronchoalveolar lavage fluid from calves. *Am. J. Vet. Res.,* 59, 727-732.

Broer, R., Boson, B., Spaan, W., Cosset, F. L. & Corver, J. 2006. Important role for the transmembrane domain of sever acute respiratory syndrome coronavirus spike protein during entry. *J. Virol.,* 80, 1302-1310.

Buchmeier, M. J., Lewicki, H. A., Talbot, P. J. & Knobler, R. L. 1984. Murine hepatitis virus-4 (strain JHM)-induced neurologic disease is modulated in vivo by monoclonal antibody. *Virology,* 132, 261-270.

Callan, R. J. & Garry, F. B. 2002. Biosecurity and bovine respiratory disease. *Vet. Clin. North Am. Food Anim. Pract.,* 18, 57-77.

Calvo, E., Escors, D., López, J. A., González, J. M., Álvarez, A., Arza, E. & Enjuanes, L. 2005. Phosphorylation and subcellular localization of transmissible gastroenteritis virus nucleocapsid protein in infected cells. *J. Gen. Virol.,* 86, 2255-2267.

Carbone, E., Ruggiero, G., Terrazzano, G., Palomba, C., Manzo, C., Fontana, S., Spits, H., Kärre, K. & Zappacosta, S. 1997. A new mechanism of NK cell cytotoxicity activation: the CD40-CD40 ligand interaction. *J. Exp. Med.,* 185, 2053-2060.

Carman, P. S. & Hazlett, M. J. 1992. Bovine coronavirus infection in Ontario, 1990-1991. *Can Vet J,* 33, 812-814.

Caul, E. O. & Egglestone, S. I. 1977. Further studies on human enteric coronaviruses. *Arch Virol,* 54, 107.

Cavanagh, D., Brian, D. A., Brinton, M. A., Enjuanes, L., Holmes, K. V., Horzinek, M. C., Lai, M. M., Laude, H., Plagemann, P. G. W., Siddell, S. G., Spaan, W., Taguchi, F. & Talbot, P. J. 1995. Coronaviridae. In: Murphy, F. A., Fauquet, C. M., Bishop, D. H. L., Ghabrial, S. A., Jarvis, A. W., Martelli, G. P., Mayo, M. A. & Summers, M. D. (eds.) *"Virus Taxonomy. Sixth Report of the International Committee on Taxonomy of viruses".* Springer-Verlag, Vienna and New York.

Cavanagh, D., Brian, D. A., Brinton, M. A., Enjuanes, L., Holmes, K. V., Horzinek, M. C., Lai, M. M. C., Laude, H., Plagemann, P. G. W., Siddell, S. G., Spaan, W., Taguchi, F. & Talbot, P. J. 1994. Revision of the taxonomy of the Coronavirus,Torovirus and Arterivirus genera. *Arch. Virol.,* 135, 227-237.

Cavanagh, D. & Davis, P. J. 1988. Evolution of avian coronavirus IBV: sequence of the matrix glycoprotein gene and intergenic region of several serotypes. *J. Gen. Virol.,* 69, 621-629.

Cavanagh, D., Davis, P. J., Darbyshire, J. H. & Peters, R. W. 1986. Coronavirus IBV: Virus Retaining Spike Glycopolypeptide S2 but Not S1 Is Unable to Induce Virus-neutralizing or Haemagglutination-inhibiting Antibody, or Induce Chicken Tracheal Protection. *J. Gen. Virol.,* 67, 1435-1442.

Cavanagh, D., Mawditt, K., Sharma, M., Drury, S. E., Ainsworth, H. L., Britton, P. & Gough, R. E. 2001. Detection of a coronavirus from turkey poults in Europe genetically related to infectious bronchitis virus of chickens. *Avian Path.*, 30, 355-368.

Chandra, R. K. 1997. Nutrition and the immune system: an introduction. *Am J Clin Nutr,* 66, 460S-463S.

Chang, K. W., Sheng, Y.-W. & Gombold, J. L. 2000. Coronavirus-induced membrane fusion requires the cyctine-rich domain in the spike protein. *Virology,* 269, 212-224.

Chen, H., Gill, A., Dove, B. K., Emmett, S. R., Kemp, C. F., Ritchie, M. A., Dee, M. & Hiscox, J. A. 2005. Mass Spectroscopic Characterization of the Coronavirus Infectious Bronchitis Virus Nucleoprotein and Elucidation of the Role of Phosphorylation in RNA Binding by Using Surface Plasmon Resonance. *J. Virol.*, 79, 1164-1179.

Chirase, N. K., Greene, W., Purdy, C. W., Loan, R. W., Auvermann, B. W., Parke, D. B., Walborg, E. F., Stevenson, D. E., Xu, Y. & JE, J. E. K. 2004. Effect of transport stress on respiratory disease, serum antioxidant status, and serum concentrations of lipid peroxidation biomarkers in beef cattle. *Am. J. Vet. Res.*, 65, 860-864.

Cho, K.-O., Halbur, P. G., Bruna, J. D., Sorden, S. D., Yoon, K.-J., Janke, B. H., Chang, K.-O. & L, J. S. 2000. Detection and isolation of coronavirus from feces of three herds of feedlot cattle during outbreaks of winter dysentery-like disease. *JAVMA*, 217, 1191-1194.

Cho, K. O., Hoet, A., Loerch, S. C., Wittum, T. E. & Saif, L. J. 2001. Evaluation of concurrent shedding of bovine coronavirus via the respiratory tract and enteric route in feedlot cattle. *Am J Vet Res,* 62, 1436-1441.

Chouljenko, V. N., Lin, X. Q., Storz, J., Kousoulas, K. G. & Gorbalenya, A. E. 2001. Comparison of genomic and predicted amino acid sequences of respiratory and enteric coronaviruses isolated from the same animal with fatal shipping pneumonia. *Journal of General Virology,* 82, 2927-2933.

Clark, M. A. 1993. Bovine coronavirus. *Br Vet J,* 149, 51-70.

Clevers, H., Alarcon, B., Wileman, T. & Terhorst, C. 1988. TheTcell receptor/CD3 complex: a dynamic protein ensemble. *Ann. Rev. Immunol.,* 6, 629.

Cole, N. A., Phillips, W. A. & Hutcheson, D. P. 1986. The effect of pre-fast diet and transport on nitrogen metabolism in calves. *Journal of Animal Science,* 62, 1719-1731.

Collins, A. R., Knobler, R. L., Powell, H. & Buchmeier, M. J. 1982. Monoclonal antibodies to murein hepatitis virus-4 strain (strain JHM) define the viral glycoprotein responsib'e for attachment and cell-cell fusion. *Virology,* 119, 358-371.

Colman, P. M. & Lawrence, M. C. 2003. The structural biology of type I viral membrane fusion. *Nat. Rev. Mol. Cell Biol.,* 4, 309-319.

Cologna, R., Spagnolo, J. F. & Hogue, B. G. 2000. Identification of nucleocapsid binding sites within coronavirus-defective genomes. *Virology*, 227, 235-249.

Compton, S. R., Rogers, D. B., Holmes, K. V., Fertsch, D., Reminick, J. & McGOWAN, J. J. 1987. In vitro replication of mouse hepatitis virus strain A59. *J. Virol.,* 61, 1814-1820.

Compton, S. R., Stephensen, C. B., Snyder, S. W., Weismiller, D. G. & Holmes, K. V. 1992. Coronavirus species specificity: murine coronavirus binds to a mouse-specific epitope on its carcinoembryonic antigen-related receptor glycoprotein. *J. Virol.,* 66, 7420-7428.

Corse, E. & Machamer, C. E. 2000. Infectious bronchitis virus E protein is targeted to the Golgi complex and directs release of virus-like particles. *J. Virol.,* 74, 4319-4326.

Corse, E. & Machamer, C. E. 2002. The cytoplasmic tail of infectious bronchitis virus E protein directs Golgi targeting. *J. Virol.,* 76, 1273-1284.

Cusack, P. M. V., McMeniman, N. & Lean, I. J. 2003. The medicine and epidemiology of bovine respiratory diseases in feedlots. *Australian Veterinary Journal,* 81, 480-487.

Dea, S. & Tijssen, P. 1988. Identification of the structural proteins of turkey enteric coronavirus. *Arch. Virol.,* 99, 173-186.

Decaro, N., Mari, V., Campolo, M., Lorusso, A., Camero, M., Elia, G., Martella, V., Cordioli, P., Enjuanes, L. & Buonavoglia, C. 2009. Recombinant Canine Coronaviruses Related to Transmissible Gastroenteritis Virus of Swine Are Circulating in Dogs. *J. Virol.,* 83, 1532-1537.

DeDiego, M. L., Álvarez, E., Almazán, F., Rejas, M. T., Lamirande, E., Roberts, A., Shieh, W.-J., Zaki, S. R., Subbarao, K. & Enjuanes, L. 2007. A Severe Acute Respiratory Syndrome Coronavirus That Lacks the E Gene Is Attenuated In Vitro and In Vivo▽. *J. Virol.,* 81, 1701-1713.

deGroot, R. J., Luytjes, W., Horzinek, M. C., Zeijst, B. A. v. d., Spaan, W. J. & Lenstra, J. A. 1987a. Evidence for a coiled-coil structure in the spike proteins of coronaviruses. *J. Mol. Biol.,* 196, 963-966.

deGroot, R. J., Maduro, J., Lenstra, J. A., Horzinek, M. C., Zeiijst, B. A. M. v. d. & Spaan, W. J. M. 1987b. cDNA cloning and sequence analysis of the gene encoding the peplomer protein of feline infectious peritonitis virus. *J. Gen. Virol.,* 68, 2639-2646.

deHaan, C. A., H, V. & Rottier, P. J. 2000. Assembly of the coronavirus envelope: Homotypic interactions between the M proteins. *J. Virol.,* 74, 4967–4978.

deHaan, C. A., Kuo, L., Masters, P. S., Vennema, H. & Rottier, P. J. 1998. Coronavirus particle assembly: Primary structure requirements of the membrane protein. *J. Virol.,* 72, 6838-6850.

deHaan, C. A. & Rottier, P. J. 2005. Molecular interactions in the assembly of coronaviruses. *Adv. Virus Res.,* 64, 165-230.

deHaan, C. A., Smeets, M., Vernooij, F., Vennema, H. & Rottier, P. J. 1999. Mapping of the coronavirus membrane protein domains involved in interaction with the spike protein. *J. Virol.,* 73.

Deliyannis, G., Boyle, J. S., Brady, J. L., Brown, L. E. & Lew, A. M. 2000. A fusion DNA vaccine that targets antigen-presenting cells increases protection from viral challenge. *Proc. Natl. Acad. Sci. USA,* 97, 6676-6680.

Delmas, B. & Laude, H. 1990. Assembly of coronavirus spike protein into trimers and its role in epitope expression. *J. Virol.,* 64, 5367-5375.

Denison, M. R., Graham, R. L., Donaldson, E. F., Eckerle, L. D. & Baric, R. S. 2011. An RNA proofreading machine regulates replication fidelity and diversity. *RNA Biol.,* 8, 270-279.

Dennis, D. E. & Brian, D. A. 1982. RNA-dependent RNA polymerase activity in coronavirus-infected cells. *J. Virol.,* 42, 153-164.

Deregt, D. & Babiuk, L. A. 1987. Monoclonal antibodies to bovine coronavirus: characteristics and topographical mapping of neutralizing epitopes on the E2 and E3 glycoproteins. *Virology,* 161, 410-420.

Deregt, D., Gifford, G. A., Ijaz, M. K., Watts, T. C., Gilchrist, J. E., Haines, D. M. & Babiuk, L. A. 1989. Monoclonal Antibodies to Bovine Coronavirus Glycoproteins E2 and E3: Demonstration of in vivo Virus-neutralizing Activity. *Journal of General Virology,* 70, 993-998.

Diebold, S. S., Kaisho, T., Hemmi, H., Akira, S. & Sousa, C. R. e. 2004. Innate antiviral responses by means of TLR7-mediated recognition of single-stranded RNA. *Science,* 303, 1529-1531.

Donkersgoed, J. V. 1992. Meta-analysis of field trials of antimicrobial mass medication for prophylaxis of bovine respiratory disease in feedlot cattle. *Canadian Veterinary Journal,* 33, 786-795.

Draper, H. H., Dhanakoti, S. N., Hadley, M. & Piche, L. A. 1988. Malondialdehyde in biological systems. In: Chow, C. K. (ed.) *Cellular Antioxidant Defense Mechanisms.* CRC Press, Florida.

Duarte, E. A., Novella, I. S., Weaver, S. C., Domingo, E., Wain-Hobson, S., Clarke, D. K., Moya, A., Elena, S. F., Torre, J. C. d. l. & Holland, J. J. 1994. RNA virus quasispecies: significance for viral disease and epidemiology. *Infect. Agents Dis.,* 3, 201-214.

Earp, L. J., Delos, S. E., Park, H. E. & White, J. M. 2005. The many mechanisms of viral membrane fusion proteins. *Curr. Top. Microbiol. Immunol.,* 285, 25-66.

Eaton, D., Rodriguez, H. & Vehar, G. A. 1986. Proteolytic processing of human factor VIII. Correlation of specific cleavages by thrombin, factor Xa, and activated protein C with activation and inactivation of factor VIII coagulant activity. *Biochemistry,* 25, 505-512.

Eickmann, M., Becker, S., Klenk, H.-D., Doerr, H. W., Stadler, K., Censini, S., Guidotti, S., Masignani, V., Scarselli, M., Mora, M., Donati, C., Han, J. H., Song, H. C., Abrignani, S., Covacci, A. & Rappuoli, R. 2003. Phylogeny of the SARS coronavirus. *Science,* 302, 1504-1505.

Enjuanes, L., Almaz´an, F., Sola, I. & niga, S. Z. 2006. Biochemical Aspects of Coronavirus Replication and Virus-Host Interaction. *Annu. Rev. Microbiol.*, 211-230.

Erles, K., Toomeya, C., Brooksa, H. W. & Brownlie, J. 2003. Detection of a group 2 coronavirus in dogs with canine infectious respiratory disease. *Virology*, 310, 216-223.

Escors, D., Camafeita, E., Ortego, J., Laude, H. & Enjuanes, L. 2001. The membraneMprotein carboxy terminus binds to transmissible gastroenteritis coronavirus core and contributes to core stability. *J. Virol.,* 75, 1312–1324.

Evans, D. E., Munks, M. W., Purkerson, J. M. & Parker, D. C. 2000. Resting B lymphocytes as APC for naive T lymphocytes: dependence on CD40 ligand/CD40. *J. Immunol.,* 164, 688-697.

Faassen, A. E., Dalke, D. P., Berton, M. T., Warren, W. D. & Pierce, S. K. 1995. CD40-CD40 ligand interactions stimulate B cell antigen processing. *Eur. J. Immunol.,* 25, 3249-3255.

Fang, X., Ye, L., Timani, K. A., Li, S., Zen, Y., Zhao, M., Zheng, H. & Wu, Z. 2005. Peptide domain involved in the interaction between membrane protein and nucleocapsid protein of SARS-associated coronavirus. *J. Biochem. Mol. Biol.*, 38, 381–385.

Fanslow, W. C., Clifford, K. N., Seaman, M., Alderson, M. R., Spriggs, M. K., Armitage, R. J. & Ramsdell, F. 1994. Recombinant CD40 ligand exerts potent biologic effects on T cells. *J. Immunol.*, 152, 4262-4269.

Filion, L. G., Willson, P. J., Bielefeldt-Ohmann, H., Babiuk, L. A. & Thomson, R. G. 1984. The possible role of stress in the induction of pneumonic pasteurellosis. *Can J Comp Med*, 48, 268-274.

Finlay, B. B. & Hancock, R. E. 2004. Can innate immunity be enhanced to treat microbial infections? *Nat. Rev. Microbiol*, 2, 497-504.

Fischer, F., Stegen, C. F., Masters, P. S. & Samsonoff, W. A. 1998. Analysis of constructed E gene mutants of mouse hepatitis virus confirms a pivotal role for E protein in coronavirus assembly. *J. Virol.*, 72, 7885-7894.

Fosmire, J. A., Hwang, K. & Makino, S. 1992. Identification and characterization of a coronavirus packaging signal. *J. Virol.*, 66, 6522-3530.

Frana, M. F., Behnke, J. N., Sturman, L. S. & Holmes, K. V. 1985. Proteolytic cleavage of the E2 glycoprotein of murine coronavirus: host-dependent differences in proteiolytic clevage and cell fusion. *J. Virol.*, 56, 912-920.

Gagneten, S., Gout, O., Dubois-Dalcq, M., Rottier, P. J. M., Rossen, & J. W. A. & Holmes, K. V. 1995. Interaction of mouse hepatitis virus (MHV) spike glycoprotein with receptor glycoprotein MHVR is required for infection with an MHV strain that expresses the hemagglutininesterase glycoprotein. *J. Virol.*, 69, 889-895.

Gallagher, T. M., Escarmis, C. & Buchmeier, M. J. 1991. Alteration of the pH-dependence of coronavirus-induced cell fusion: Effect of mutations in the spike glycoprotein. *J. Virol.*, 65, 1916-1928.

Gallagher, T. M., Parker, S. E. & Buchmeier, M. J. 1990. Neutralization-resistant variants of a neurotropic coronavirus are generated by deletions within the amino-terminal half of the spike glycoprotein. *J. Virol.*, 64, 731-741.

Gares, S. L., Fischer, K. P., Congly, S. E., Lacoste, S., Addision, W. R., Tyrrell, D. L. & Gutfreund, K. S. 2006. Immunotargeting with CD154 (CD40 Ligand) Enhances DNA Vaccine Responses in Ducks. *Clin. Vaccine Immunol.*, 13, 958-965.

Gauchat, J.-F., Henchoz, S., Fattah, D., Mazzei, G., Aubry, J.-P., Jomotte, T., Dash, L., Page, K., Solari, R., Aldebert, D., Capron, M., Dahinden, C. & Bonnefoy, J.-Y. 1995. CD40 ligand is functionally expressed on human eosinophils. *Eur. J. Immunol.,* 25, 863-865.

Gauchat, J.-F., Henchoz, S., Mazzai, G., Aubry, J.-P., Brunner, T., Blasey, H., Life, P., Talabot, D., Flores-Romo, L., Thompson, J., Kishi, K., Butterfield, J., Dahinden, C. & Bonnefoy, J.-Y. 1993. Induction of human IgE synthesis in B cells by mast cells and basophils. *Nature,* 365.

Gitlin, L., Barchet, W., Gilfillan, S., Cella, M., Beutler, B., Flavell, R. A., Diamond, M. S. & Colonna, M. 2006. Essential role of mda-5 in type I IFN responses to polyriboinosinic:polyribocytidylic acid and encephalomyocarditis picornavirus. *Proceedings of the National Academy of Sciences,* 103, 8459-8464.

Godet, M., Grosclaude, J., Delmas, B. & Laude, H. 1994. Major receptor-binding and neutralization determinants are located within the same domain of the transmissible gastroenteritis virus (coronavirus) spike protein. *J. Virol.,* 68, 8008-8016.

Godet, M., Vautherot, R. L. H. J.-F. & Laude, H. 1992. TGEV corona virus ORF4 encodes a membrane protein that is incorporated into virions. *Virology,* 188, 666-675.

Goffard, A. & Dubuisson, J. 2003. Glycosylation of hepatitis C virus envelope proteins. *Biochemie,* 85, 295-301.

Gombold, J. L., Hingley, S. T. & Weiss, S. R. 1993. Fusion-defective mutants of mouse hepatits virus A59 contain a mutation in the spike protein cleavage signal. *J. Virol.,* 67, 4504-4512.

Grewal, I. S. & Flavell, R. A. 1998. CD40 and CD154 in cell-mediated immunity. *Annu. Rev. Immunol.,* 16, 111-135.

Guillen, J., Perez-Berna, A. J., Moreno, M. R. & Villalain, J. 2005. Identification of the membrane-active regions of severe acute respirtaory syndrom coronavirus spike membrane glycoprotein using a 16/18-mer peptide scan: implications for the viral fusion mechanism. *J. Virol.,* 79, 1743-1752.

Ha, Y., Stevens, D. J., Skehel, J. J. & Wiley, D. C. 2002. H5 avian and H9 swine influenza virus haemagglutinin structures: possible origin of influenza subtypes. *EMBO J.,* 21, 865-875.

Harrison, R. L. & Jarvis, D. L. 2006. Protein N-glycosylation in the baculovirus-insect cell expression system and engineering of insect cells to produce ‘mammalianised’ recombinant glycoproteins. *Adv. Virus Res.,* 68, 159-191.

Hasoksuz, M., Lathrop, S. L., Gadfield, K. L. & Saif, L. J. 1999. Isolation of bovine respiratory coronaviruses from feedlot cattle and comparison of their biological and antigenic properties with bovine enteric coronaviruses. *Am J Vet Res,* 60, 1227-1233.

Hasoksuz, M., Sreevatsan, S., Cho, K.-O., Hoet, A. E. & Saif, L. J. 2002. Molecular analysis of the S1 subunit of the spike glycoprotein of respiratory and enteric bovine coronavirus isolates. *Virus Res.,* 84, 101-109.

Heald-Sargent, T. & Gallagher, T. 2012. Ready, Set, Fuse! The Coronavirus Spike Protein and Acquisition of Fusion Competence. *Viruses,* 4, 557-580.

Heil, F., Hemmi, H., Hochrein, H., Ampenberger, F., Kirschning, C., Akira, S., Lipford, G., Wagner, H. & Bauer, S. 2004. Species-specific recognition of single-stranded RNA via toll-like receptor 7 and 8. *Science,* 303, 1481-1482.

Hellebø, A., Vilas, U., Falk, K. & Vlasak, R. 2004. Infectious Salmon Anemia Virus Specifically Binds to and Hydrolyzes 4-O-Acetylated Sialic Acids. *J. Virol.,* 78, 3055-3062.

Hermann, P., Van-Kooten, C., Gaillard, C., Banchereau, J. & Blanchard, D. 1995. CD40 ligand-positive CD8+ T cell clones allow B cell growth and differentiation. *Eur. J. Immunol.,* 25, 2972-2977.

Hill, G. M. 1987. Vitamin E and selenium supplementation of cattle. *Proc. Georgia Nutrition Conference.* Atlanta, GA.

Hoek, L. v. d., Maarten, K. P., Jebbink, F., Vermeulen-Oost, W., Berkhout, R. J. M., Wolthers, K. C., Dillen, P. M. E. W.-v., Kaandorp, J., Spaargaren, J. & Berkhout, B. 2004. Identification of a new human coronavirus. *Nature Med.,* 10, 368-373.

Hogue, B. G. 1995. Bovine coronavirus nucleocapsid protein processing and assembly. *Adv. Exp. Med. Biol.,* 380, 259-263.

Hogue, B. G. & Brian, D. A. 1986. Structural proteins of human respiratory coronavirus OC43. *Virus Res.,* 5, 131-144.

Holland, J. J., Torre, J. C. D. L. & Steinhauer, D. A. 1992. RNA virus populations as quasispecies. *Curr. Top Microbiol. Immunol.,* 176, 1-20.

Holmes, K. V. 1990. Coronaviridae and their replication. In: al., B. N. F. e. (ed.) *Virology.* Raven Press, New York.

Holmes, K. V. 2005. Adaptation of SARS coronavirus to humans. *Science,* 309, 1822-1823.

Holmes, K. V., Doller, E. W. & Sturman, L. S. 1981. Tunicamycin-resistant glycosylation of coronavirus glycoprotein: demonstration of a novel type of viral glycoprotein. *Virology,* 115, 334-344.

Holmgren, J. & Czerkinsky, C. 2005. Mucosal immunity and vaccines. *Nature Med.,* 11, S45-S53.

Hornung, V., Ellegast, J., Kim, S., Brzózka, K., Jung, A., Kato, H., Poeck, H., Akira, S., Conzelmann, K. K., Schlee, M., Endres, S. & Hartmann, G. 2006. 5'-Triphosphate RNA is the ligand for RIG-I. *Science,* 314, 994-997.

Howard, M. W., Travanty, E. A., Jeffers, S. A., Smith, M. K., Wennier, S. T., Thackay, L. B. & Holmes, K. V. 2008. Aromatic amino acids in the juxtamembrane domain of severe acute respiratory syndrome coronavirus spike glycoprotein are important for receptor-dependent virus entry and cell-cell fusion. *J. Virol.,* 82, 2883-2894.

Hurst, K. R., L. Kuo, L., Koetzner, C. A., Ye, R., B. Hsue, B. & Masters, P. S. 2005. A major determinant for membrane protein interaction localizes to the carboxy-terminal domain of the mouse coronavirus nucleocapsid protein. *J Virol,* 79, 13285-13297.

Imler, J.-L. 1995. Adenovirus vectors as recombinant viral vaccines. *Vaccine,* 13, 1143-1151.

Inaba, K., Witmer-Pack, M., Inaba, M., Hathcock, K. S., Sakuta, H., Azuma, M., Yagita, H., Okumura, K., Linsley, P. S., Ikehara, S., Muramatsu, S., Hodes, R. J. & Steinman, R. M. 1994. The tissue distribution of the B7-2 costimulator in mice: abundant expression on dendritic cells in situ and during maturation in vitro. *J. Exp. Med.,* 180, 1849-1860.

Iwasaki, A. & Medzhitov, R. 2004. Toll-like receptor control of the adaptive immune responses. *Nat. Immunol.,* 5, 987-995.

Jacobs, L., Zeijst, B. A. M. v. d. & Horzinek, M. C. 1986. Chacterization and translation of transmissible gastroentertis virus mRNAs. *J. Virol.,* 57, 1010-1015.

Janeway, C. A. 1989. Approaching the asymptote? Evolution and revolution in immunology. *Cold Spring Harb. Symp. Quant. Biol.,* Cold Spring Harbor.

Jarvis, D. L. 2003. Developing baculovirus–insect cell expression systems for humanized recombinant glycoprotein production. *Virology,* 310, 1-7.

Jericho, K. W. F. & Langford, E. V. 1978. Pneumonia in Calves Produced with Aerosols of Bovine Herpesvirus 1 and Pasteurella haemolytica. *Can. J. Comp. Med.,* 42, 269-277.

Jonassen, C. M., Kofstad, T., Larsen, I. L., Løvland, A., Handeland, K., Follestad, A. & Lillehaug, A. 2005. Molecular identification and characterization of novel coronaviruses infecting graylag geese (Anser anser), feral pigeons (Columbia livia) and mallards (Anas platyrhynchos). *J. Gen. Virol.,* 86, 1597-1607.

Rausch, J. M., Gallagher, W. R., Garry, R. F. & Wimley, W. C. 2005. Identification and characterization of the putative fusion peptide of the severe acute respiratory syndrom-associated coronavirus spike protein. *J. Virol.,* 79, 7195-7206.

Cho, K.-O., D., Halbur, P. G., Bruna, J. D., Sorden, S. D., Yoon, K.-J., Janke, B. H., Chang, K.-O. & Saif, L. J. 2000. Detection and isolation of coronavirus from feces of three herds of feedlot cattle during outbreaks of winter dysentery-like disease. *J Am Vet Med Assoc,* 217, 1191-1194.

Kang, D. C., Gopalkrishnan, R. V., Wu, Q., Jankowsky, E., Pyle, A. M. & Fishe, P. B. 2002. MDA-5: An interferon-inducible putative RNA helicase with double-stranded RNA-dependent ATPase activity and melanoma growth-suppressive properties. *Proc. Natl. Acad. Sci. USA,* 99, 637-642.

Kanneganti, T. D., Lamkanfi, M. & Nunez, G. 2007. Intracellular NOD-like receptors in host defense and disease. *Immuntiy,* 27.

Kapil, S., Pomeroy, K. A., Goyal, S. M. & Trent, A. M. 1991. Experimental infection with a virulent pneumoenteric isolate of bovine coronavirus. *J vet Diagn Invest,* 3, 88-89.

Kapke, P. A. & Brian, D. A. 1986. Sequence analysis of the porcine transmissible gastroenteritis coronavirus nucleocapsid protein gene. *Virology,* 151, 41-49.

Kato, H., Takeuchi, O., Mikamo-Satoh, E., Hirai, R., Kawai, T., Matsushita, K., Hiiragi, A., Dermody, T. S., Fujita, T. & S. Akira, S. 2008. Length-dependent recognition of double-stranded ribonucleic acids by retinoic acid-inducible gene-I and melanoma differentiation-associated gene 5. *J. Exp. Med.,* 205, 1601-1610.

Kato, H., Takeuchi, O., Sato, S., Yoneyama, M., Yamamoto, M., Matsui, K., Uematsu, S., Jung, A., Kawai, T., Ishii, K. J., Yamaguchi, O., Otsu, K., Tsujimura, T., Koh, C. S., Sousa, C. R. e., Matsuura, Y., Fujita, T. & Akira, S. 2006. Differential roles of MDA5 and RIG-I helicases in the recognition of RNA viruses. *Nature,* 441, 101-105.

Kawai, T., Takahashi, K., Sato, S., Coban, C., Kumar, H., Kato, H., Ishii, K. J., Takeuchi, O. & Akira, S. 2005. IPS-1, an adaptor triggering RIG-I- and Mda5-mediated type I interferon induction. *Cell,* 122, 981-988.

Kennedy, M. K., Mohler, K. M., Shanebeck, K. D., Baum, P. R., Picha, K. S., Otten-Evans, C. A., Jr., C. A. J. & Grabstein, K. H. 1994. Induction of B cell costimulatory function by recombinant murine CD40 ligand. *Eur. J. Immunol.,* 24, 116-123.

Kientzle, T. E., Abraham, S., Hogue, B. G. & Brian, D. A. 1990. Structure and Orientation of Expressed Bovine Coronavirus Hemagglutinin-Esterase Protein. *J. Virol.,* 64, 1834-1838.

King, B. & Brian, D. A. 1982. Bovine coronavirus structural proteins. *J. Virol.,* 42, 700-707.

KIng, B., Potts, B. J. & Brian, D. A. 1985. Bovine coronavirus hemagglutinin protein. *Virus Res.,* 2, 433-443.

Klumperman, J., Locker, J. K., Meijer, A., Horzinek, M. C., Geuze H. J. & Rottier, P. J. M. 1994. Coronavirus M proteins accumulate in the golgi complex beyond the site of virion budding. *J. Virol.,* 68, 6523-6534.

Kovacsovics, M., Martinon, F., Micheau, O., Bodmer, J. L., Hofmann, K. & Tschopp, J. 2002. Overexpression of Helicard, a CARD-containing helicase cleaved during apoptosis, accelerates DNA degradation. *Curr. Biol.,* 12, 838-843.

Krijnse-Locker, J., Griffiths, G., Horzinek, M. C. & Rottier, P. J. M. 1992. O-glycosilation of the coronavirus M protein; differential localization of sialyltransferases in N- and O-linked glycosylation. *J. Biol. Chem.,* 267, 14094-14101.

Kubo, H., Yamada, Y. K. & Taguchi, F. 1994. Localization of neutralizing epitopes and the receptor-binding site within the amino-terminal 330 amino acids of the murine coronavirus spike protein. *J. Virol.,* 68, 5403-5410.

Kumar, H., Kawai, T., Kato, H., Sato, S., K.Takahashi, Coban, C., Yamamoto, M., Uematsu, S., Ishii, K. J., Takeuchi, O. & Akira, S. 2006. Essential role of IPS-1 in innate immune responses against RNA viruses. *J. Exp. Med.,* 203, 1795-1803.

Kuo, L., Godeke, G.-J., Raamsman, M. J. B., Masters, P. S. & Rottier, P. J. M. 2000. Retargeting of Coronavirus by Substitution of the Spike Glycoprotein Ectodomain: Crossing the Host Cell Species Barrier. *J. Virol.,* 24, 1393-1406.

Kuo, L. & Masters, P. S. 2002. Genetic evidence for a structural interaction between the carboxy termini of the membrane and nucleocapsid proteins of mouse hepatitis virus. *J. Virol.,* 76, 4987–4999.

Lai, M. M. C., Patton, C. D., Baric, R. S. & Stohlman, S. A. 1983. Presence of leader sequences in the mRNA of mouse haptitis virus. *J. Virol.,* 46, 1027-1033.

Larsen, J. E., Lund, O. & Nielsen, M. 2006. Improved method for predicting linear B-cell epitopes. *Immunome. Res.,* 2, 2.

Larson, R. L. & Bradley, J. S. 1996. Immunologic principles and immunization strategy. *Comp. Cont. Ed. Prac. Vet.,* 18, 963-970.

Lathrop, S. L., Wittum, T. E., Brock, K. V. & Saif, L. J. 2000. Association between infection of the respiratory tract attributable to bovine coronavirus and health and growth performance of cattle in feedlots. *Am J Vet Res,* 61, 1062-1066.

Lau, S. K. P., Woo, P. C. Y., Li, K. S. M., Huang, Y., Tsoi, H.-W., Wong, B. H. L., Wong, S. S. Y., Leung, S.-Y., Chan, K.-H. & Yuen, K.-Y. 2005. Severe acute respiratory syndrome coronavirus-like virus in Chinese horseshoe bats. *Proc. Natl. Acad. Sci. USA,* 102, 14040-14045.

Laude, H. & Masters., P. S. 1995. The coronavirus nucleocapsid protein. In: Siddell, S. G. (ed.) *The Coronaviridae.* Plenum Press, New York, NY.

Lauring, A. S. & Andino, R. 2010. Quasispecies Theory and the Behavior of RNA Viruses. *PLOS Pathog.,* 6, 1-8.

Leibowitz, J. L., Perlman, S., Weinstock, G., Devries, J. R., Budzilowicz, C., Weissmann, J. M. & Weiss, S. R. 1988. Detection of a murine coronavirus nonstructural protein encoded in a downstream open reading frame. *Virology,* 164, 156-164.

Lenschow, D. J., Sperling, A. I., Cooke, M. P., Freeman, G., Rhee, L., Decker, D. C., Gray, G., Nadler, L. M., Goodnow, C. C. & Bluestone, J. A. 1994. Differential up-regulation of the B7-1 and B7-2 costimulatory molecules after Ig receptor engagement by antigen. *J. Immunol.,* 153, 1990-1997.

Li, W., Shi, Z., Yu, M., Ren, W., Smith, C., Epstein, J. H., Wang, H., Crameri, G., Hu, Z., Zhang, H., Zhang, J., McEachern, J., Field, H., Daszak, P., Eaton, B. T., Zhang, S. & Wang, L.-F. 2005. Bats Are Natural Reservoirs of SARS-Like Coronaviruses. *Science,* 310, 676-679.

Liao, Y., Yuana, Q., Torresa, J., Tama, J. P. & Liu, D. X. 2006. Biochemical and functional characterization of the membrane association and membrane permeabilizing activity of the severe acute respiratory syndrome coronavirus envelope protein. *Virology,* 349, 264-275.

Lin, Y. P., Shaw, M., Gregory, V., Cameron, K., Lim, W., Klimov, A., Subbarao, K., Guan, Y., Krauss, S., Shortridge, K., Webster, R., Cox, N. & Hay, A. 2000.

Avian-to-human transmission of H9N2 subtype influenza A viruses: relationship between H9N2 and H5N1 human isolates. *Proc. Natl. Acad. Sci. USA,* 97, 9654-9658.

Liu, D. X., and S. C. Inglis. 1991. Association of the infectious bronchitis virus 3c protein with the virion envelope. *Virology,* 185, 911-917.

Lontok, E., Corse, E. & Machamer, C. E. 2004. Intracellular Targeting Signals Contribute to Localization of Coronavirus Spike Proteins near the Virus Assembly Site. *J. Virol.,* 78, 5913-5922.

Lopez, A., Thomson, R. G. & Savan, M. 1976. The pulmonary clearance of Pasteurella hemolytica in calves infected with bovine parainfluenza-3 virus. *Can J Comp Med,* 40, 385-391.

Lopez, L. A., Riffle, A. J., Pike, S. L., Gardner, D. & Hogue, B. G. 2008. Importance of Conserved Cysteine Residues in the Coronavirus Envelope Protein▽. *J. Virol.,* 82, 3000-3010.

Lund, J. M., Alexopoulou, L., Sato, A., Karow, M., Adams, N. C., Gale, N. W., Iwasaki, A. & Flavell, R. A. 2004. Recognition of single-stranded RNA viruses by Toll-like receptor 7. *Proc. Natl. Acad. Sci. USA,* 101, 5598-5603.

Luytjes, W., Bredenbeek, P. J., Noten, A. F., Horzinek, M. C. & Spaan, W. J. 1988. Sequence of mouse hepatitis virus A59 mRNA2: indications for RNA-recombination between coronaviruses and influenza C virus. *Virology,* 166, 415-422.

Luytjes, W., Sturman, L. S., Bredenbeek, P. J., Charite, J., Zeijst, B. A. v. d., Horzinek, M. C. & Spaan, W. J. 1987. Primary structure of the glycoprotein E2 of coronavirus MHV-A59 and identification of the trypsin clevage site. *Virology,* 161, 479-487.

Mackey, M. F., Barth, R. J. & Noelle, R. J. 1998. The role of CD40/CD154 interactions in the priming, diVerentiation, and eVector function of helper and cytotoxic T cells. *J. Leukoc. Biol.,* 63, 418-428.

Macnaughton, M. R. & Davies, H. A. 1978. Ribonucleoprotein-like Structures from Coronavirus Particles. *J. Gen. Virol.,* 39, 545-549.

Maeda, J., J. F. Repass, A. Maeda, and S. Makino. 2001. Membrane topology of coronavirus E protein. *Virology,* 281, 163-169.

Manoj, S., Griebel, P., Babiuk, L. A. & Hurk, S. V. D. L.-v. d. 2004. Modulation of immune responses to bovine herpesvirus-1 in cattle by immunization with a DNA

vaccine encoding glycoprotein D as a fusion protein with CD154. *Immunol.,* 112, 238-338.

Manoj, S., Griebel, P. J., Babiuk, L. A. & Hurk, S. V. D. L.-V. D. 2003. Targeting with bovine CD154 enhances humoral immune responses induced by a DNA vaccine in sheep. *J. Immunol.,* 170, 989-996.

Marrack, P., Kappler, J. & Mitchell, T. 1999. Type I interferons keep activated T cells alive. *J. Exp. Med.,* 189, 521-530.

Maruyama, K. & Sugano, S. 1994. Oligo-capping: a simple method to replace the cap structure of eukaryotic mRNAs with oligoribonucleotides. *Gene,* 138, 171-174.

Masters, P. S. 2006. The Molecular Biology of Coronaviruses. *Adv. Virus Res.,* 66, 193-292.

Masters, P. S., Koetzner, C. A., Kerr, C. A. & Heo, Y. 1992. Optimization of Targeted RNA Recombination and Mapping of a Novel Nucleocapsid Gene Mutation in the Coronavirus Mouse Hepatitis Virus. *J. Virol.,* 68, 328-337.

Maue, A. C., Waters, W. R., Palmer, M. V., Whipple, D. L., Minion, F. C., Brown, W. C. & Estes, D. M. 2004. CD80 and CD86, but not CD154, augment DNA vaccine-induced protection in expreimental bovine tuberculosis. *Vaccine,* 23.

Mazzei, G. J., Edgerton, M. D., Losberger, C., Lecoanet-Henchoz, S., Graber, P., Durandy, A., Gauchat, J.-F., Bernard, A., Allet, B. & Bonnefoy, J.-Y. 1995. Recombinant Soluble Trimeric CD40 Ligand Is Biologically Active. *J. Biol. Chem.,* 270, 7025-7028.

McCartney, S. A. & Colonna, M. 2009. Viral sensors: diversity in pathogen recognition. *Immunol. Rev.,* 227, 87-94.

McIntosh, K. 1974. Coronaviruses: a comparative review. *Curr. Top Microbiol. Immunol.,* 63, 85-129.

Medzhitov, R. 2007. Recognition of microorganisms and activation of the immune response. *Nature,* 449, 819-826.

Melikyan, G. B., Markosyan, R. M., Hemmati, H., Delmedico, M. K., Lambert, D. M. & Cohen, F. S. 2000. Evidence that the transition of HIV-1 gp41 into a six-helix bundle, not the bundle configuration, induces membrane fusion. *J. Cell Biol.,* 151, 413-423.

Mesecar, A. D. & Ratia, K. 2008. Viral destruction of cell surface receptors. *Proc. Natl. Acad. Sci. USA,* 105, 8807-8808.

Mockett, A. P. A., Cavanagh, D. & Brown, T. D. K. 1984. Monoclonal antibodies to the S1 soike and membrane proteins of avian infectious bronchitis coronavirus strain Massachusetts M41. *J. Gen. Virol.,* 65, 2281-2286.

Molenkamp, R. & Spaan, W. J. M. 1997. Identification of a specific interaction between the coronavirus mouse hepatitis virus A59 nucleocapsid protein and packaging signal. *Virology,* 239, 78-86.

Morrison, L. A. 2004. The toll of herpes simplex virus infection. *Trends Microbiol.,* 12, 353-356.

Nakanaga, K., Yamanouchi, K. & Fujiwara, K. 1986. Protective effect of monoclonal antibodies on lethal mouse hepatitis virus infection in mice. *J. Virol.,* 59, 168-171.

Nal, M., Chan, C., Kie, F., Siu, L., Tse, J., Chu, K., Kam, J., Staropoli, I., Crescenzo-Chaigne, B., Escriou, N., Werf, S. v. d., Yuen, K. Y. & Altmeyer, R. 2005. Differential maturation and subcellular localization of severe acute respiratory syndrome coronavirus surface proteins S, M and E. *J. Gen. Virol.,* 86, 1423-1434.

Narayanan, K., Chen, C. J., Maeda, J. & Makino, S. 2003. Nucleocapsid-independent specific viral RNA packaging via viral envelope protein and viral RNA signal. *J. Virol.,* 77, 2922-2927.

Nash, T. C. & Buchmeier, M. J. 1997. Entry of mouse hepatitis virus into cells by endosomal and non-endosomal pathways. *Virology,* 23, 1-8.

Nashar, T. O. & Drake, J. R. 2005. The pathway of antigen uptake and processing dictates MHC class II-mediated B cell survival and activation. *J. Immunol.,* 174, 1306-1316.

Navas, S., Seo, S.-H., Chua, M. M., Sarma, J. D., Lavi, E., Hingley, S. T. & Weiss, S. R. 2001. Murine Coronavirus Spike Protein Determines the Ability of the Virus To Replicate in the Liver and Cause Hepatitis. *J. Virol.,* 75, 2452-2457.

Navas, S. & Weiss*, S. R. 2003. Murine Coronavirus-Induced Hepatitis: JHM Genetic Background Eliminates A59 Spike-Determined Hepatotropism. *J. Virol.,* 77, 4972-4978.

Nelson, G. W. & Stohlman, S. A. 1993. Localization of the RNA-binding domain of mouse hepatitis virus nucleocapsid protein. *J. Gen. Virol.,* 74, 1975-1979.

Nelson, G. W., Stohlman, S. A. & Tahara, S. M. 2000. High affinity interaction between nucleocapsid protein and leader/intergenic sequence of mouse hepatitis virus RNA. *J. Gen. Virol.,* 81, 181-188.

Nguyen, V. P. & Hogue, B. G. 1997. Protein interactions during coronavirus assembly. *J. Virol.,* 71, 9278–9284.

Opstelten, D. J. E., Raamsman, M. J. B., Wolfs, K., Horzinek, M. C. & Rottier, P. J. M. 1995. Coexpression and association of the spike and the membrane protein of mouse hepatitis virus. *Adv. Exp. Med. Biol.,* 380, 921-297.

Oshiumi, H., Matsumoto, M., Funami, K., Akazawa, T. & Seya, T. 2003. TICAM-1, an adaptor molecule that participates in Toll-like receptor 3-mediated interferon-beta induction. *Nat. Immunol.,* 4, 161-167.

Parker, J. M., Guo, D. & Hodges, R. S. 1986. New hydrophilicity scale derived from high-performance liquid chromatography peptide retention data: correlation of predicted surface residues with antigenicity and X-ray-derived accessible sites. *Biochemistry,* 25, 5425-5432.

Parker, M. D., Cox, G. J., Deregt, D., Fitzpatrick, D. R. & Babiuk, L. A. 1989. Cloning and in vitro expression of the gene for the E3 haemagglutinin glycoprotein of bovine coronavirus. *J. Gen. Virol.,* 70, 155-164.

Pasquini, S., Xiang, Z., Wang, Y., He, Z., Deng, H., Blaszczyk-Thurin, M. & Ertl, H. C. 1997. Cytokines and costimulatory molecules as genetic adjuvants. *Immunol. Cell. Biol.,* 75, 397-401.

Payne, H. R. & Storz, J. 1990. Coronavirus antigens in the host cell plasmallema. *Exp. Mol. Pathol.,* 53, 152-159.

Petit, C. M., Chouljenko, V. N., Iyer, A., Colgrove, R., Farzan, M., Knipe, D. M. & Kousoulas, K. G. 2007. Palmitoylation of the cyctine-rich domain endodomain of the SARS-coronavirus spike glycoprotein is important for spike-mediated cell fusion. *Virology*, 360, 264-274.

Petrilli, V., Dostert, C., Muruve, D. A. & Tschopp, J. 2007. The inflammasome: a danger sensing complex triggering innate immuntiy. *Curr. Opin. Immunol.,* 19, 615-622.

Phillips, J. J., Chua, M. M., Seo, S.-h. & Weiss, S. R. 2001. Multiple regions of the murine coronavirus spike glycoprotein influence neurovirulence. *J. Neuro. Virol.,* 7, 421-431.

Pichlmair, A., Schulz, O., Tan, C. P., Naslund, T. I., Liljestrom, P., Weber, F. & Sousa, C. R. e. 2006. RIG-I-mediated antiviral responses to single-stranded RNA bearing 50-phosphates. *Science,* 314, 997-1001.

Pike, B. V. & Garwes, D. J. 1977. Lipids of transmissible gastroenteritis virus and their relation to those of two different host cells. *J. Gen. Virol.,* 54, 531-535.

Poon, L. L., Chu, D. K., Chan, K. H., Wong, O. K., Ellis, T. M., Leung, Y. H., Lau, S. K., Woo, P. C., Suen, K. Y., Yuen, K. Y., Guan, Y. & Peiris, J. S. 2005. Identification of a novel coronavirus in bats. *J. Virol.,* 79, 2001-2009.

Popova, R. & Zhang, X. 2002. The spike but not the hemagglutinin/esterase protein of bovine coronavirus is necessary and sufficient for viral infection. *Virology,* 294, 222-236.

Potgieter, L. N. D. 1977. Current concepts on the role of viruses in respiratory tract diseases of cattle. *Bovine Pract.,* 10, 75-81.

Qiu, Z., Hingley, S. T., Simmons, G., Yu, C., Sarma, J. D., Bates, P. & Weiss, S. R. 2006. Endosomal Proteolysis by Cathepsins Is Necessary for Murine Coronavirus Mouse Hepatitis Virus Type 2 Spike-Mediated Entry. *J. Virol.,* 80, 5768-5776.

Raamsman, M. J., Locker, J. K., Hooge, A. d., Vries, A. A. d., Griffiths, G., Vennema, H. & Rottier, P. J. 2000. Characterization of the coronavirus mouse hepatitis virus strain A59 small membrane protein E. . *J. Virol.,* 74, 2333-2342.

Ranheim, E. A. & Kipps, T. J. 1993. Activated T cells induce expression of B7/BB1 on normal or leukemic B cells through a CD40-dependent signal. *J. Exp. Med.,* 177, 925-935.

Regl, G., Kaser, A., Iwersen, M., Schmid, H., Kohla, G., Strobl, B., Vilas, U., Schauer, R. & Vlasak, R. 1999. The Hemagglutinin-Esterase of Mouse Hepatitis Virus Strain S Is a Sialate-4-O-Acetylesterase. *J. Virol.,* 73, 4721-4727.

Reynolds, D. J., Debney, T. G., Hall, G. A., Thomas, L. H. & Parsons, K. R. 1984. Studies on the relationship between coronaviruses from the intestinal and respiratory tracts of calves. *Arch Virol,* 85, 71-83.

Risco, C., Anto, I. M., Enjuanes, L. & Carrascosa, J. L. 1996. The Transmissible Gastroenteritis Coronavirus Contains a Spherical Core Shell Consisting of M and N Proteins. *J. Virol.,* 70, 4773-4777.

Robbins, S. G., Frana, M. F., McGowen, J. J., Boyle, J. F. & K. V. Holmes, K. V. 1986. RNA-binding proteins of coronavirus MHV: detection of monomeric and multimeric N protein with an RNA overlay-protein blot assay. *Virology,* 150, 402-410.

Roeber, D. L., Speer, N. C., Gentry, j. G., Tatum, J. D., Smith, C. D., Whittier, J. C., Jones, G. F., Belk, K. E. & Smith, G. C. 2001. Feeder cattle health management: Effects on morbidity rates, feedlot performance, carcass characteristics, and beef palatability. *Professional Animal Scientist,* 17, 39-44.

Rosenthal, P. B., Zhang, X., Formanowski, F., Fitz†, W., Wong, C.-H., Meier-Ewert, H., Skehelk, J. J. & Wiley, D. C. 1988. Structure of the haemagglutinin-esterase fusion glycoprotein of influenza C virus. *Nature,* 396, 92-96.

Rothenfusser, S., Goutagny, N., DiPerna, G., Gong, M., Monks, B. G., Schoenemeyer, A., Yamamoto, M., Akira, S. & Fitzgerald, K. A. 2005. The RNA helicase Lgp2 inhibits TLR-independent sensing of viral replication by retinoic acid-inducible gene-I. *J. Immunol.,* 175, 5260-5268.

Rottier, P. J., Brandenburg, D., Armstrong, J., Zeijst, B. v. d. & Warren, G. 1984. Assembly in vitro of a spanning membrane protein of the endoplasmic reticulum: the E1 glycoprotein of coronavirus mouse hepatitis virus A59. *Proc. Natl. Acad. Sci. USA,* 81, 1421-1425.

Rottier, P. J., Horzinek, M. C. & Zeijst, B. A. M. v. d. 1981. Viral protein synthesis in mouse hepatitis virus strain A59-infected cells: effect of tuicamyacin. *J. Virol.,* 40, 350-357.

Rottier, P. J. & Rose, J. K. 1987. Coronavirus E1 glycoprotein expressed from a clones cDNA localizes in teh golgi region. *J. Virol.,* 61, 2042-2045.

Rottier, P. J., Welling, G. W., Welling-Wester, S., Niesters, H. G., Lenstra, J. A. & Zeijst, B. A. M. v. d. 1986. Predicted membrane topology of the coronavirus protein E1. *Biochemistry,* 25, 1335-1339.

Rottier, P. J. M. 1995. The coronavirus membrane glycoprotein. In: Siddell, S. G. (ed.) *The Coronaviridae.* Plenum Press, New York, NY.

Roy, M., AruVo, A., Ledbetter, J., Linsley, P., Kehry, M. & Noelle, R. 1995. Studies on the interdependence of gp39 and B7 expression and function during antigen-speciWc immune responses. *Eur. J. Immunol.,* 25, 596-603.

Ruggiero, G., Cáceres, C. E. M., Voordouw, A., Noteboom, E., Graf, D., Kroczek, R. A. & Spits, H. 1996. CD40 expressed on thymic epithelial cells provides costimulation for proliferation but not for apoptosis of human thymocytes. *J. Immunol.,* 156, 3737-3746.

Russell, C. J., Jardetzky, T. S. & Lamb, R. A. 2001. Membrane fusion machines of paramyxoviruses: capture of intermediates of fusion. *EMBO J.,* 20, 4024-4034.

Sad, S., Krishnan, L., Bleackley, R. C., Kagi, D., Hengartner, H. & Mosmann, T. R. 1997. Cytotoxicity and weak CD40L expression of CD8+ type 2 cytotoxic T cells restricts their potential B cell helper activity. *Eur. J. Immunol.,* 27.

Saif, L. J. 2004. Animal coronavirus vaccines: lessons for SARS. *Dev. Biol.,* 119, 129-140.

Saito, T., Hirai, R., Loo, Y.-M., Owen, D., Johnson, C. L., Sinha, S. C., Akira, S., Fujita, T. & M. Gale, J. 2007. Regulation of innate antiviral defenses through a shared repressor domain in RIG-I and LGP2. *Proc. Natl. Acad. Sci. USA*, 104, 582-587.

Saito, T. & M. Gale, J. 2008. Differential recognition of double-stranded RNA by RIG-I like receptors in antiviral immunity. *J. Exp. Med.*, 205, 1523-1527.

Saito, T., Owen, D. M., Jiang, F., Marcotrigiano, J. & M. Gale, J. 2008. Innate immunity induced by composition-dependent RIG-I recognition of hepatitis C virus RNA. *Nature,* 454, 523-527.

Sawicki, S. G. & D. L. Sawicki, D. L. 1995. Coronaviruses use discontinuous extension for synthesis of subgenome-length negative strands. *Adv. Exp. Med. Biol.,* 380, 499-506.

Sawicki, S. G. & D. L. Sawicki, D. L. 1998. A new model for coronavirus transcription. *Adv. Exp. Med. Biol.,* 440, 215-219.

Sawicki, S. G. & Sawicki, D. L. 1990. Coronavirus transcription: subgenomic mouse hepatitis virus replicative intermediates function in RNA synthesis. *J. Virol.,* 64, 1050-1056.

Schmaljohn, C. S., Y.-K. CHU, Schmaljohn, A. L. & Dalrymple, J. M. 1990. Antigenic Subunits of Hantaan Virus Expressed by Baculovirus and Vaccinia Virus Recombinants. *J. Virol.,* 64, 3162-3170.

Schultze, B., Wahn, K., Klenk, H.-D. & Herrler, G. 1991. Isolated HE-protein from hemagglutinating encephalomyelitis virus and bovine coronavirus has receptor-destroying and receptor-binding activity. *Virology,* 180, 221-228.

Shalk, A. F. & Hawn, M. C. 1931. An apparently new disease of chicks. *J Am Vet Med Assoc,* 78, 413-422.

Sharpee, R. L., Mebus, C. A. & Bass, E. P. 1976. Characterization of a calf diarrheal coronavirus. *J. Vet. Res.,* 37, 1031-1041.

Siddell, S. 1983. Coronavirus JHM: boding assignments of subgenomic mRNAs. *J. Gen. Virol.,* 64, 113-125.

Siddell, S., Wege, H., Barthel, A. & Meulen, V. T. 1981. Coronavirus JHM: intracellular protein synthesis. *J. Virol.,* 33.

Siddell, S., Wege, H. & Meulen, V. t. 1983. The biology of coronaviruses. *J. Gen. Virol.,* 64, 761-776.

Siddell, S. G. 1995. The Coronaviridae: An Introduction. In: Siddell, S. G. (ed.) *The Coronaviridae: An Introduction.* Plenum Pres, New York, NY.

Smith, D. B. & Corcoran, L. M. 1990. Current Protocols in Molecular Biology. In: Ausubel, F. M., Brent, R., R. E. Kingston, Moore, D. D., Seidman, J. G., Smith, J. A. & Struhl, K. (eds.) *Current Protocols in Molecular Biology.* Wiley, New York.

Sousa, C. R. e. 2004. Activation of dendritic cells: translating innate into adaptive immunity. *Curr. Opin. Immunol.,* 16, 21-25.

Spaan, W., Cavanagh, D. & Horzinek, C. 1988. Coronaviruses: Structure and genome expression. *J. Gen. Virol.,* 69, 2939-2952.

Spaan, W., Delius, H., Skinner, M., Armstrong, J., Rottier, P., Smeekens, S., Zeijst, B. A. M. v. d. & Siddell, S. G. 1983. Coronavirus mRNA synthesis involves fusion of non-contiguous sequences. *EMBO J.,* 2, 1839-1844.

Stamenkovic, I., Clark, E. A. & Seed, B. 1989. A B-lymphocyte activation molecule related to the nerve growth factor receptor and induced by cytokines in carcinomas. *EMBO J.,* 8, 1403-1410.

Stauber, R., Pfleiderer, M. & Siddell, S. 1993. Proteolytic clevage of the murine coronavirus surface glycoprotein is not required for fusion. *J. Gen. Virol.,* 74, 183-191.

Stern, D. F. & Sefton, B. M. 1982a. Coronavirus proteins: structure and finction of the oligosaccharides of the avian infectious bronchitis virus glycoproteins. *J. Virol.,* 44, 804-812.

Stern, D. F. & Sefton, B. M. 1982b. Coronavirus proteins: biogenesis of anvian infectious bronchitis virus virion proteins. *J. Virol.,* 44, 794-803.

Stetson, D. B. & Medzhitov, R. 2006. Type I interferons in host defense. *Immunity,* 25, 373-381.

Stohlman, S. A., Baric, R. S., Nelson, G. N., Soe, L. H., Welter, L. M. & Deans, R. J. 1988. Specific interaction between coronavirus leader RNA and nucleocapsid protein. *J. Virol.,* 62, 4288-4295.

Stohlman, S. A., Brayton, P. R., Fleming, J. O., Weiner, L. P. & Lai, M. M. 1982. Murine coronaviruses: Isolation and characterization of two plaque morphology variants of the JHM neurotropic strain. *J. Gen. Virol.,* 63.

Stohlman, S. A. & Lai, M. M. C. 1979. Phosphoproteins of murine hepatitis viruses. *J. Virol.,* 32, 672-675.

Stohlman, S. A., Matsushima, G. K., Casteel, N. & Weiner, L. P. 1985. In vivo effects of coronavirus-specific T cell clones: DTH inducer cells prevent a lethal infection but do not inhibit virus replication. *J. Immunol.,* 136, 3052-3056.

Storz, J., Purdy, C. & Lin, X. B. M. 2000. Isolation of respiratory bovine coronavirus, other cytocidal virus, and *Pasturella* spp. from cattle involved in two natural outbreaks of shipping fever. *Journal of the Veterinary Medical Association,* 216, 1599-1604.

Storz, j., Stine, L., Liem, A. & Anderson, G. A. 1996. Coronavirus isolation from nasal swab samples in cattle with signs of respiratory tract disease after shipping. *Journal of the Veterinary Medical Association,* 208, 1452-1455.

Sturman, L. S. 1977. Characterization of a coronavirus I. Structural proteins: effects of preparative conditions on the migration of protein in polyacrylamide gels. *Virology,* 77, 637-649.

Sturman, L. S. & Holmes, K. V. 1983. The molecular biology of coronaviruses. *Adv. Virus Res.,* 28, 35-112.

Sturman, L. S., Holmes, K. V. & Behnke, J. 1980. Isolation of coronavirus envelope glycoproteins and interaction with the viral nucleocapsid. *J. Virol.,* 33, 449-462.

Sturman, L. S., Ricard, C. S. & Holmes, K. V. 1985. Proteolytic clevage of the E2 glycoprotein of murine coronavirus: activation of cell-fusing activity of virions by trypsin and separation if two different 90K clevage fragments. *J. Virol.*, 56, 904-911.

Sugiyama, K. & Amano, Y. 1981. Morphological and biological properties of new corona- virus associated with diarrhea in infant mice. *Arch. Virol.,* 67, 241-251.

Suzuki, N., Suzuki, S. & Yeh, W.-C. 2002. IRAK-4 as the central TIR signaling mediator in innate immunity. *Trends in Immunol.,* 23, 503-506.

Taguchi, F. 1993. Fusion formation by the uncleaved spike protein of murine coronavirus JHM variant cl-2. *J. Virol.,* 67, 1195-1202.

Takahashi, K., Kawai, T., Kumar, H., Sato, S., Yonehara, S. & Akira, S. 2006. Roles of caspase-8 and caspase-10 in innate immune responses to double-stranded RNA. *J. Immunol.*, 176, 4520-4524.

Takeuchi, O. & Akira, S. 2007. Recognition of viruses by innate immunity. *Immunol. Rev.,* 220, 214-224.

Takeuchi, O. & Akira, S. 2009. Innate immuntiy to virus infection. *Immunol. Rev.,* 227, 75-86.

Theofilopoulos, A. N., Baccala, R., Beutler, B. & Kono, D. H. 2005. Type I interferons (alpha/beta) in immunity and autoimmunity. *Annu. Rev. Immunol.,* 23, 307-336.

Thomas, C., Young, N. J., Heaney, J., Collins, M. E. & Brownlie, J. 2009. Evaluation of efficacy of mammalian and baculovirus expressed E2 subunit vaccine candidates to bovine viral diarrhoea virus. *Vaccine,* 27, 2387-2393.

Thomas, L. H., Gourlay, R. N., Stott, E. J., Howard, C. J. & Bridger, J. C. 1982. A search for new microorganisms in pneumonia by the inoculation of gnotobiotic calves. *Res Vet Sci,* 33, 170-182.

Tooze, J., Tooze, S. & Warren, G. 1984. Replication of coronavirus MHV-A59 in sac-cells: determination fo the first site of budding of progeny virions. *Eur. J. Cell Biol.,* 33, 281-293.

Tooze, S. A., Tooze, J. & Warren, G. 1988. Site of addition of N- acetyl-galactosamine to the E1 glycoprotein of mouse hepatitis virus -A59. *J. Cell Biol.,* 106, 1475-1487.

Torres, J., Wang, J., Parthasarathy, K. & Liu, D. X. 2005. The Transmembrane Oligomers of Coronavirus Protein E. *Biophys. J.,* 88, 1283-1290.

Tough, D. F. 2004. Type I interferon as a link between innate and adaptive immunity through dendritic cell stimulation. *Leuk. Lymphoma,* 45, 257-264.

Tsunemitsu, H., el-Kanawati, Z. R., Smith, D. R., Reed, H. H. & Saif, L. J. 1995. Isolation of coronaviruses antigenically indistinguishable from bovine coronavirus from wild ruminants with diarrhea. *J. Clin. Microbio.,* 33, 3264-3269.

Vander Most, R. G., Bredenbeek, P. J. & Spaan, W. J. M. 1991. A domain at the 3* end of the polymerase gene is essential for the encapsidation of coronavirus Defective Interfering RNAs. *J. Virol.,* 65, 3219-3226.

Van Kooten, C. & Banchereau, J. 1996. CD40±CD40 ligand: a multifunctional receptor±ligand pair. *Adv. Immunol.,* 61, 1-77.

Van Kooten, C. & Banchereau, J. 2000. CD40-CD40 ligand. *J. Leukoc. Biol.,* 67, 2-17.

Venkataraman, T., Valdes, M., Elsby, R., Kakuta, S., Caceres, G., Saijo, S., Iwakura, Y. & Barber, G. N. 2007. Loss of DExD/H box RNA helicase LGP2 manifests disparate antiviral responses. *J. Immunol.,* 178, 6444-6455.

Vennema, H., Godeke, G. J., Rossen, J. W. A., Voorhout, W. F., Horzinek, M. C., Opsteltein, D.-J. E. & Rottier, P. J. M. 1996. Nucleocapsid-independent assembly of coronavirus-like particles by co-expression of viral envelope protein genes. *EMBO J.,* 15, 2020-2028.

Verheije, M. H., Hagemeijer, M. C., Ulasli, M., Reggiori, F., Rottier, P. J., Masters, P. S. & deHaan, C. A. 2010. The coronavirus nucleocapsid protein is dynamically associated with the replication-transcription complexes. *J Virol,* 84, 11575-11579.

Vijgen, L., Keyaerts, E., Lemey, P., Moes, E., Li, S., Vandamme, A.-M. & Ranst, M. V. 2005. Circulation of genetically distinct contemporary human coronavirus OC43 strains. *Virology,* 337, 85-92.

Vlasak, R., Luytjes, W., Spaan, W. & Palese, P. 1988. Human and bovine coronaviruses recognize sialic acid-containing receptors similar to those of influenza C viruses. *Proc. Natl. Acad. Sci. USA,* 85, 4526-4529.

Vries, A. A. F. d., Horzinek, M. C., Rottier, P. J. & Groot, R. J. d. 1997. The genome organization of the Nidovirales: similarities and differences between arteri-, toro- and coronaviruses. *Semin. Virol.,* 8, 33-47.

Wang, W., Singh, S., Zeng, D. L., King, K. & Nema, S. 2007. Antibody Structure, Instability, and Formulation. *J. Pharm. Sci.,* 96, 1-26.

Warr, G. W., Magor, K. E. & Higgins, D. A. 1995. IgY: clues to the origins of modern antibodies. *Immunol. Today,* 16, 392-398.

Wege, H., Dorries, R. & Wege, H. 1984. Hybridoma antibodies to the murine coronavirus JHM: characterization of epitopes on the peplomer protein (E2). *J. Gen. Virol.,* 65, 1931-1942.

Weismiller, D. G., Sturman, L. S., Buchmeier, M. J., Fleming, J. O. & Holmes, K. V. 1990. Monoclonal antibodies to the peplomer glycoprotein of coronavirus mouse hepatitis virus identify two subunits and detect a conformational change in the subunit released under mild alkaline conditions. *J. Virol.,* 64, 3051-3055.

Weiss, S. R. & Leibowitz, J. L. 2011. Coronavirus Pathogenesis. *Advances in Virus Research,* 81, 85-164.

Weissman, A. M., Bonifacino, J. S., Klausner, R. D., Samelson, L. E. & O'Shea, J. J. 1989. T cell antigen receptor: structure, assembly and function *Year Immunol.,* 4, 207.

Wildman, B. K., Perrett, T., Abutarbush, S. M., Guichon, P. T., Pittman, T. J., Booker, C. W., Schunicht, O. C., Fenton, R. K. & Jim, G. K. 2008. A comparison of 2 vaccination programs in feedlot calves at ultra-high risk of developing undifferentiated fever/bovine respiratory disease. *Can. Vet. J.,* 49, 463-472.

Williams, G. D., Chang, R.-I. & Brian, D. A. 1999. A Phylogenetically Conserved Hairpin-Type 39 Untranslated Region Pseudoknot Functions in Coronavirus RNA Replication. *J. Virol.,* 73, 8349-8355.

Williams, R. K., Jiang, G. S. & Holmes, K. V. 1991. Receptor for mouse hepatitis virus is a member of the carcinoembryonic antigen family of glycoproteins. *Proc. Natl. Acad. Sci. USA,* 88, 5533-5536.

Wilson, I. A., Skehel, J. J. & Wiley, D. C. 1981. Structure of the haemagglutinin membrane glycoprotein of influenza virus at 3A resolution. *Nature,* 289, 366-373.

Woo, P. C., Lau, S. K., Chu, C. M., Chan, K. H., Tsoi, H. W., Huang, Y., Wong, B. H., Poon, R. W., Cai, J. J., Luk, W. K., Poon, L. L., Wong, S. S., Guan, Y., Peiris, J. S. & Yuen, K. Y. 2005. Characterization and complete genome sequence of a novel coronavirus, coronavirus HKU1, from patients with pneumonia. *J. Virol.,* 79, 884-895.

Wu, Y., Xu, J. C., Shinde, S., Grewal, I., Henderson, T., Flavell, R. A. & Y. Liu. 1995. Rapid induction of a novel costimulatory activity on B cells by CD40 ligand. *Curr. Biol.,* 5, 1303-1311.

Xiao, X., Feng, Y., Chakraborti, S. & Dimitrov, D. S. 2004. Oligomerization of the SARS-CoV S glycoprotein: dimerization of the N-terminus and trimerization of the ectodomain. *Biochem. Biophys. Res. Comm.,* 322, 93-99.

Xu, L. G., Wang, Y. Y., Han, K. J., Li, L. Y., Zhai, Z. & Shu, H. B. 2005. VISA is an adapter protein required for virus-triggered IFN-beta signaling. *Mol. Cell,* 19, 727-740.

Yamadaa, Y. K., Yabea, M., Ohtsukib, T. & Taguchib, F. 2000. Unique N-linked glycosylation of murine coronavirus MHV-2 membrane protein at the conserved O-linked glycosylation site *Virus Res.,* 66, 149-154.

Yamamoto, M., Sato, S., Mori, K., Hoshino, K., Takeuchi, O., Takeda, K. & Akira, S. 2002. Cutting edge: a novel Toll/IL-1 receptor domain-containing adapter that preferentially activates the IFN-beta promoter in the Toll-like receptor signaling. *J. Immunol.,* 169, 6666-6672.

Yao, Q., Fischer, K. P., Li, L., Agrawal, B., Berhane, Y., Tyrrell, D. L., Gutfreund, K. S. & Pasick, J. 2010. Immunogenicity and protective efficacy of a DNA vaccine encoding a chimeric protein of avian influenzahemagglutinin subtype H5 fused to CD154 (CD40L) in Pekin ducks. *Vaccine,* 28, 8147-8156.

Yokomori, K., Baker, S. C., Stohlman, S. A. & Lai, M. M. C. 1991. Hemagglutinin-Esterase-Specific Monoclonal Antibodies Alter the Neuropathogenicity of Mouse Hepatitis Virus. *J Virol,* 66, 2865-2874.

Yokomori, K., Banner, L. R. & Lai, M. M. C. 1991. Heterogeneity of gene expression of the hemagglutinin-esterase (HE) protein of murine coronaviruses. Virology 183:647-657. *Virology,* 183, 647-657.

Yokomori, k., Monica, N. L., Makino, S., Shieh, C.-K. & Lai., M. M. C. 1989. Biosynthesis, structure, and biological activities of envelope protein gp65 of murine coronavirus. *Virology,* 173, 683-691.

Yoneyama, M., Kikuchi, M., Natsukawa, T., Shinobu, N., Imaizumi, T., Miyagishi, M., Taira, K., Akira, S. & Fujita, T. 2004. The RNA helicase RIG-I has an essential function in double-stranded RNA-inducedinnate antiviral responses. *Nat. Immunol.,* 5, 730-737.

Yu, X., Bi, W., Weiss, S. R. & Leibowitz, J. L. 1994. Mouse hepatitis virus gene 5b protein is a new virions envelope protein. *Virology,* 202, 1018-1023.

Zeng, Q., Langereis, M. A., Vlie, A. L. W. v., Huizinga, E. G. & Groot, R. J. d. 2008. Structure of coronavirus hemagglutinin-esteraseoffers insight into corona and influenza virus evolution. *Proc. Natl. Acad. Sci. USA,* 105, 9065–9069.

Zhang, S. Y., Jouanguy, E., Sancho-Shimizu, V., Bernuth, H. v., Yang, K., Abel, L., Picard, C., Puel, A. & Casanova, J. L. 2007. Human Toll-like receptor-dependent induction of interferons in protective immunity to viruses. *Immunol. Rev.,* 2007, 225-236.

Zhang, X., Kousoulas, K. G. & Storz, J. 1991. The hemagglutinin/esterase glycoprotein of bovine coronavirus: sequence and functional comparisons between virulent and avirulent strains. *Virology,* 185, 847-852.

Zhang, X. M., Herbst, W., Kousoulas, K. G. & Storz, J. 1994. Biological and genetic characterization of a hemagglutinating coronavirus isolated from a diarrhoeic child. *J. Med. Virol.,* 44, 152-161.

Zhou, M. & Collisson, E. W. 2000. The amino and carboxyl domains of the infectious bronchitis virus nucleocapsid protein interact with 3′ genomic RNA. *Virus Res.,* 67, 31-39.

CHAPTER III
BRCoV VACCINOLOGY

Introduction

The greatest health-associated impact on beef cattle profitability is Bovine Respiratory Disease (BRD), commonly known as “shipping fever”, a disease complex typically associated with multiple etiologies (Smith, 1998). Predisposing factors commonly associated with the risk of BRD development include stress associated with fasting and transport, introduction of microbial pathogens via stressful comingling of calves, rapid environmental and weather changes, age, and sudden nutritional alterations (Callan and Garry, 2002; *reviewed by* Cusack et al., 2003).

Of the numerous microbial agents known to contribute to the development of BRD, one of the most consistently isolated is Bovine Respiratory Coronavirus (BRCoV; Storz et al., 1996; Storz et al., 2000a,b), although this virus is not solely responsible for development of BRD, as a number of other viruses have also been implicated in the development of the disease complex, including BVDV, BHV-1, BRSV, and PI-3. Furthermore, previous research has strongly suggested that respiratory virus infection alone is insufficient for the development of BRD (Martin et al., 1998), although these infections are generally thought to play a pivotal role in potentiating development of the complex (Dunn et al., 1991). The development of BRD is generally thought to follow a common progression involving viral-bacterial synergism (Jericho and Langford, 1978), starting with some form of immune suppression and followed by exposure to respiratory viral pathogen, either in the environment, or, most commonly, carried by other animals and spread during the comingling of animals from different farms during shipping to feedlots (Lathrop et al., 2000). The viral infections are typically followed by

opportunistic overgrowth of commensal bacterial species (Lopez et al., 1976) commonly inhabiting the nasopharynx of healthy animals, some of the most commonly isolated being *Mannheimia haemolytica* and *Pasteurella multocida* (Allen et al., 1991).

Coronaviruses belong to the *Coronaviridae* family of viruses (Cavanagh et al., 1994, 1995) within a relatively newly established order, *Nidovirales*. Coronaviruses are large, approximately 120 nm in diameter pleomorphic virions possessing a cell membrane-derived bi-layer lipid envelope (Pike and Garwes, 1977), from which project numerous prominent, 17-20 nm petal-shaped spikes (McIntosh, 1974), glycoproteins (gp) composed of heavily glycosylated class I fusion proteins anchored within the lipid envelope of the virion. These viruses contain linear, non-segmented, positive sense, single stranded genomic RNA, and possess the largest genomes of the RNA viruses, up to 30 kb for some coronavirus species. Coronaviruses have an impressive host range, infecting a wide variety of mammalian and avian hosts, although host range for each species of virus is typically narrow and well defined, although exceptions to this general rule do exist. For instance, BCoV has been well-documented in its ability sporadically engage in cross-species transmission (Saif, 2004), as viruses very closely related to BCoV have been isolated from wild ruminants (Tsunemitsu et al., 1995), domestic dogs (Erles et al., 2003), and, in one case, a human child (Zhang et al., 1994). One would be remiss in failing to mention the species jump made by the SARS-CoV from its unknown natural reservoir to the palm civet, and from the palm civet to humans (Li et al., 2006).

Although it has been identified as an important factor in the development and progression of the BRD complex, there is currently no effective vaccine for protection against BRCoV infection or the development of BRD, as this disease complex continues

to be a major threat in feedlot environments, in spite of considerable use of various vaccines against other viral agents of BRD (Van Donkersgoed, 1992). There are, however, vaccines commercially available for the prevention of infection by the enteropathic strain of the virus, bovine enteric coronavirus (BECoV), and some research purports that the two strains of BCoV are, in fact, antigenically related and cross-reactive (Hasoksuz et al., 1999), suggesting that a single vaccine developed against BECoV, if administered nasally, may be protective against the respiratory strain of the virus (Decaro et al., 2009; Plummer et al., 2004; Cho et al., 2001). However, additional research needs to be performed to this end, as other researchers have reported that, although BECoV and BRCoV are almost genetically indistinguishable, the two strains have distinct differences in the amino acid sequences, especially for the gene encoding the spike glycoprotein (S; Chouljenko et al, 2001), which is a major antigenic site containing important epitopes for recognition of neutralizing antibody (Deregt et al., 1989). Furthermore, the majority of vaccines commonly used in feedlots for the prevention of BRD have proven to be ineffective against the development of respiratory disease in feedlot animals (Martin, 1983). In addition, IgA-associated mucosal immunity, which would be the primary response to a vaccine administered via the intranasal (IN) route, is in most cases not associated with effective long-term protection from viral infection (*reviewed by* Holmgren and Czerkinsky, 2005), thus necessitating the need for the development of a BRCoV-specific vaccine that results in the development of, preferably, a long-lasting IgG-associated immune response.

The concept of using DNA for vaccine purposes is not a new one, and in many cases it is thought that DNA may be superior in this capacity to both killed virus and live,

attenuated virus vaccines. Firstly, DNA poses no risk of infection as long as infectious viral DNA genomes are not used for vaccination. This is especially important when considering the use of live, attenuated RNA viruses for vaccination purposes. As a result of the use of virus-encoded RDRP for replication purposes, these viruses are notoriously unstable, as this polymerase lacks for the most part any proofreading capability. This is especially true of RNA viruses with particularly large genomes, such as coronaviruses, although some evidence exists suggesting that the coronavirus-encoded RDRP may possess some proofreading capability (Denison et al., 2011), providing the virus some degree of fidelity during genome replication. However, as a result of RDRP-directed replication, even these viruses still undergo a considerable amount of mutation while replicating within even a single host (Holland et al., 1992; Duarte et al., 1994; Lauring and Andino, 2010). In fact, within one host exist a variable mélange of viral quasispecies, rather than a single virus strain. Thus, attenuated RNA viruses are inherently capable of reverting to wild type, as has been shown with the live, attenuated oral Sabin vaccine strain of poliomyelitis (Dunn et al., 1990; Abraham et al., 1993). Secondly, because they contain no viral replicative component, DNA vaccines pose no risk of persistence or the establishment of latency. Although they have shown to be effective, the use of adenoviruses as vaccine vectors has been questioned due to the fact that these DNA viruses are capable of undergoing additional rounds of replication following the initial infection within the host (Imler, 1995). As such, these viral vaccine vectors have the potential to recrudesce, resulting in infection of the host. Additionally, DNA vaccines are relatively easy to construct, and can be designed and manufactured with considerable ease, requiring the use of common cloning techniques, essentially every day molecular

laboratory applications. Furthermore, these DNA vaccines are fairly inexpensive to design and produce and remain stable during transport and storage. Finally, contributing to their overall efficacy is the ability of DNA to essentially self-adjuvant. Recognition of foreign DNA by Toll-like receptors of the innate immune results in interferon release and recruitment of antigen presenting cells such as dendritic cell and macrophages, which are then available for capture of recombinant viral antigen resulting from expression of the DNA vaccine plasmid taken up by cells surrounding the vaccination site.

CD154, also known as CD40 ligand (CD40L) is present primarily on the surface of activated CD4+ T cells (Roy et al., 1993), but also found on the surface of CD8+ T cells (Hermann et al., 1995; Sad et al., 1997), eosinophils (Gauchatet al., 1995), mast cells (Gauchat et al., 1993), and natural killer (NK) cells (Carbone et al., 1997). This integral membrane protein is a 39 kDa type II integral membrane protein and a member of the TNF superfamily (*reviewed by* Grewal and Flavell, 1998; van Kooten and Banchereau, 2000). CD154 ligation with CD40 on DCs results in production of signals required for the activation and survival of both DC and T cells (Banchereau et al., 1998), while ligation of CD154 with CD40 on the surface of B cells influences the maturation of B cells, inducing the secretion of various cytokines as well as the process of class switching (Burden et al., 1996), processes vital to the induction of a robust humoral immune response. The use of CD154 as an immunomodulator in vaccine therapy has its roots in the observation that antigens linked to or administered in conjunction with molecules targeting them to APCs generally increases the response of the immune system versus administration of the antigen alone (Deliyannis et al., 2000). The development of methods for production and expression of recombinant fusion proteins and cDNA

vaccines for the *in vivo* expression of their protein products has paved the way for the use of CD154 fusion to a plethora of antigens as potential vaccines, the idea being that CD154 fused to the expressed recombinant protein will target the relatively small quantities of expressed antigen specifically to APCs within the tissues in which they are expressed. This in turn should result in significantly more efficient antigen uptake and presentation, in turn eliciting a faster and potentially more robust immune response (Manoj et al., 2004). Furthermore, by not only increasing the potential number of secondary signals available for both T and B cell stimulation, but by also mimicking the development of the immunological synapse by clustering both the primary MHC-TCR or TCR-BCR signals and secondary CD40-CD154 signals together in one location, the likelihood that all signals necessary for DC, T cell, and B cell activation will be received may be increased.

Our goal in this study was to develop an effective, robust IgG-stimulating vaccine against BRCoV. In addition, we wanted to compare the ability of soluble antigens alone in eliciting a strong, protective neutralizing antibody response to that of the immunostimulatory effects that have been previously reported for antigens fused to CD154. To this end we chose to compare two prime-boost vaccination strategies: one using DNA expressing either the soluble portion of the BRCoV S gp either alone and boosted with the same purified recombinant protein expressed in a baculovirus system compared with a DNA vaccine expressing the same portion of the S gp fused to the soluble portion of bovine CD154 boosted with its respective purified protein, also expressed via a baculovirus system.

Materials and methods

Construction of a plasmid vector for transient expression of the extracellular domain of the BRCoV S glycoprotein (Sopt)

The DNAworks program (Hoover and Lubkowski, 2002) was used to design synthetic oligonucleotides to be utilized in a PCR-based system for the generation of a codon-optimized BRCoV S glycoprotein (Sopt) corresponding to the S sequence of isolates obtained from a calf having succumbed to fatal pneumonia during a bovine shipping fever epizootic (Chouljenko et al., 2001). Since the S gps differ between the pneumopathogenic and enteropathogenic strains by only seven amino acids, the codon optimized respiratory and enteropathic S gps were first constructed via PCR-assisted overlap extension (Aiyar, Xiang, and Leis, 1996). The BCoV-Lun Sopt 3xFL and BCoV-Ent Sopt 3xFL plasmids were then generated by cloning the respective codon-optimized BCoV S gene, either BCoV-Lun Sopt or BCoV-Ent Sopt, lacking the DNA sequence coding for the signal peptide, into the p3XFLAG-CMV-9 plasmid vector (Sigma, St. Louis, MO).

Cells

African green monkey kidney (Vero) cells were obtained from the American Type Culture Collection (Rockville, MD) and were propagated and maintained in Dulbecco's Modified Eagle Media (DMEM; Invitrogen, Carlsbad, CA) containing sodium bicarbonate, 25 mM HEPES (Invitrogen, Carlsbad, CA), and 10% heat-inactivated fetal bovine serum (FBS).

Cells of the 18-G clone of a human rectal tumor cell line (HRT-18G) were obtained from the American Type Culture Collection (Rockville, MD) and propagated

and maintained in Dulbecco's Modified Eagle Media (DMEM; Invitrogen, Carlsbad, CA) containing sodium bicarbonate, 25 mM HEPES (Invitrogen, Carlsbad, CA), and 10% heat-inactivated FBS. Cells were maintained at 37° C in a 5% CO_2 atmosphere.

SF9 cells, derived from *Spodoptera frugiperda* (Fall Armyworm) IPLB-Sf21-AE cells, were obtained from Invitrogen (Carlsbad, CA). Cells were propagated and maintained in serum-free SF900-II SFM (Invitrogen, Carlsbad, CA) containing 1% penacillin-streptomyacin solution (Invitrogen, Carlsbad, CA), either as attached cells in a monolayer or as a suspension culture. Cells were maintained at 29° C in a 0% CO_2 atmosphere.

Virus

A respiratory coronavirus isolate, BCoV-Lun, was obtained from a calf having succumbed to fatal pneumonia during a bovine shipping fever epizootic (Chouljenko et al., 2001). A viral stock was propagated from virus stored at -80°C by inoculation onto the G clone of an HRT-18 cell line, derived from human rectal tumor cells (Thompkins et al., 1974; Storz et al., 1996). The viral stock was maintained for a low number of passages through HRT-18G cells in culture. Passage 6 viral stock, 0.5 mL, was inoculated onto a tightly confluent monolayer of HRT-18G cells in 2 x T^{150} flasks and rocked at room temperature for 1h to permit virus adsorption onto monolayer. Cells were then incubated at 37°C for the remainder of the infection period. Approximately 48 h following initial infection, cytopathic effects were evident as numerous clumps of dead and dying cells were observed in the cell culture supernatant, indicative of successful infection for this strain of BCoV. Cells were harvested by submitting cell cultures in T^{150} flasks to single freeze-thaw cycle at -80° C. The resulting cell suspension was then

sonicated to further release any remaining cell-associated viral particles and clarified via low-speed centrifugation at 1,000 rpm for 10 min. The resulting supernatant was then separated from the debris pellet, and the viral stock was then aliquoted and stored at -80°C.

Recombinant protein production

The Bac-to-Bac Baculovirus protein expression system (Invitrogen, Carlsbad, CA) was used to produce two versions of the truncated, soluble portion of the Bovine Respiratory coronavirus (BRCoV) codon-optimized spike glycoprotein (Sopt): the soluble portion of Sopt, from amino acid 19 through amino acid 1296 (an EcoRV site; Sol-Sopt), and the second consisting of the same fragment fused after amino acid 1296 to the soluble portion of bovine CD154 (Sopt-CD154). These proteins were designed to contain a 5' 3X Flag sequence and a 3' 9-histidine tag for detection and purification purposes, respectively, and were over-expressed in SF9 insect cells infected with recombinant baculovirus carrying the appropriate expression cassette, either that of Sol-Sopt or Sopt-CD154. Briefly, SF9 cells were seeded into SF900-II cell culture media (Invitrogen, Carlsbad, CA) at a density of $2x10^6$ cells/ mL and infected with recombinant baculovirus carrying the expression cassette for either Sol-Sopt or Sopt-CD154 at an MOI of 5. Cell suspension cultures were maintained at 27°C in an orbital incubator. Cell supernatants were harvested approximately 72 h post-infection, and soluble protein present in the supernatant was isolated and purified via two rounds of cobalt-based immobilized metal affinity chromatography (IMAC) using the Talon Metal Affinity resin (ClonTech Laboratories, Inc., Mountainview, CA). Briefly, SF9 cell cultures were decanted into 50 mL centrifuge tubes and centrifuged at 3000 rpm for 10 min at 27°C.

The resulting supernatant was then decanted into clean 50 mL centrifuge tubes and placed on ice, while the cell pellets were stored at -80°C. A 20% Igepal® CA-630 (Sigma, St. Louis, MO) solution was then added to each supernatant for a final concentration of 1% Igepal (v/v) and inverted to gently mix. Supernatants were then centrifuged for 30 min at 8,000 rpm at 4°C. The resulting supernatants were then decanted into new 50 mL centrifuge tubes and Talon Metal Affinity resin (ClonTech Laboratories, Inc., Mountainview, CA) was added 1:100 (v/v) to each aliquot. Supernatants were then rocked overnight at 4°C to allow binding of His-tagged proteins. Following overnight incubation, supernatants were centrifuged at 4,000 rpm at 4°C. The resulting supernatant was decanted from the pellet, which consisted of the affinity resin bound to His-tagged proteins. Beads were then washed 4 times with native wash buffer (50 mM NaH_2PO_4, 300 mM NaCl, 10 mM Imidazole, pH 7.4). Bound proteins were then eluted twice with 0.5 mL each of native elution buffer (50 mM NaH_2PO_4, 300 mM NaCl, 250 mM Imidazole, pH 7.4) and stored at -80°C until further analysis. The purified proteins were verified via expected size using western immunoblot analysis, using mouse anti-flag antibody (Sigma, St. Louis, MO) as the primary detection antibody. The purified protein concentration was then determined using the Pierce BCA protein quantification assay (Thermo Fisher Scientific, Inc., Rockford, IL), according to manufacturer's instructions.

Immunofluorescence assay

In order to determine viral titer, an immunofluorescence assay (IFA) was performed. Briefly, HRT-18G cells were cultured overnight in 6-well tissue culture plates to obtain a confluent monolayer. Serial 10-fold dilutions of virus from 10^{-2} to 10^{-6} were

prepared in DMEM and 1 mL of these dilutions used to infect individual wells. Plates were then rocked at room temperature for 1h to permit virus adsorption onto monolayer. The cell culture medium was then removed from each well, and wells washed twice with PBS. Fresh cell culture medium was then added to each well and plates incubated at 37°C. After 12h culture medium was removed and cells washed with two volumes of PBS, followed by 1mL ice-cold methanol to fix cells. Cells were incubated in methanol for 15 minutes, followed by washing with ice-cold PBS containing 2% bovine serum albumin (BSA). Wells were then blocked for 1h with PBS containing 2% BSA. To each well was then added the anti-BCoV spike hyperimmune rabbit serum, obtained as discussed previously, diluted 1:2500 in PBS containing 2% BSA and incubated 2h at room temperature with rocking. Cells were then washed twice with PBS containing 2% BSA. Alexafluor 488-conjugated goat anti-rabbit secondary antibody (Invitrogen, Carlsbad, CA) diluted 1:500 in PBS containing 2% BSA was added to each well and incubated at room temperature for 1h with rocking. Infected cells were then visualized and counted via an Olympus fluorescence microscope at an excitation of 488 nm in order to determine the number of infectious virus particles per mL.

Screening of BCoV-negative calves

Veinipuncture was performed on 128 crossbred calves ranging from 7 to 5 mo of age using red top Vacutainer tubes. Blood was allowed to stand for a minimum of 1h, followed by centrifugation at 4,000 rpm for 20 min. The resulting serum supernatant was removed from the red blood cell pellet and aliquoted into 1 mL and 4 mL aliquots. Sera were then centrifuged a second time at 10,000 rpm for 10 min to remove any remaining erythrocytes. Sera samples were then stored at

-80° C until analysis.

To perform the ELISA screening assays, BCoV-Lun virus grown in HRT-18G cells and HRT-18G cell lysates were prepared by submitting cell cultures in T^{75} flasks to two freeze-thaw cycles at -80° C. The resulting cell suspension was then clarified via centrifugation at 4,000 rpm for 30 min., followed by filtering through a 0.45 nm filter. BCoV-Lun and HRT-18G cell lysates were then adsorbed onto 96-well NUNC plates overnight at 4° C as follows: wells A1 through D12 were each coated with 100 μL BCoV-Lun stock diluted 1:10 in ELISA coating buffer, pH 9.6, while wells E1 through H12 were coated with HRT-18G cell lysate diluted 1:10 in ELISA coating buffer (100 mM Na2CO3, 100 mM NaHCO3, pH 9.6). Wells were then washed 4 times with ELISA wash buffer (25 mM Tris, 0.15 M NaCl.0.05% Tween-20) and each well blocked with 100 μL PBS containing 5% goat serum for 1h at room temperature. Wells were then washed 4 times with ELISA wash buffer. Serum samples were diluted 1:500 in PBS containing 5% goat serum and 100 μL added to wells in duplicate. Serum samples taken from cows previously vaccinated and boosted with a commercially available BCoV vaccine were used as high and low positive controls, while gamma-irradiated FBS (γi-FBS) was used a negative control. Following overnight incubation with rocking at 4° C, wells were washed 4 times with ELISA wash buffer. Secondary rabbit anti-cow IgG heavy and light chain antibody conjugated to alkaline phosphatase (ALP; AbCam, Cambridge, MA) was diluted 1:1000 in PBS containing 5% goat serum and 100 μL added to each well. Following 2 h incubation at room temperature with rocking, wells were again washed 4 times with ELISA wash buffer. To each well was then added 50 μL p-nitrophenyl phosphate (p-NPP) and wells incubated bench top for 45 min, followed by

the addition of 50 μL 0.75 M NaOH to stop the reaction. Absorbances were read at 405 nm on a SpectraMax M2 Multimode Plate reader (Molecular Devices, LLC, Sunnyvale, CA). Based on OD_{405} values obtained for the positive and negative controls, a cut-off value of 0.2 was set, and all calves with an $OD_{405} \leq 0.2$ were selected for a second round of screening.

In an attempt to increase the sensitivity of the assay, a second round of screening was designed. As described previously, plates were coated with both BCoV and HRT-18G cell lysates, each diluted 1:10 in ELISA coating buffer, pH 9.6. Serum samples were diluted 1:10, 1:250, and 1:500 in PBS containing 5% goat serum and 100 μL of each added to wells in duplicate per dilution. The assays were then completed as described previously, including treatment with the same secondary antibody. Absorbances were then again read at 405 nm on a SpectraMax M2 Multimode Plate reader (Molecular Devices, LLC, Sunnyvale, CA). Absorbance values obtained for serum on wells coated with HRT-18G cell lysate alone were then subtracted from those obtained for serum on wells coated with BVC-Lun, and seronegative animals were designated as those animals with an OD_{405} for the 1:10 serum dilution < 0.2, as the negative control for each plate read was < 0.1, while the positive control was ≥ 0.55.

Experimental vaccine protocol

Crossbred calves (n=18) weighing, on average, 283.5 kg, previously screened and found to be seronegative for anti-BCoV antibodies were obtained from the LSU AgCenter Reproductive Biology Center in St. Gabriel, LA and delivered to the LSU AgCenter Infectious Disease Isolation Facility (IDIF). Upon arrival on d -7, calves were weighed and blood collected using 10 mL Vacutainer tubes (BD, Franklin Lakes, NJ),

then allotted by sex, 2 steers and 1 heifer per treatment, to one of the following treatment groups: Sol-Sopt vaccinated/uninfected (n=3), Sol-Sopt vaccinated/BCoV-Lun infected (n=3), Sopt-CD154 vaccinated/uninfected (n=3), Sopt-CD154 vaccinated/BCoV-Lun infected (n=3), Mock vaccinated/uninfected (n=3), or Mock vaccinated/BCoV-Lun infected (n=3). Calves were housed 3 per room in negative-pressure, temperature controlled isolation rooms with rubber-coated concrete flooring and fed a formulated, commercially available complete ration once daily. Blood was collected from each animal on d -7, d 0, and every 7 d afterwards for a total of 49 d. Rectal temperatures were obtained for each animal on d 0 and every 7 d afterwards until trial termination on d 49. Nasal swabs were collected for each animal on d 28, 35, and 42 of the experiment and stored in DMEM containing 0.2% Primocin (InvivoGen, San Diego, CA) and Nystatin (24,000 U/mL; Sigma, St. Louis, MO) stored at -80°C until analysis. Likewise, fecal samples were collected on d 28, 35, and 42 and stored at -80°C until analysis. All animal protocols and procedures were approved by the Louisiana State University Agricultural Center Animal Care and Use Committee (IACUC approval no. A2011-09) and all recombinant DNA and infectious agent procedures were approved by the Louisiana State University Inter-Institutional Biological and Recombinant DNA Safety Committee.

DNA vaccine production

The codon-optimized BRCoV spike glycoprotein (Sopt) truncated at nucleotide 3888 and cloned into the pFastBac Dual shuttle vector (Invitrogen, Carlsbad, CA) was used to generate two versions of a DNA vaccine: one encoding only the soluble portion of the S gp (Sol-Sopt), and one encoding the same soluble portion of the S gp fused in frame with the soluble portion of the bovine CD154 molecule (Sopt-CD154**;** GenBank

accession Z48469.1). Polymerase chain reaction utilizing primers specific for each of the two cDNA fragments, Sol-Sopt and Sopt-CD154, and Taq Polymerase (Invitrogen, Carlsbad, CA) were then used to amplify the respective cDNA, resulting in cDNA fragments with overhanging adenosine residues. These overhanging adenosine residues were then used for TOPO TA ligation to clone the resulting PCR fragments into the mammalian expression vector pcDNA3.1 using the pcDNA™3.1/V5-His® TOPO® TA Expression Kit (Invitrogen, Carlsbad, CA). The resulting plasmids were designated pcDNA-Sol-Sopt and pcDNA-Sopt-CD154. Plasmid sequences and correct insert orientation were then verified via sequencing on an ABI Prism 377 DNA sequencer (PE Applied Biosystems). To verify expression of the Sol-Sopt and SoptCD154 recombinant proteins by the mammalian expression vector in mammalian cells, Vero cells were cultured overnight in 6-well tissue culture plates to approximately 95% confluence. Cells were then transfected in duplicate with 4 μg of either pcDNA-Sol-Sopt or pcDNA-Sopt-CD154 per well via Lipofectamine transfection reagent (Invitrogen, Carlsbad, CA) according to manufacturer's specifications**.** A mock transfection was also performed in which cells received PBS containing no plasmid DNA. After 72 h incubation at 37°C, transfected Vero cells were harvested to verify expression of recombinant proteins. Briefly, culture media was removed and cells washed once with PBS. Cells were then removed from each well via gentle mechanical scraping and contents of duplicate wells combined in the same microcentrifuge tube. Following centrifugation and removal of resulting supernatant, cell pellet was lysed using NP-40 containing proteolytic inhibitors for 30 min on ice with intermittent agitation. Following centrifugation at 10,000 rpm for 10 min, the resulting pellet and supernatant were separated and equal volume of Laemmli

sample buffer (Bio-Rad, Hercules, CA) containing 5% β-mercaptoethanol added to each for separate analyses via SDS-PAGE gel electrophoresis and western immunoblot.

DNA and recombinant protein immunization

Plasmids pcDNA-Sol-Sopt and pcDNA-SoptCD154 were amplified in *E. coli* Max Efficiency® DH5α™-T1^{R} competent cells (Invitrogen, Carlsbad, CA), extracted, purified on Qiagen columns (QIAGEN, Inc., Mississauga, ON, Canada), quantified via spectrophotometry, and stored at -20°C until use. On d 0 of the trial, each calf was vaccinated with the DNA vaccine for its respective treatment group, with Sol-Sopt and SoptCD154 vaccinated calves receiving 500 μg plasmid DNA containing the construct of interest in two injections, each containing 250 μg DNA in PBS in a 1 mL volume, while mock-vaccinated calves received 1 mL PBS. Injections were given intramuscularly (IM) on each side of the neck, in the trapezius, pars cervicalis muscle. The initial priming vaccination was then followed 14 days later, on d 14 of the trial, by a booster vaccination containing the purified protein product, either Sol-Sopt or Sopt-CD154, expressed in SF9 insect cells and purified from SF9 insect cell culture supernatant. Calves were inoculated with 20 μg of the respective purified protein in native elution buffer emulsified with TiterMax Gold (TiterMax, Norcross, GA) for a total volume of 1 mL per calf. Injections were given intramuscularly (IM) on the left side of the neck, in the trapezius, pars cervicalis muscle. On this day, in addition to the purified protein product booster vaccine, calves were also administered a second 500 μg dose of the plasmid DNA vaccine containing the appropriate construct of interest, either Sol-Sopt or Sopt-CD154, in two injections, each containing 250 μg of plasmid DNA in PBS in a 1 mL volume, again administered IM on each side of the neck, in the trapezius, pars cervicalis muscle.

Animal challenge protocol

Prior to inoculation with p8 BCoV-Lun on d 28 of the trial, animals were withheld feed for 24 h and water for 12 h, as fasting has long been understood, albeit usually in conjunction with transport, to predispose cattle to development of BRD (Draper et al., 1988; Cole et al., 1986). In addition, 12 h prior to exposure to BCoV-Lun, the previously segregated animals were moved out of their respective rooms and comingled in a common pen, as the stress of establishment of social hierarchy has been associated with increased risk for development of disease in cattle (Martin et al., 1982; Brakel and Leis, 1976). Animals were then first worked through a hydraulic squeeze chute, where pre-infection blood, fecal, and nasal swab samples were taken in an attempt to further stress the animals, as, again, stress has commonly been implicated in the development of respiratory illness in cattle (Filion et al., 1984). Following the sampling procedures, animals were then experimentally infected, with mock-infected animals first receiving an HRT-18 G cell lysate in DMEM intranasally in a 4 mL volume, 2 mL per nostril, via a modified sandblasting gun designed to effectively aerosolize droplets of liquid for introduction into the nasal passages. Animals allotted to groups to be infected with BCoV-Lun were then administered 10^7 infectious virus particles in a 4 mL volume of DMEM containing an HRT-18G cell lysate, with 2 mL administered into each nostril. This was also administered via use of the modified sandblasting gun in order to effectively aerosolize the liquid in which the virus was prepared. Following infection on d 21, animals were observed daily for clinical symptoms of disease.

Bronchoalveolar lavage

Bronchoalveolar lavage was performed on all calves at d 35 of the study as described previously (Brennan et al., 1998). Briefly, a specially designed speculum was used to gain access to the larynx of standing, restrained calves. Once in pace, a guarded culture tube was inserted into the speculum and down the trachea. A sterile, 4 mm outer diameter polyethylene tubing was then passed through the guarded culture tube and seated into a 4 mm diameter airway of the lung. Thirty milliliters of sterile PBS followed by 30 mL of air was then injected into the tube using a sterile 50 mL syringe. Approximately 10 to 20 mL of fluid was then drawn out and collected in 50 mL culture tubes. Lavage fluid was stored at -80°C until analysis.

Virus isolation and real time PCR

In an attempt to determine if animals were actively shedding infectious virus post-infection, cell culture propagation for virus isolation was performed on d 28, 35, and 42 nasal swab and fecal samples, as well as d 35 BAL samples from all calves sampled. Fecal samples were prepared as described previously (Kapil et al., 1991), with minor changes. Briefly, 20% (w/v) fecal samples were prepared in sterile PBS and homogenized via vortexing for 10 s. Samples were then centrifuged at 1000 rpm, 27°C for 15 m, and a 1:10 dilution of the resulting supernatant was prepared in DMEM containing 0.2% Primocin (InvivoGen, San Diego, CA) and Nystatin (24,000 U/mL; Sigma, St. Louis, MO). Diluted fecal samples were then cleared via filtration through a 0.45 μm HT Tuffryn Acrodisc syringe filter (Pall Corp., Ann Arbor, MI), through which 500 μL DMEM containing 0.2% Primocin (InvivoGen, San Diego, CA) and Nystatin (24,000

U/mL; Sigma, St. Louis, MO) was first passed to limit virus adsorbance to the filter membrane.

Nasal swab samples remained at -80°C until preparation for analysis. Briefly, swabs kept in DMEM containing 0.2 % Primocin and Nystatin (24,000 U/mL; Sigma, St. Louis, MO) were allowed to thaw on ice. Swabs were then homogenized in DMEM storage solution via vigorous vortexing for approximately 10 s, followed by centrifugation at 1000 rpm for 15 min at 27°C. Samples were then filtered through a 0.45 μm HT Tuffryn Acrodisc syringe filter (Pall Corp., Ann Arbor, MI), having first passed approximately 500 μL DMEM containing 0.2% Primocin (InvivoGen, San Diego, CA) and Nystatin (24,000 U/mL; Sigma, St. Louis, MO) through the filter to limit virus adsorbance to the filter membrane. Lavage fluid samples were prepared in a similar fashion to the nasal swab samples, except that BAL samples were not diluted in DMEM prior to filtration through 0.45 μm HT Tuffryn Acrodisc syringe filters (Pall Corp., Ann Arbor, MI).

Prepared clinical samples were then used to inoculate HRT-18G cells in culture. Briefly, HRT-18G cells were seeded onto 6-well plates overnight. The resulting tightly confluent monolayers were then washed once with PBS and infected with 500 μL nasal swab, BAL filtrate, or fecal sample filtrate in duplicate per sample and rocked for 30 min at 27°C. Culture plates were then placed into a 37°C incubator, under a 5% CO_2 atmosphere for an additional 30 min. Afterwards, 1 mL DMEM containing 0.2% Primocin (InvivoGen, San Diego, CA) and 2% γ-irradiated FBS (γ-I FBS; Invitrogen, Carlsbad, CA) was added to each well and plates returned to 37°C incubator, under a 5% CO_2 atmosphere. Infection was allowed to proceed for approximately 72 hours, at which

time virus was passaged onto newly confluent monolayer of HRT-18G cells. Following 3 such blind passages in which 1 mL cell culture supernatants were used to inoculate fresh HRT-18G monolayers, cultures were harvested via 3 cycles of freeze-thaw followed by storage at -80°C until analysis via PCR.

Virus neutralization assay

To determine BRCoV specific serum antibody titer in sera samples collected on d -7 and 28 of the study, a series of virus neutralization assays utilizing FACS were developed. The first experiments were designed to verify the positive and negative controls. To this end, HRT-18G cells were seeded to confluence in 24-well plates and allowed to attach at 37°C overnight. Positive control serum samples, those obtained from cows vaccinated and boosted with a commercially available BCoV vaccine and expected, based on ELISA results, to have titers of circulating anti-BCoV antibodies, and negative control samples, γ-i FBS and a serum-free positive infection control, were serially diluted 5-fold, from 1:5 to 1:625 in DMEM containing 0.2% Primocin (InvivoGen, San Diego, CA) but no FBS. Diluted sera were then mixed 1:1 with the BVC-Lun virus stock and incubated on a BD Adams nutator rotational mixer (BD, Franklin Lakes, NJ) at 27°C for 30 min. After the 30 min neutralization period, the serum-treated viruses were then used to infect HRT-18G cells in individual wells of the 24-well plates prepared the day before, 0.15 mL per well, in triplicate per dilution per sample. Following 1 h rocking at 27°C to allow virus attachment, plates were washed once with PBS. Fresh DMEM containing 0.2% Primocin (InvivoGen, San Diego, CA) but no FBS was then added to each well and cultures were then incubated 16 h at 37°C. Following the 16 h infection period, cells were washed once with 0.5 mL PBS and trypsinized with 0.2 mL TrypLE (Invitrogen,

Carlsbad, CA) per well at 37°C until approximately 90% of the cells were no longer attached. Goat serum was then added (Invitrogen, Carlsbad, CA), 50 μL per well, to quench the action of the TrypLE. Remaining attached cells were then dislodged and separated via pipetting, followed by the transfer of the entire contents of each well to a new well within a 96-well U-bottom plate. The 96-well plate containing the transferred cells was then centrifuged at 400 rcf, 4°C, for 7 min. Resulting supernatants were removed from each well and the remaining cell pellets were washed with 0.2 mL ice-cold FACS wash buffer (PBS containing 2.5 mM EDTA and 1% goat serum) and centrifuged again using the previously mentioned conditions. Supernatants were again discarded and cells were resuspended in 100 μL PBS containing 2% goat serum and primary antibody, rabbit serum containing polyclonal antibody against the Sopt-CD154 purified protein, diluted 1:2500 and incubated at 4°C for 30 min. Following a wash with 0.2 mL ice-cold FACS wash buffer, cells were then resuspended in 100 μL PBS containing 2% goat serum and secondary antibody, goat-anti rabbit IgG (heavy and light chains) conjugated to Alexafuor488 (2 mg/mL; Invitrogen, Carlsbad, CA), diluted 1:500 and incubated at 4°C for 30 min. Cells were then washed in 0.2 mL ice-cold FACS wash buffer and centrifuged as outlined previously. Cells were then resuspended in 0.15 mL ice-cold FACS wash buffer and analyzed via the Accuri Flow Cytometer (Ann Arbor, MI). Following verification of the controls as outlined, serum samples were evaluated for ability to actively neutralize BRCoV using the same protocol as outlined above, using the same 5-fold serial dilution scheme. The percentage of cells positively staining for the presence of membrane-associated S gp was determined via flow cytometry and used to

calculate the 50% inhibitory concentration (IC_{50}), the dilution of serum at which approximately 50% of the virus was neutralized.

Results

Construction and expression of gene constructs encoding Sol-Sopt and Sol-Sopt-CD154 fusion protein

An alignment of the amino acid sequences of CD154 genes encoded by different animal species was performed using the COBALT Constraint-based Multiple Protein Alignment Tool available through the National Center for Biotechnology Information (NCBI). The resulting alignment revealed a high degree of conservation among CD154 proteins of rabbit (GenBank accession number AFA36650), bovine (GenBank accession number NP_777049.1), human (GenBank accession number CAA48077.1), mouse (GenBank accession number NP_035746.2), and rat (GenBank accession number NP_445805.1) origin, suggesting potential conservation of CD154 functions among different animal species (Fig. 3.1).

Previous work has shown that the extracellular portion of the CD154 molecule retains the ability to bind its ligand CD40 and function as a adjuvant for the enhancement of immune responses against specific protein antigens (Mazzei et al., 1995). Therefore, the extracellular portion of the CD154 protein spanning amino acids 1-216 were utilized as a potential adjuvant for the enhancement of immune responses against the BRCoV S glycoprotein. A gene segment encoding amino acids 1-216 of the bovine CD154 was

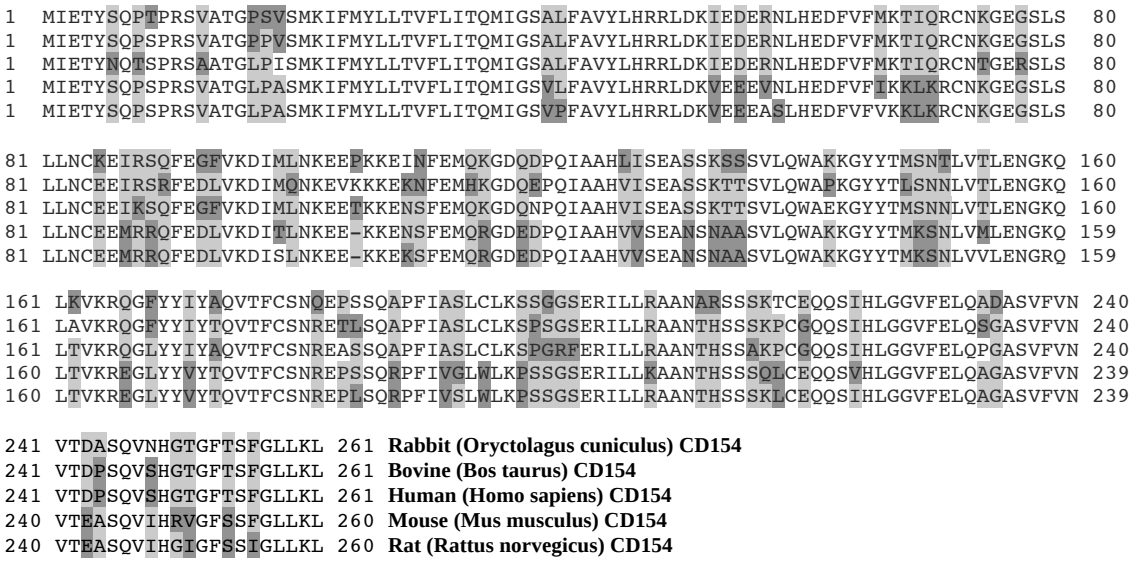

Figure 3.1. Alignment of CD154 amino acid sequences encoded by multiple species shows considerable conservation amongst species.

cloned in-frame with the Sol-Sopt portion of the BRCoV S glycoprotein spanning amino acids 19-1296 into the transient expression vector pCDNA3.1 (Invitrogen, Carlsbad, CA). In addition, the gene segment encoding the Sol-Sopt portion of the S gene was cloned alone for control purposes (Fig. 3.2A). Both of the gene constructs contained a 3XFL epitope tag inserted in-frame at the amino terminus of each protein. Expression of both gene constructs was detected using anti-FLAG monoclonal antibody following transient transfection into Vero cells. Multiple protein species were detected by western immunoblots in cellular extracts derived from Vero cells transfected with either gene construct. Specifically, the Sol-Sopt and Sopt-CD154 proteins were detected in both the cell culture supernatants and cell pellets of transfected cells (Fig. 4.2B: lanes, 1,2, 3, 4). The Sol-Sopt predominant protein species migrated with apparent molecular masses of 150, 75 and 50 kDa. The slowest migrating protein species of 150 kDa corresponded to

the predicted molecular mass of the 1277 aa sequence after post-translational modification (i.e glycosylation). Similarly, the Sol-Sopt-CD154 fusion protein profile revealed a slowly migrating protein species with the apparent molecular mass of approximately 190 kDa, while other protein species with faster migrating mobilities were also detected. The 190 kDa protein species correlated well with the predicted molecular mass of the Sol-Sopt-CD154 protein (1512 aa), considering the effect of glycosylation of the Sol-Sopt portion of the molecule in Vero cells. Both proteins were detected in supernatants of transfected cells in substantial amounts considering that a small volume of supernatants were tested in comparison to cell pellets, which were concentrated in much smaller volumes.

Construction of recombinant baculoviruses expressing Sol-Sopt and Sopt-CD154 proteins in insect cells

To enable the production of relatively large amounts of proteins suitable for vaccine testing, recombinant baculoviruses were constructed expressing the Sol-Sopt and Sopt-CD154 gene constructs as described in Materials and Methods. Sf9 cellular extracts obtained after infection with a recombinant baculovirus expressing either Sol-Sopt or Sopt-CD154 were tested for the presence of the proteins in western immunoblots reacted with anti-3XFL antibody (Fig. 3.3). The slowest migrating protein species of 150 and 190 kDa corresponding to the Sol-Sopt and Sopt-CD154 proteins (lanes 3-4 and 1-2, respectively) were readily detected in both supernatant (lanes 2 and 4) and cellular extract (lanes 1 and 3) samples, as was previously detected in transient expression in Vero cells (Fig. 4.2). A relatively large amount of each recombinant protein was detected in supernatant samples in comparison with samples obtained from cellular extracts,

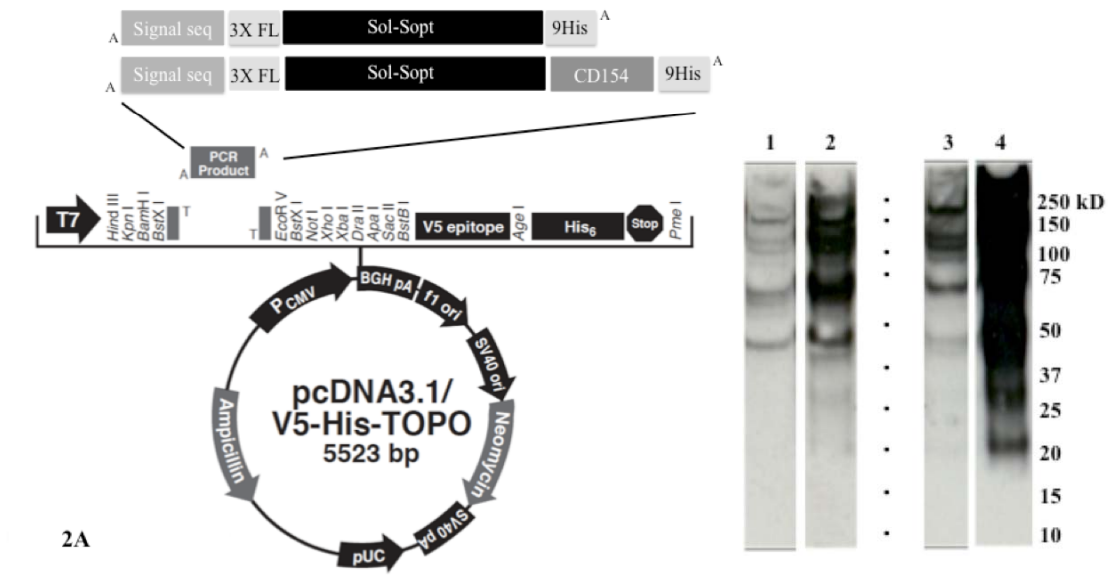

Figure 3.2. Sol-Sopt and Sopt-CD154 constructs were cloned into the pcDNA3.1 mammalian expression vector and transiently transfected into Vero cells. A high level of expression of both recombinant proteins was observed in cell pellets as well as within cell culture supernatants.

suggesting that both proteins were efficiently secreted into extracellular spaces (Fig.3.3).

Animal vaccination protocol

Calves (n=129) were pre-screened for the presence of anti-BRCoV antibodies using an indirect ELISA developed for this purpose and animals were selected for the vaccination experiments, based on their apparent lack of anti-BRCoV antibody (see Materials and Methods). The animals were allotted into two treatment groups based on sex. A prime-boost vaccination strategy involving priming with the pcDNA gene constructs followed by a booster vaccination with mixtures of purified proteins (Sol-Sopt or Sopt-CD154) mixed with pcDNA gene constructs expressing each protein, respectively was administered depending on animal treatment group (Figure 3.4). All animals were infected intranasally with BRCoV at d 28 post vaccination and sacrificed at

day 42 post vaccination after bronchial and blood samples were obtained at different time intervals as described in Materials and Methods.

Humoral immune responses of vaccinated animals.

The relative amounts of anti-BRCoV antibodies were obtained for the different animal groups at different times post vaccination by an indirect ELISA. The highest amounts of circulating anti-BRCoV antibodies were detected on d 35 in the group of animals vaccinated with the Sopt-CD154 gene and purified protein mixture that were then challenged intranasally with BRCoV in comparison to animals that received either Mock-vaccination ($p = 0.0184$) or the Sol-Sopt gene and protein mixtures and challenged by BRCoV ($p = 0.0663$). In addition, on d 35 of the study antibody responses of animals immunized with either vaccine and challenged were higher than that of mock-vaccinated animals challenged with virus ($p \leq 0.0001$). All other pairwise comparisons failed to show any statistically significant differences (Fig. 3.5). ELISA profiles of average relative circulating antibody concentrations within treatment group revealed a time-dependent increase of antibody levels between day 0 and day 35 for animals vaccinated with either Sol-Sopt or Sopt-CD154 gene and protein mixtures. The greatest increase was observed for the Sopt-CD154 immunized animals from day 0 to day 35 ($p< 0.0012$; Fig. 3.6A) in comparison to that of all other animals (Fig. 3.6). Antibody neutralization assays revealed that only animals vaccinated with the Sopt-CD154 gene and protein mixtures produced a significant increase in IC_{50} titers from day -7 to day 28 post vaccination.

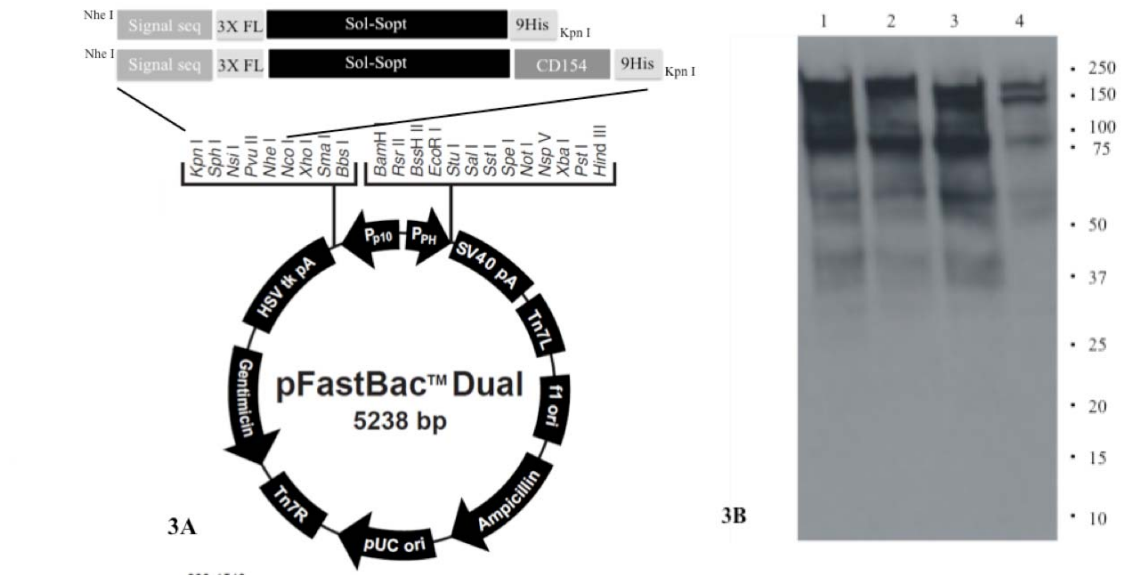

Figure 3.3. Sol-Sopt and Sopt-CD154 constructs were cloned into the pFastBac Dual baculovirus shuttle vector and used to construct recombinant baculoviruses. A high level of expression of both recombinant proteins was observed in infected SF9 cell pellets as well as cell culture supernatants.

Discussion

Fusion proteins containing the soluble portion of CD154 have been extensively utilized for the augmentation of humoral and cellular immune responses against a variety of protein antigens. In this work, we constructed and tested fusion proteins consisting of the soluble portion of the bovine CD154 fused-in-frame to the extracellular domain of the BRCoV S glycoprotein. Vaccination and challenge experiments revealed that the bovine CD154 protein enhanced humoral immune responses of vaccinated animals, suggesting that it can be effectively utilized for the production of subunit vaccines capable of eliciting robust humoral responses against multiple antigens in cattle.

Purified Sol-Sopt-CD154 protein was initially utilized to immunize rabbits (see chapter IV). These immunizations resulted in the production of high titer antibody that

specifically reacted with BRCoV S glycoprotein in western immunoblots (see chapter IV). It is highly possible that the high degree of amino acid conservation observed between the rabbit and bovine CD154 proteins allowed for the bovine CD154 to function in rabbits as an adjuvant, suggesting that the bovine CD154 may be useful in generating monospecific antibodies against specific proteins in this species. It is important to note that the coronavirus S glycoprotein is known to form dimers and trimers, suggesting that multimeric forms of the Sopt-CD154 proteins are formed (Xiao et al., 2004), which may then very likely further potentiate the adjuvant properties of the CD154 moieties by enhanced development of the immunological synapse between APCs, T cells, and B cells.

Efficient expression of the Sol-Sopt-CD154 protein was observed in both transient expression in Vero cells, as well as in insect cells after infection with recombinant baculoviruses. Of particular interest was the fact that this protein was readily secreted to extracellular spaces despite its high molecular mass. These results suggest that this rather large fusion protein may be readily purified and concentrated from supernatants of cell cultures, substantially lowering the costs associated with purification from cellular extracts. Furthermore, expression of these proteins in a mammalian expression system may result in post-translational modifications more similar to those observed within the native host, as the insect cell and mammalian post-translational pathways, especially those involved in glycosylation, differ considerably (Thomas et al., 2009). Post translational modification of this fusion protein may result in an even more robust immune response and the production of higher-affinity neutralizing antibodies targeting conformational epitopes.

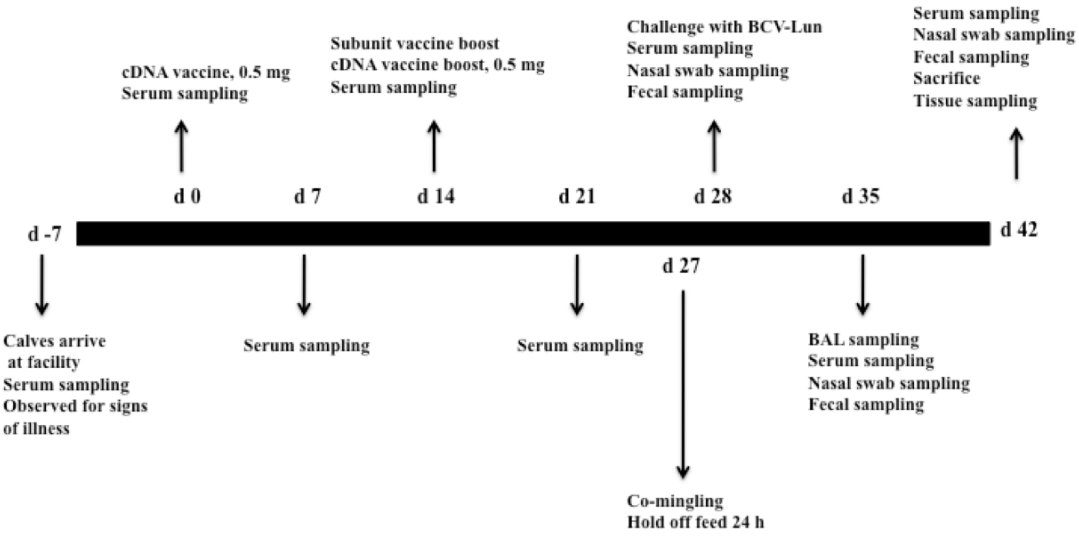

Figure 3.4. Timeline of animal vaccination and experimental protocol.

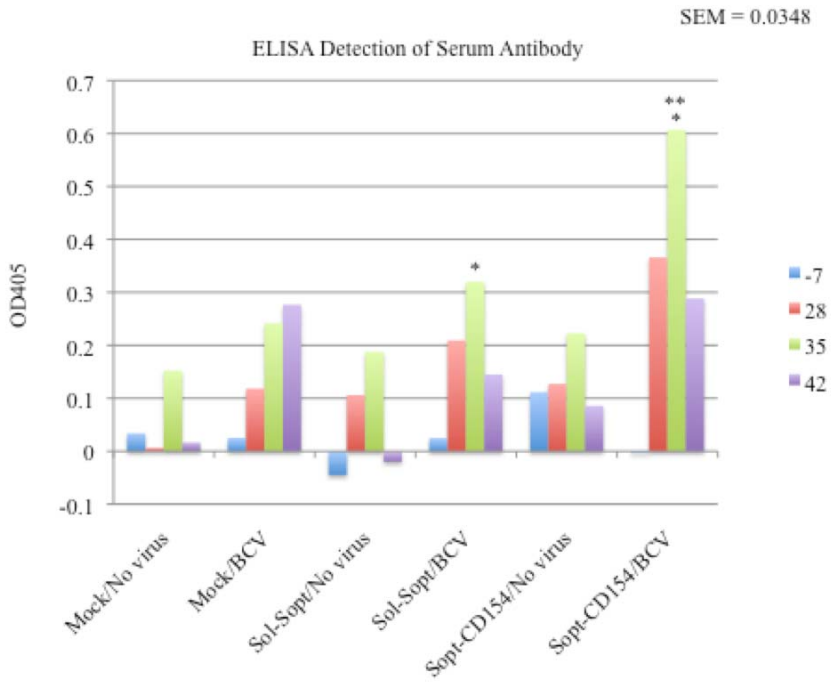

Figure 3.5. ELISA detection of circulating serum anti-BRCoV S glycoprotein antibodies in calves vaccinate with either the mock, Sol-Sopt, or Sopt-CD154 vaccines and infected or not infected with BRCoV.

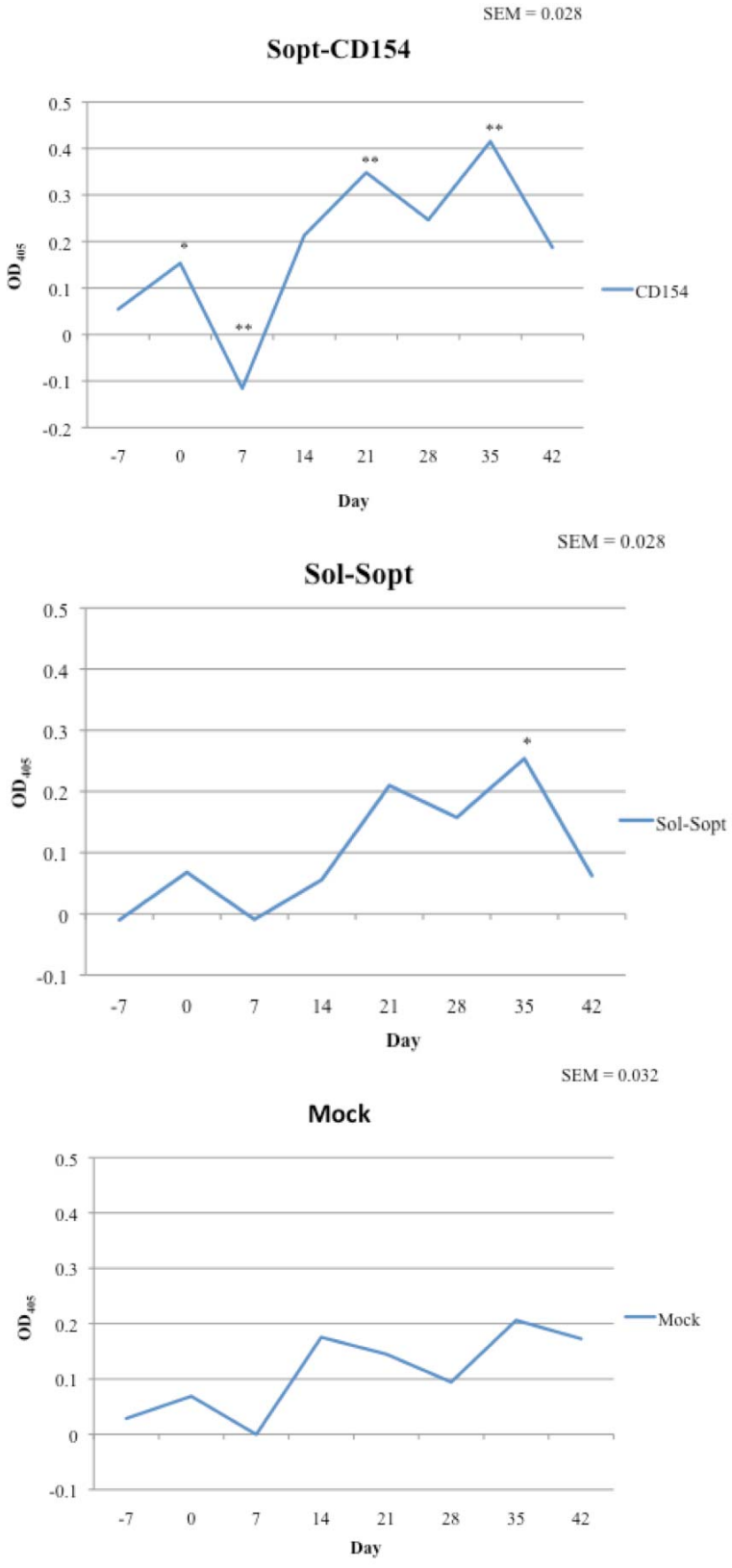

Figure 3.6. ELISA data expressed as group means by day.

Animal vaccination experiments strongly suggested that prior immunization with the Sopt-CD154 gene and protein mixtures generated the strongest immune response after challenge with the virus, suggesting that the presence of CD154 protein was responsible for the observed enhancement of humoral responses. The fact that this enhancement was observed only after challenge with the virus suggests that a strong memory immune response was present that was not detected in the absence of viral infection. This observation, in turn, then suggests that infection completes immunological stimulation initiated by the CD154 molecule. Additional experiments would be required to assess whether long-term immunological memory exists in animals immunized with the Sopt-CD40L fusion protein.

Previous attempts to utilize the bovine CD154 for the production of subunit vaccines for bovine herpes virus type-1 showed strong humoral immune responses in sheep, but not in cattle (Manoj et al., 2003; 2004). Manoj and colleagues reported that fusion of the gene encoding bovine CD154 to that encoding a truncated version of BHV-1 gD and inserted into a plasmid for use as a DNA vaccine elicited a significantly enhanced antibody response in sheep versus animals vaccinated with a DNA plasmid expressing only the truncated portion of BHV-1 gD (2003). However, when this study was performed in cattle the researchers failed to see the same response (Manoj et al., 2004). It is possible that the positive results obtained with the Sopt-CD154 fusion proteins are due to the ability of the S protein to efficiently form multimeric complexes predicted to augment humoral immune responses.

The experiments described here were not able to discern whether humoral immune responses against the BRCoV S glycoprotein may be protective against BRCoV

infection largely because there were minimal clinical signs and practically no disease symptoms observed in infected animals other than a transient temperature elevation and the recovery of infectious virus from fecal samples of one of three animals infected after being mock-vaccinated. The notable exception that one animal that relatively high titers of virus were detected in fecal samples of one-of-three mock-vaccinated animals, while no virus was detected in vaccinated animals. Additional experiments are needed using gnotobiotic calves to maximize disease parameters associated with BRCoV infection. Moreover, BRCoV virulent strains serially passaged in gnotobiotic calves may be needed to ensure preservation of their virulence characteristics, since it is known that only few passages of BRCoV strains in cell culture results in the generation of BRCoV quasispecies potentially significantly decreasing the virulence characteristics of viral stocks (Chouljenko and Kousoulas, unpublished). Given these results, it is highly likely that cocktails of fusion proteins and gene constructs expressing multiple BRCoV antigens, as well as antigens specified by other pathogens involved in shipping fever could be combined to produce efficacious vaccine approaches that can protect animals against multiple viral and bacterial pathogens involved in BRD. In this regard, both DNA immunogens and easily purified fusion proteins containing the bovine CD154 protein portions may constitute a cost effective strategy to immunize cattle against a variety of pathogens.

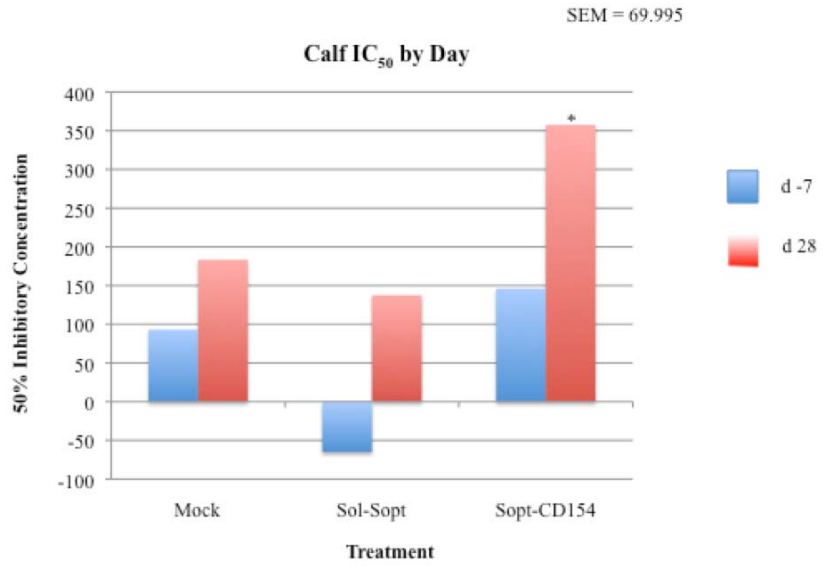

Figure 3.7. Serum virus neutralization expressed as 50% inhibitory concentration (IC_{50}).

References

Abraham, R., Minor, P., Dunn, G., Modlin, J. F. & Ogra, P. L. 1993. Shedding of virulent poliovirus revertants during immunization with oral poliovirus vaccine after prior immunization with inactivated polio vaccine. *J. Infect. Dis.,* 168**,** 1105-1109.

Aiyar, A., Xiang, Y. & Leis, J. 1996. Site-directed mutagenesis using overlap extension PCR. *Methods Mol. Biol.,* 57**,** 177-191.

Allen, J. W., Viel, L., Bateman, K. G., Rosendal, S., Shewen, P. E. & Physick-Sheard, P. 1991. The microbial flora of the respiratory tract in feedlot calves: associations between nasopharyngeal and bronchoalveolar lavage cultures. *Can. J. Vet. Res.,* 55**,** 341-346.

Banchereau, J. & Steinman, R. M. 1998. Dendritic cells and control of immunity. *Nature,* 392**,** 245-252.

Brakel, W. J. & Leis, R. A. 1976. Impact of social disorganization on behavior, milk yield, and body weight of dairy cows. *Journal of Dairy Science,* 59**,** 716-721.

Brennan, R. E., Corstvet, R. E. & Paulsen, D. B. 1998. Antibody responses to Pasterella haemolytica 1:A and three of its outer embrane proteins in serum, nasal

secretions, and bronchoalveolar lavage fluid from calves. *Am. J. Vet. Res.,* 59**,** 727-732.

Callan, R. J. & Garry, F. B. 2002. Biosecurity and bovine respiratory disease. *Vet. Clin. North Am. Food Anim. Pract.,* 18**,** 57-77.

Carbone, E., Ruggiero, G., Terrazzano, G., Palomba, C., Manzo, C., Fontana, S., Spits, H., Kärre, K. & Zappacosta, S. 1997. A new mechanism of NK cell cytotoxicity activation: the CD40-CD40 ligand interaction. *J. Exp. Med.,* 185**,** 2053-2060.

Cavanagh, D., Brian, D. A., Brinton, M. A., Enjuanes, L., Holmes, K. V., Horzinek, M. C., Lai, M. M., Laude, H., Plagemann, P. G. W., Siddell, S. G., Spaan, W., Taguchi, F. & Talbot, P. J. 1995. Coronaviridae. In: Murphy, F. A., Fauquet, C. M., Bishop, D. H. L., Ghabrial, S. A., Jarvis, A. W., Martelli, G. P., Mayo, M. A. & Summers, M. D. (eds.) *"Virus Taxonomy. Sixth Report of the International Committee on Taxonomy of viruses".* Springer-Verlag, Vienna and New York.

Cavanagh, D., Brian, D. A., Brinton, M. A., Enjuanes, L., Holmes, K. V., Horzinek, M. C., Lai, M. M. C., Laude, H., Plagemann, P. G. W., Siddell, S. G., Spaan, W., Taguchi, F. & Talbot, P. J. 1994. Revision of the taxonomy of the Coronavirus,Torovirus and Arterivirus genera. *Arch. Virol.,* 135**,** 227-237.

Cho, K. O., Hoet, A., Loerch, S. C., Wittum, T. E. & Saif, L. J. 2001. Evaluation of concurrent shedding of bovine coronavirus via the respiratory tract and enteric route in feedlot cattle. *Am J Vet Res,* 62**,** 1436-1441.

Chouljenko, V. N., Lin, X. Q., Storz, J., Kousoulas, K. G. & Gorbalenya, A. E. 2001. Comparison of genomic and predicted amino acid sequences of respiratory and enteric coronaviruses isolated from the same animal with fatal shipping pneumonia. *Journal of General Virology,* 82**,** 2927-2933.

Cole, N. A., Phillips, W. A. & Hutcheson, D. P. 1986. The effect of pre-fast diet and transport on nitrogen metabolism in calves. *Journal of Animal Science,* 62**,** 1719-1731.

Cusack, P. M. V., McMeniman, N. & Lean, I. J. 2003. The medicine and epidemiology of bovine respiratory diseases in feedlots. *Australian Veterinary Journal,* 81**,** 480-487.

Decaro, N., Mari, V., Campolo, M., Lorusso, A., Camero, M., Elia, G., Martella, V., Cordioli, P., Enjuanes, L. & Buonavoglia, C. 2009. Recombinant Canine Coronaviruses Related to Transmissible Gastroenteritis Virus of Swine Are Circulating in Dogs. *J. Virol.,* 83**,** 1532-1537.

Deliyannis, G., Boyle, J. S., Brady, J. L., Brown, L. E. & Lew, A. M. 2000. A fusion DNA vaccine that targets antigen-presenting cells increases protection from viral challenge. *Proc. Natl. Acad. Sci. USA,* 97**,** 6676-6680.

Denison, M. R., Graham, R. L., Donaldson, E. F., Eckerle, L. D. & Baric, R. S. 2011. An RNA proofreading machine regulates replication fidelity and diversity. *RNA Biol.,* 8**,** 270-279.

Deregt, D., Gifford, G. A., Ijaz, M. K., Watts, T. C., Gilchrist, J. E., Haines, D. M. & Babiuk, L. A. 1989. Monoclonal Antibodies to Bovine Coronavirus Glycoproteins E2 and E3: Demonstration of in vivo Virus-neutralizing Activity. *Journal of General Virology,* 70**,** 993-998.

Donkersgoed, J. V. 1992. Meta-analysis of field trials of antimicrobial mass medication for prophylaxis of bovine respiratory disease in feedlot cattle. *Canadian Veterinary Journal,* 33**,** 786-795.

Draper, H. H., Dhanakoti, S. N., Hadley, M. & Piche, L. A. 1988. Malondialdehyde in biological systems. In: Chow, C. K. (ed.) *Cellular Antioxidant Defense Mechanisms.* CRC Press, Florida.

Duarte, E. A., Novella, I. S., Weaver, S. C., Domingo, E., Wain-Hobson, S., Clarke, D. K., Moya, A., Elena, S. F., Torre, J. C. d. l. & Holland, J. J. 1994. RNA virus quasispecies: significance for viral disease and epidemiology. *Infect. Agents Dis.,* 3**,** 201-214.

Dunn, G., Begg, N. T., Cammack, N. & Minor, P. D. 1990. Virus excretion and mutation by infants following primary vaccination with live oral poliovaccine from two sources. *J. Med. Virol.,* 32**,** 92-95.

Filion, L. G., Willson, P. J., Bielefeldt-Ohmann, H., Babiuk, L. A. & Thomson, R. G. 1984. The possible role of stress in the induction of pneumonic pasteurellosis. *Can J Comp Med,* 48**,** 268-274.

Gauchat, J.-F., Henchoz, S., Fattah, D., Mazzei, G., Aubry, J.-P., Jomotte, T., Dash, L., Page, K., Solari, R., Aldebert, D., Capron, M., Dahinden, C. & Bonnefoy, J.-Y. 1995. CD40 ligand is functionally expressed on human eosinophils. *Eur. J. Immunol.,* 25**,** 863-865.

Gauchat, J.-F., Henchoz, S., Mazzei, G., Aubry, J.-P., Brunner, T., Blasey, H., Life, P., Talabot, D., Flores-Romo, L., Thompson, J., Kishi, K., Butterfield, J., Dahinden, C. & Bonnefoy, J.-Y. 1993. Induction of human IgE synthesis in B cells by mast cells and basophils. *Nature,* 365.

Grewal, I. S. & Flavell, R. A. 1998. CD40 and CD154 in cell-mediated immunity. *Annu. Rev. Immunol.,* 16**,** 111-135.

Hasoksuz, M., Lathrop, S. L., Gadfield, K. L. & Saif, L. J. 1999. Isolation of bovine respiratory coronaviruses from feedlot cattle and comparison of their biological and antigenic properties with bovine enteric coronaviruses. *Am J Vet Res,* 60**,** 1227-1233.

Hermann, P., Van-Kooten, C., Gaillard, C., Banchereau, J. & Blanchard, D. 1995. CD40 ligand-positive CD8+ T cell clones allow B cell growth and differentiation. *Eur. J. Immunol.,* 25**,** 2972-2977.

Holland, J. J., Torre, J. C. D. L. & Steinhauer, D. A. 1992. RNA virus populations as quasispecies. *Curr. Top Microbiol. Immunol.,* 176**,** 1-20.

Holmgren, J. & Czerkinsky, C. 2005. Mucosal immunity and vaccines. *Nature Med.,* 11**,** S45-S53.

Hoover, D. M. & Lubkowski, J. 2002. DNAWorks: an automated method for designing oligonucleotides for PCR-based gene synthesis. *Nucleic Acids Res.,* 30**,** e43.

Imler, J.-L. 1995. Adenovirus vectors as recombinant viral vaccines. *Vaccine,* 13**,** 1143-1151.

Jericho, K. W. F. & Langford, E. V. 1978. Pneumonia in Calves Produced with Aerosols of Bovine Herpesvirus 1 and Pasteurella haemolytica. *Can. J. Comp. Med.,* 42**,** 269-277.

Kapil, S., Pomeroy, K. A., Goyal, S. M. & Trent, A. M. 1991. Experimental infection with a virulent pneumoenteric isolate of bovine coronavirus. *J vet Diagn Invest,* 3**,** 88-89.

Lathrop, S. L., Wittum, T. E., Brock, K. V. & Saif, L. J. 2000. Association between infection of the respiratory tract attributable to bovine coronavirus and health and growth performance of cattle in feedlots. *Am J Vet Res,* 61**,** 1062-1066.

Lauring, A. S. & Andino, R. 2010. Quasispecies Theory and the Behavior of RNA Viruses. *PLOS Pathog.,* 6**,** 1-8.

Lopez, A., Thomson, R. G. & Savan, M. 1976. The pulmonary clearance of Pasteurella hemolytica in calves infected with bovine parainfluenza-3 virus. *Can J Comp Med,* 40**,** 385-391.

Manoj, S., Griebel, P., Babiuk, L. A. & Hurk, S. V. D. L.-v. d. 2004. Modulation of immune responses to bovine herpesvirus-1 in cattle by immunization with a DNA vaccine encoding glycoprotein D as a fusion protein with CD154. *Immunol.,* 112**,** 238-338.

Manoj, S., Griebel, P. J., Babiuk, L. A. & Hurk, S. V. D. L.-V. D. 2003. Targeting with bovine CD154 enhances humoral immune responses induced by a DNA vaccine in sheep. *J. Immunol.,* 170**,** 989-996.

Martin, S. W. 1983. Vaccination: Is it effective in preventing respiratory disease or influencing weight gains in feedlot calves? *Canadian Veterinary Journal,* 24.

Martin, S. W., Meek, A. H. & Davis, D. G. 1982. Factors associated with mortality and treatment costs in feedlot calves: The Bruce County Beef Project, years 1978, 1979, 1980. *Can J Comp Med,* 46**,** 341-349.

Martin, S. W., Nagy, E., Shewen, P. E. & Harland, R. J. 1998. The association of titer to bovine coronavirus with treatment for bovine respiratory disease and weight gain in feedlot calves *Can J Vet Res,* 62**,** 257-261.

Mazzei, G. J., Edgerton, M. D., Losberger, C., Lecoanet-Henchoz, S., Graber, P., Durandy, A., Gauchat, J.-F., Bernard, A., Allet, B. & Bonnefoy, J.-Y. 1995. Recombinant Soluble Trimeric CD40 Ligand Is Biologically Active. *J. Biol. Chem.,* 270**,** 7025-7028.

Pike, B. V. & Garwes, D. J. 1977. Lipids of transmissible gastroenteritis virus and their relation to those of two different host cells. *J. Gen. Virol.,* 54**,** 531-535.

Plummer, P. J., Rohrbach, B. W., Daugherty, R. A., Daugherty, R. A., Thomas, K. V., Wilkes, R. P., Duggan, F. E. & Kennedy, M. A. 2004. Effect of intranasal vaccination against bovine enteric coronavirus on the occurrence of respiratory tract disease in a commercial backgrounding feedlot. *Journal of the Veterinary Medical Association,* 225**,** 726-731.

Roy, M., AruVo, A., Ledbetter, J., Linsley, P., Kehry, M. & Noelle, R. 1995. Studies on the interdependence of gp39 and B7 expression and function during antigen-speciWc immune responses. *Eur. J. Immunol.,* 25**,** 596-603.

Sad, S., Krishnan, L., Bleackley, R. C., Kagi, D., Hengartner, H. & Mosmann, T. R. 1997. Cytotoxicity and weak CD40L expression of CD8+ type 2 cytotoxic T cells restricts their potential B cell helper activity. *Eur. J. Immunol.,* 27.

Saif, L. J. 2004. Animal coronavirus vaccines: lessons for SARS. *Dev. Biol.,* 119**,** 129-140.

Smith, R. A. 1998. Impact of disease on feedlot performance: a review. . *Journal of Animal Science,* 76**,** 272-274.

Storz, J., Purdy, C. & Lin, X. B. M. 2000a. Isolation of respiratory bovine coronavirus, other cytocidal virus, and *Pasturella* spp. from cattle involved in two natural

outbreaks of shipping fever. *Journal of the Veterinary Medical Association,* 216**,** 1599-1604.

Storz, j., Stine, L., Liem, A. & Anderson, G. A. 1996. Coronavirus isolation from nasal swab samples in cattle with signs of respiratory tract disease after shipping. *Journal of the Veterinary Medical Association,* 208**,** 1452-1455.

Storz, J., XiaoQing, L., Purdy, C. W., Chouljenko, V. N., Kousoulas, K. G., Enright, F. M., Gilmore, W. C., Briggs, R. E. & Loan, R. W. 2000b. Coronavirus and pasteurella infections in bovine shipping fever pneumonia and Evans criteria for causation. *Journal of Clinical Microbiology,* 38**,** 3291-3298.

Tsunemitsu, H., el-Kanawati, Z. R., Smith, D. R., Reed, H. H. & Saif, L. J. 1995. Isolation of coronaviruses antigenically indistinguishable from bovine coronavirus from wild ruminants with diarrhea. *J. Clin. Microbio.,* 33**,** 3264-3269.

Van Kooten, C. & Banchereau, J. 2000. CD40-CD40 ligand. *J. Leukoc. Biol.,* 67**,** 2-17.

Xiao, X., Feng, Y., Chakraborti, S. & Dimitrov, D. S. 2004. Oligomerization of the SARS-CoV S glycoprotein: dimerization of the N-terminus and trimerization of the ectodomain. *Biochem. Biophys. Res. Comm.,* 322**,** 93-99.

Zhang, X. M., Herbst, W., Kousoulas, K. G. & Storz, J. 1994. Biological and genetic characterization of a hemagglutinating coronavirus isolated from a diarrhoeic child. *J. Med. Virol.,* 44**,** 152-161.

CHAPTER IV
DESIGN OF DIAGNOSTIC TOOLS AND APPLICATIONS

Introduction

The use of antibodies within the molecular biology laboratory is a particularly common one, as they have a plethora of applications, including immunohistochemistry, receptor-site blocking and binding, and western blotting. Antibodies can be created against virtually any protein molecule of sufficient size and relative antigenicity. Even those proteins not possessing adequate size may act as haptans when fused to or recombined with larger, more antigenic peptides. Antibody applications abound in the field of virology, where both polyclonal and monoclonal antibodies are used in receptor binding assays, virus detection and microscopy studies, protein-protein interaction assays, and fluorescence-assisted cell sorting, just to name a few. In fact, the argument could easily be made that a vast amount of what we in the field of virology understand about viruses has been a result of the use of antibody applications in the laboratory.

Antibodies are generated by activated B cells and plasma cells of the immune system in response to exposure to foreign antigen. These immunoglobulins may be divided into 5 different classes: IgM, IgD, IgG, IgE, and IgA. Avians are an exception to this, as they express a variation of IgG called IgY (Warr et al., 1985). The class designation of antibody is based on its C region, a result of genetic rearrangement of the μ, γ, δ, ε, and α heavy chain genes, respectively, during B cell maturation as discussed previously. The majority of Ig are monomers, with IgM and IgA being exceptions; these molecules are, in soluble form, pentamers and dimers, respectively, linked by co-expressed J chain molecules. Antibodies are roughly Y-shaped in structure and may interact to form aggregates. The top of the Y-structure contains the V, or variable, region,

containing three hypervariable sequences that undergo affinity maturation during B cell maturation and are responsible for providing the extreme specificity usually associated with antibody, as it is these areas that recognize and interact with antigen. The bottom, or stem, of the Y contains the C, or constant, region, responsible for interacting with effector cells and molecules. This structure is composed of two heavy chains and two light chains linked both to each other as well as to one another via disulfide bonds (*reviewed by* Wang et al., 2007).

The spike gp (S) of coronaviruses is arguably the most distinctive coronaviral protein, as it projects some 17 to 20 nm out from the surface of the viral envelope, giving the virus the appearance of a crown. The gp is large, ranging anywhere from 1160 amino acids in the IBV S to 1452 in FCV and contains numerous glycosylation sites, ranging in number anywhere from 21 to 35, all of which are exclusively N-linked (Holmes et al., 1981; Rottier et al., 1981). Responsible for facilitating not only host receptor recognition and binding (Collins et al., 1982; Godet et al., 1994; Kubo et al., 1994) but also virus-host and host-host membrane fusion and viral entry (Gallagher et al., 1991; Qiu et al., 2006), S plays a vital role in promoting infection and has been implicated as a significant factor influencing virulence (Navas et al., 2001), as well as both tissue (Navas et al., 2001; Phillips et al., 2001; Navas and Weiss, 2003) and host tropism (Li et al, 2006). The protein exists on the virion surface as a trimer (Delmas and Laude, 1990), with the S1 subunits, the approximately N-terminal one-half of the polypeptide, interacting to form the globular head and the S2 subunits, comprised of the approximately C-terminal one-half of the polypeptide, interacting to form the transmembrane stalk (de Groot et al., 1987).

The Coronavirus S can be divided into two approximately 90 kD subunits, the S1 and S2 domains of the protein, which can be cleaved from one another in the presence of trypsin (Hogue and Brian, 1986), the latter of the two being acylated (Sturman et al., 1985). Most of the MHV S proteins, with the exception of those belonging to MHV-2, are cleaved postranslationally by a cellular furan-like protease into the S1 and S2, which remain bound via a non-covalent linkage (Frana et al., 1985; Sturman et al., 1985). Being the primary viral protein involved in host cell binding, and, ultimately, the determinant of host cell infectivity, it is perhaps no surprise that the S gp is also the primary target of the host adaptive immune response (Collins et al. 1982; Stohlman et al., 1985; Williams et al., 1991; Compton et al., 1992), with antibodies developed against this protein generally associated with strong protection against viral infection (Buchmeier et al., 1984; Nakanaga, 1986). Studies performed with Mab produced against the S gp of IBV have shown that strongly neutralizing antibody formation was associated primarily with the S1 subunit of S (Mockett et al., 1984), and, in fact, research utilizing IBV in which the S1 portion of the S gp had been removed via treatment with urea, while the S2 portion was retained, failed to induce production of protective antibody (Cavanagh et al., 1986).

There are few, if any, commercially available antibodies that specifically recognize the S gp of BRCoV. For this reason our laboratory undertook the process of designing, expressing, and purifying recombinant spike gps to be used in the development of anti-spike polyclonal antiserum. Our goal was to generate a robust antiserum for the recognition of the BRCoV, to be utilized in laboratory procedures commonly used in the study of viruses.

Materials and methods

Cells

African green monkey kidney (Vero) cells were obtained from the American Type Culture Collection (Rockville, MD) and were propagated and maintained in Dulbecco's Modified Eagle Media (DMEM; Invitrogen, Carlsbad, CA) containing sodium bicarbonate, 25 mM HEPES (Invitrogen, Carlsbad, CA), and 10% heat-inactivated fetal bovine serum (FBS).

SF9 cells, derived from *Spodoptera frugiperda* (Fall Armyworm) IPLB-Sf21-AE cells, were obtained from Invitrogen (Carlsbad, CA). Cells were propagated and maintained in serum-free SF900-II SFM (Invitrogen, Carlsbad, CA) containing 1% penacillin-streptomyacin solution (Invitrogen, Carlsbad, CA), either as attached cells in a monolayer or as a suspension culture. Cells were maintained at 29° C in a 0% CO_2 atmosphere.

Sopt plasmid

The DNAworks program (Hoover and Lubkowski, 2002) was used to design synthetic oligonucleotides to be utilized in a PCR-based system for the generation of a codon-optimized BRCoV S glycoprotein (Sopt) corresponding to the S sequence of isolates obtained from a calf having succumbed to fatal pneumonia during a bovine shipping fever epizootic (Chouljenko et al., 2001). Since the S gps only differ between the pneumopathogenic and enteropathogenic strains by seven amino acids, the codon optimized enteropathic S gp was first constructed via PCR overlap extension (Aiyar, et al., 1996). The BCoV-Lun Sopt 3xF and BCoV-Ent Sopt 3xF plasmids were then generated by cloning the respective codon-optimized BCoV S gene, either BCoV-Lun

Sopt or BCoV-Ent Sopt, lacking the DNA sequence coding for the signal peptide, into the p3XFLAG-CMV-9 plasmid vector (Sigma, St. Louis, MO).

Recombinant protein production

The Bac-to-Bac Baculovirus protein expression system (Invitrogen, Carlsbad, CA) was used to produce two versions of the truncated, soluble portion of the Bovine Respiratory coronavirus (BRCoV) codon-optimized spike glycoprotein (Sopt): the soluble portion of Sopt, from amino acid 19 through amino acid 1296 (an EcoRV site; Sol-Sopt), and the second consisting of the same fragment fused after amino acid 1296 to the soluble portion of bovine CD154 (SoptCD154). These proteins were designed to contain a 5' 3X Flag sequence and a 3' 9-histadine tag for detection and purification purposes, respectively, and were over-expressed in SF9 insect cells infected with recombinant baculovirus carrying the appropriate expression cassette, either that of Sol-Sopt or Sopt-CD154. Briefly, SF9 cells were seeded into SF900-II cell culture media (Invitrogen, Carlsbad, CA) at a density of $2x10^6$ cells/ mL and infected with recombinant baculovirus carrying the expression cassette for either Sol-Sopt or SoptCD154 at an MOI of 5. Cell suspension cultures were maintained at 27°C in an orbital incubator. Cell supernatants were harvested approximately 72 h post-infection, and soluble protein present in the supernatant was isolated and purified via two rounds of cobalt-based immobilized metal affinity chromatography (IMAC) using the Talon Metal Affinity resin (ClonTech Laboratories, Inc., Mountainview, CA). Briefly, SF9 cell cultures were decanted into 50 mL centrifuge tubes and centrifuged at 3000 rpm for 10 min at 27°C. The resulting supernatant was then decanted into clean 50 mL centrifuge tubes and placed on ice, while the cell pellets were stored at -80°C. A 20% Igepal® CA-630

(Sigma, St. Louis, MO) solution was then added to each supernatant for a final concentration of 1% Igepal (v/v) and inverted to gently mix. Supernatants were then centrifuged for 30 min at 8,000 rpm at 4°C. The resulting supernatants were then decanted into new 50 mL centrifuge tubes and Talon Metal Affinity resin (ClonTech Laboratories, Inc., Mountainview, CA) was added 1:100 (v/v) to each aliquot. Supernatants were then rocked overnight at 4°C to allow binding of His-tagged proteins. Following overnight incubation, supernatants were centrifuged at 4,000 rpm at 4°C. The resulting supernatant was decanted from the pellet, which consisted of the affinity resin bound to His-tagged proteins. Beads were then washed 4 times with native wash buffer (50 mM NaH_2PO_4, 300 mM NaCl, 10 mM Imidazole, pH 7.4). Bound proteins were then eluted twice with 0.5 mL each of native elution buffer (50 mM NaH_2PO_4, 300 mM NaCl, 250 mM Imidazole, pH 7.4) and stored at -80°C until further analysis. The purified proteins were verified via expected size using western blot analysis, using mouse anti-flag antibody (Sigma, St. Louis, MO) as the primary detection antibody. The purified protein concentration was then determined using the Pierce BCA protein quantification assay (Thermo Fisher Scientific, Inc., Rockford, IL), according to manufacturer's instructions.

Polyclonal anti-BRCoV spike glycoprotein production

Purified Sopt-CD154 protein was used to inoculate an immunologically naïve rabbit via IM injection, 50 μg in 0.5 mL phosphate buffered saline (PBS) emulsified with an equal volume TiterMax Gold (TiterMax, Norcross, GA) into each hind leg. Two weeks later the rabbit was administered a booster inoculation of 50 μg purified Sopt-CD154 protein in the same manner as previously described. Following an additional two

weeks, the rabbit was placed under general anesthesia and exsanguinated via cardiac puncture. Blood was then allowed to clot at room temperature for 1 h, followed by centrifugation for 30 min at 4,000 rpm. The resulting serum was then aliquoted into to clean 1.5 mL centrifuge tubes and again centrifuged at 10,000 rpm for 20 min to remove any remaining solid or insoluble blood components. Serum was then stored at -80° C until analysis.

Antiserum verification (Western immunoblot analysis)

To verify the specificity of any antibodies against BRCoV-Sopt that may be present in the rabbit serum obtained as described previously, a western immunoblot was performed. To each the wells of a 4-20% Tris-HEPES denaturing protein electrophoresis gel (Thermo Scientific, Rockford, IL) was added 7.5 μL of one of the following: purified Sopt-CD154, purified Sopt-CD154, or BCoV-Lun virus culture, each prepared in Laemmli sample buffer (Bio-Rad, Hercules, CA) containing 5 % β-mercaptoethanol 1:1 and boiled at 100° C for 5 min, such that the total volume added to each well was 15 μL. The resulting nitrocellulose immunoblot was then incubated with rabbit serum diluted 1:1000, and previously verified western-positive mouse anti-flag antibody (1:4000) was utilized as a positive control. Naïve rabbit serum obtained from the rabbit prior to the initial inoculation with Sopt-CD154 was used as a negative control. Following 1 h incubation, goat anti-rabbit or goat anti-mouse secondary antibody conjugated to HRP was added at a dilution of 1:10,000 to each immunoblot and incubated 1 h.

Immunofluorescence assay

In order to further determine the ability of the rabbit-derived anti-S gp antiserum to detect viral S gp, an IFA was performed. Briefly, HRT-18G cells were cultured

overnight in 6-well tissue culture plates to obtain a confluent monolayer. Serial 10-fold dilutions of virus from 10^{-2} to 10^{-6} were prepared in DMEM and 1 mL of these dilutions used to infect individual wells. Plates were then rocked at room temperature for 1h to permit virus adsorption onto monolayer. The cell culture medium was then removed from each well, and wells washed twice with PBS. Fresh cell culture medium was then added to each well and plates incubated at 37°C. After 12h culture medium was removed and cells washed with two volumes of PBS, followed by 1mL ice-cold methanol to fix cells. Cells were incubated in methanol for 15 minutes, followed by washing with ice-cold PBS containing 2% bovine serum albumin (BSA). Wells were then blocked for 1h with PBS containing 2% BSA. To each well was then added the anti-BCoV spike hyperimmune rabbit serum, obtained as discussed previously, diluted 1:2500 in PBS containing 2% BSA and incubated 2h at room temperature with rocking. Cells were then washed twice with PBS containing 2% BSA. Alexafluor 488-conjugated goat anti-rabbit secondary antibody (Invitrogen, Carlsbad, CA) diluted 1:500 in PBS containing 2% BSA was added to each well and incubated at room temperature for 1h with rocking. Infected cells were then visualized and counted via an Olympus fluorescence microscope at an excitation of 488 nm.

Sopt hydrophobicity and antigenicity analysis

The Sopt nucleotide sequence corresponding to the S1 region was analyzed for its hydrophilicity as it related to potential antigenic sites, based on predicted amino acid sequence (Parker et al., 1986) utilizing the web-based analysis tool, IEDB analysis resource (http://tools.immuneepitope.org/tools/bcell/reference.jsp). The Sopt nucleotide sequence was also analyzed for predicted linear epitopes based on the predicted amino

acid sequence (Larsen et al., 2006) utilizing the same web-based analysis resource. As a result of these combined analyses, two regions within the S1 subunit, termed “region 1” (Sopt-R1; Sopt bases 60-1200) and “region 2” (Sopt-R2; Sopt bases 1200-2100) were selected for recombinant protein and antibody production based on their relative hydrophilicity, suggesting they were exposed surface peptides not hidden within secondary structure, and potential as linear epitopes, as these regions should be recognized by B-cell receptors as linear molecules not reliant on B-cell recognition of secondary structure, which could be significantly compromised in truncated versions of the proteins.

Plasmid production

Primers were designed for use in PCR to amplify each of the regions of interest corresponding to Sopt-R1 and Sopt-R2. Using overlap extension PCR, an EcoRI restriction site was added to the 5’ end of each PCR fragment, Sopt-R1 and Sopt-R2, respectively using the forward primers, *5’TATATAGAATTCAAATGCACCACAGTGAGC ATCAATGAC 3’* for R1 and *5’ TATATAGAATTCCGGAAGGTGGATCTGCAGC TGGGAAA 3’* for R2; additionally, an XhoI site was added to the 3’ end of each PCR fragment, Sopt-R1 and Sopt-R2, respectively using the primers *5’TATATACTCGAGGT TAGGGATTGCGAACTTATCAATTGT 3’* for amplification of Sopt-R1 and *5’TATATACT CGAGGGTTCGCTGCTGTTAGCGTGAAATGC 3’* for Sopt-R2. For purification purposes, the plasmid pGEX6.1 (Figure 4.1; GE LifeSciences, Picastaway, NJ) was chosen for insertion into and expression of the Sopt-R1 and Sopt-R2 PCR fragments, as this plasmid allows for the 5’ in-frame fusion of a cleavable GST molecule to the inserted gene’s translation product. The *pGEX-R1* and *pGEX-R2* plasmids were then generated by

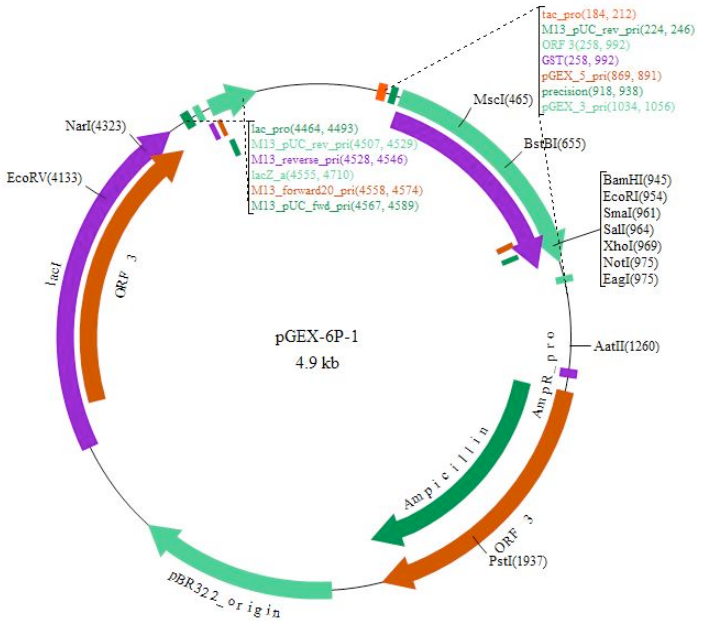

Figure 4.1. The pGEX-6P-1 cloning vector (GE LifeSciences, Picastaway, NJ) for expression of GST fusion proteins in *E. coli*.

cloning the respective PCR fragments into the pGEX6.1 plasmid vector (GE LifeSciences, Picastaway, NJ), using the New England BioLabs Quick Ligation™ Kit (New England BioLabs, Inc., Ipswitch, MA). The resulting plasmids, *pGEX-R1* and *pGEX-R2*, were amplified in *E. coli* Max Efficiency® DH5α™-T1^{R} competent cells (Invitrogen, Carlsbad, CA), extracted, purified on Qiagen columns (QIAGEN, Inc., Mississauga, ON, Canada), quantified via spectrophotometry, and stored at -20°C until use. Plasmid sequences and correct insert orientation were then verified via sequencing on an ABI Prism 377 DNA sequencer (PE Applied Biosystems) using the forward PCR primers *5' GTGTGGAATTGTGAGCGGATAAC 3'* and *5' GGGCTGGCAAGCCACGT TTGGTG 3'* in conjunction with the reverse primer *5'CGGGAGCTGCATGTGTC*

AGAGG 3'.

Recombinant protein expression

Purified *pGEX-R1* and *pGEX-R2* were used to transform *E. coli* One Shot® BL21 competent cells (Invitrogen, Carlsbad, CA) for expression of the recombinant proteins Sopt-R1-GST and Sopt-R2-GST. Additionally, as a GST control, empty pGEX6.1 plasmid expressing GST alone was also used to transform BL21 *E. coli*. Transformation-positive colonies were inoculated into LB broth containing ampicillin (100 μg/mL) and incubated at 37°C with 225 rpm rotation. To determine when cell density was high enough to induce expression of the recombinant proteins, OD_{600} was measured at 1 h intervals until OD_{600} = 0.6-0.8, at which time expression of the recombinant protein was induced via addition of 1 mM isopropyl β-D-1-thiogalactopyranoside (IPTG). The bacterial culture was then allowed to continue incubating for an additional 3 h post-induction, with 1 mL samples taken at 0, 1.5, and 3 h post-induction. Following 3 h incubation, cultures were removed, cells pelleted at 4,000 rcf for 10 minutes, and frozen at -80°C until analysis. For comparison and optimization purposes, cultures were also induced at OD_{600} = 1.0, and with three different concentrations of IPTG: 1, 0.5, and 0.1 mM IPTG. In addition, recombinant protein yield was also compared for cultures grown at 32°C and 37°C.

Recombinant protein isolation and purification

To isolate recombinant proteins, lysis conditions first required optimization. To this end, bacterial pellets were thawed on ice and lysis was first attempted using B-Per Lysis Buffer (Thermo Fisher Scientific, Rockford, IL) containing 1 mM phenylmethylsulfonyl fluoride (PMSF; Sigma, St. Louis, MO) and 10 mg/mL lysozyme

(Sigma, St. Louis, MO), according to manufacturer's specifications. Briefly, 4 mL B-Per was added to each 1 g weight of wet cells and the pellet homogenized in B-per solution via pipetting action. Homogenization was then followed by incubation for 10 to 15 min at room temperature. The resulting lysate was then centrifuged at 15,000 rcf for 5 min in order to separate soluble from insoluble proteins. Cell lysate (soluble) and cell pellet (insoluble) fractions were then each prepared for Western immunoblot analysis under denaturing conditions in order to determine whether the Sopt-R1-GST and Sopt-R2-GST recombinant proteins were both adequately expressed and soluble.

In an attempt to free the expressed Sopt-R1-GST and Sopt-R2-GST recombinant proteins from bacterial inclusion bodies and thus improve their solubility and yield, an alternative lysis buffer and method were utilized. The cell pellet was first thawed to room temperature and washed once with bacterial lysis buffer II (50 mM Tris-HCL, 300 mM NaCl). Following centrifugation and discard of resulting supernatant, 1 mL lysis buffer II was added to the pellet, followed by shearing via a 21 gauge needle in order to resuspend the entire pellet. Once the pellet was completely resuspended in lysis buffer II, an additional 5 mL lysis buffer II was added to the suspension, which was then vortexed thoroughly to mix. To the bacterial pellet suspended in lysis buffer II was added 500 mM EDTA for a final concentration of 5 mM EDTA; solution was again vortexed thoroughly to mix. To this suspension was then added 25 mg/mL lysozyme (Sigma, St. Louis, MO) for a final concentration of 1 mg/mL, followed by mixing via gentle inversion shaker for 30 minutes at room temperature. Benzonase nuclease (Sigma, St. Louis, MO) was then added to the solution for a final concentration of 5 U/mL and pellet in solution returned to the inversion shaker for an additional 30 min at room temperature. Following mixing,

solution was centrifuged 16,000 rcf for 20 min at 4ºC and resulting supernatant discarded. To the remaining pellet was added 1 mL lysis buffer II and 50 μL of 500 mM EDTA. Pellet was once again resuspended in solution via use of a 21” needle. Approximately 4 mL lysis buffer II was then added to the resulting solution followed by mixing via brief vortexing. Once mixture was homogeneous, 1 M dithiothreitol (DTT; Sigma, St. Louis, MO) was added to a final concentration of 5 mM DTT and solution was again subjected to vortexing. A solution of 10% sarkosyl (v/v; Sigma, St. Louis, MO) was added to the bacterial pellet solution, 200 μL per approximately 5 mL of bacterial pellet suspension, which was then mixed by gentle inversion on an inversion shaker for 30 min at room temperature. This was followed by overnight incubation with inversion at 4ºC. Following the lysis incubation period, bacterial suspension was subjected to sonication 3 to 4 times on ice in 12 to 15 s intervals using an output control of 7 and a 20% duty cycle. A 1 min rest period was used to allow sonicated suspension to cool between sonications. Sonicated suspension was then centrifuged at 16,000 rcf for 30 min at 4ºC and resulting supernatant decanted into new conical tubes, while the resulting pellets were returned to ice for later analysis. To the remaining supernatant was added 750 μL of a 10% solution of Triton X (Sigma, St. Louis, MO) in ddH2O (v/v), followed by gentle inversion to ensure complete mixing of solutions. Samples were then either purified via Profinia (Bio-Rad, Hercules, CA) according to manufacturer’s instructions using GST-binding columns or stored for no longer than 24 h at 4ºC until purification procedure could be performed.

Results

Recombinant Sol-Sopt and Sopt-CD154 are expressed to high levels in an SF9 cell culture system

The recombinant Sopt protein was expressed using the baculovirus expression system in insect cells to allow for post-translational modification that may increase the immunogenicity of the protein. (Goffard and Dubuisson, 2003; Harrison and Jarvis, 2006). The proteins were found to be expressed at high levels (Fig. 4.2) using this system, not only in the SF9 cells themselves (lanes 1 and 3), but also as soluble proteins secreted into the extracellular space and detectable in the cell culture supernatant (lanes 2 and 4).

Both *in vitro* expressed and wild type S gp are recognized by Sopt gp-specific antiserum

In an attempt to create a stock of BRCoV S gp-specific antiserum for use in BRCoV studies, an immunologically naïve rabbit was inoculated with SF9-expressed Sopt-CD154 and boosted 14 days later. Serum was then harvested from this rabbit via exsanguination and tested for its ability to recognize both recombinant Sopt protein purified from SF9 cell supernatants, as well as S gp on the surface of wild-type BRCoV isolated from a calf that succumbed to fatal pneumonia during a shipping fever epizootic. To determine the ability of this antiserum to detect S gp, a western immunoblot was performed (Figure 4.3) using the serum as the primary antibody against recombinant Sol-Sopt purified from SF9 cell supernatants, recombinant Sopt-CD154 purified from SF9 cell supernatants, or whole virus particles (lanes 5, 4, and 6, respectively). For comparison purposes, a second immunoblot was performed simultaneously using

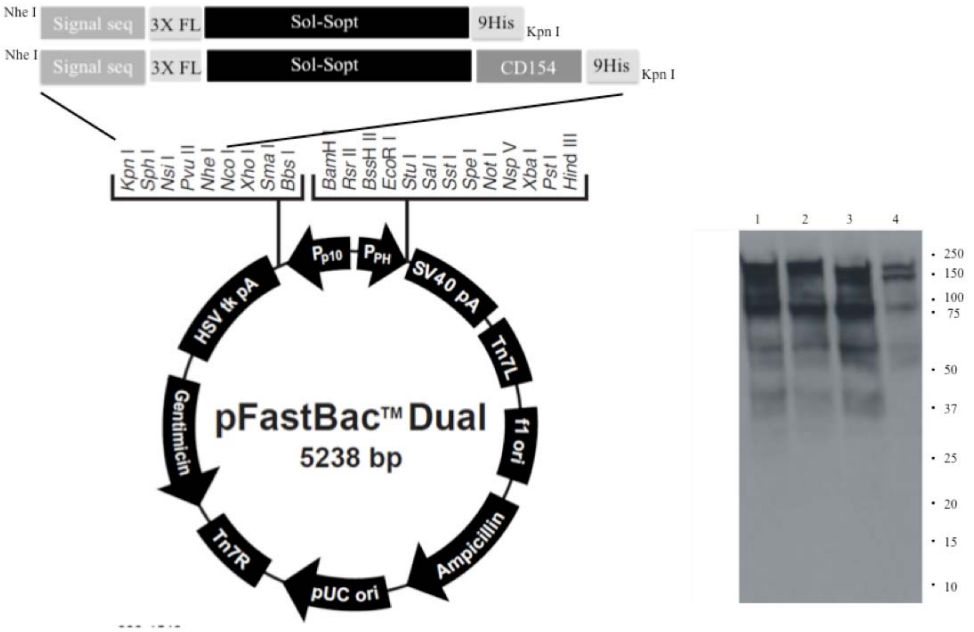

Figure 4.2. Sopt-CD154 (lanes 1 and 2) and Sol-Sopt (lanes 3 and 4) expressed in SF9 cells and isolated from SF9 cell culture supernatants.

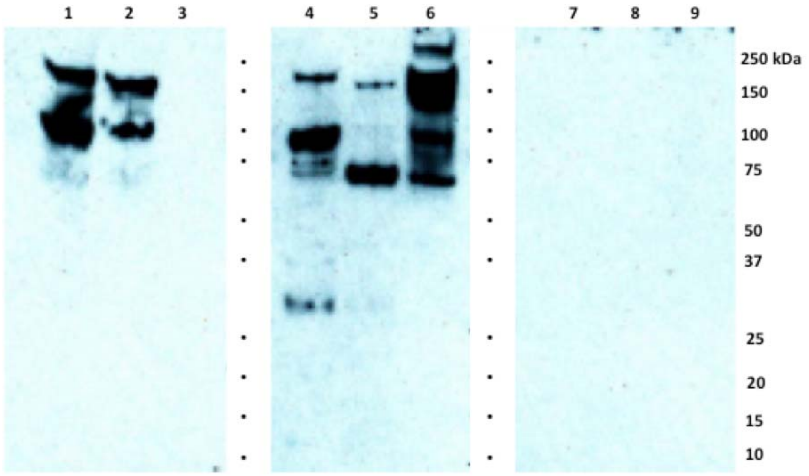

Figure 4.3. Rabbit-derived anti-Sopt-CD154 antiserum detects both recombinant Sol-Sopt and Sopt-CD154 expressed expressed from a baculovirus expression system, as well as wild-type S gp from the laboratory strain BCoV-Lun (lanes 5, 4, and 6, respectively), while naïve rabbit serum from the same rabbit pre-vaccination does not (lanes 8, 7, and 9, respectively).

anti-3XFL antibody (Sigma, St. Louis, MO) as the primary detection antibody (lanes 2, 1, and 3, respectively). As expected, an approximately 150 kDa band was observed in lanes corresponding to the recombinant Sol-Sopt in both anti-3XFL and rabbit antiserum-treated immunoblots. Likewise, a slightly larger 190 kDa band was observed in lanes corresponding to the recombinant Sopt-CD154 in both anti-3X-FL and rabbit serum-treated immunoblots. The ant 3XFL antibody did not, however, react with the S protein from the BRCoV-Lun virus located in lane 3, while rabbit-derived anti-serum was able to detect bands varying in size, predominantly those migrating as 150, 190, and possibly 250 kDa species, in the lane corresponding to BRCoV-Lun virus (lane 6). Furthermore, naïve serum taken from the rabbit prior to the initial exposure to Sopt-CD154 antigen yielded no signal as compared with serum isolated from the same rabbit following a second exposure to antigen (lanes 7-9).

To further evaluate its usefulness in BRCoV-related laboratory applications, the rabbit-derived anti-S gp antiserum was tested for its ability to detect wild-type S gp expressed on the surface of fixed cells in an immunofluorescence assay system. The serum was used in the assay at a relatively low dilution, 1:2500, resulting in low amounts of background or non-specific staining. As predicted, the anti-S gp antiserum reacted with S gp expressed on the surface of fixed HRT-18G cells and was detectable by secondary goat anti-rabbit antibody conjugated to Alexafluor 488 (Invitrogen, Carlsbad,CA), resulting in easily observable infected cells that stained fluorescent green when viewed under a fluorescent light microscope (Figure 4.4).

The S1 portion of the S gp contains regions suggestive of hydrophilic, linear epitopes

In order to determine the most hydrophilic regions of the S1 subunit of the S gp that may contain linear epitopes conducive to antibody response, the Sopt predicted amino acid sequence was analyzed using an available web-based analysis tool, IEDB analysis resource, which makes available a number of various prediction logarithms for nucleotide sequence analysis. Based on the results of the Emini Surface Accessibility (Emini et al., 1985; Figure 4.5) and Parker Hydrophilicity Prediction plots (Figure 4.6), the Bepipred Linear Epitope Prediction plot (Figure 4.7), two regions within the S1 subunit of the BRCoV S gp were selected for recombinant protein production. These regions, termed Sopt-R1 and Sopt-R2, were found to be considerably hydrophilic with respect to the rest of the gp, and were areas predicted most likely to contain linear

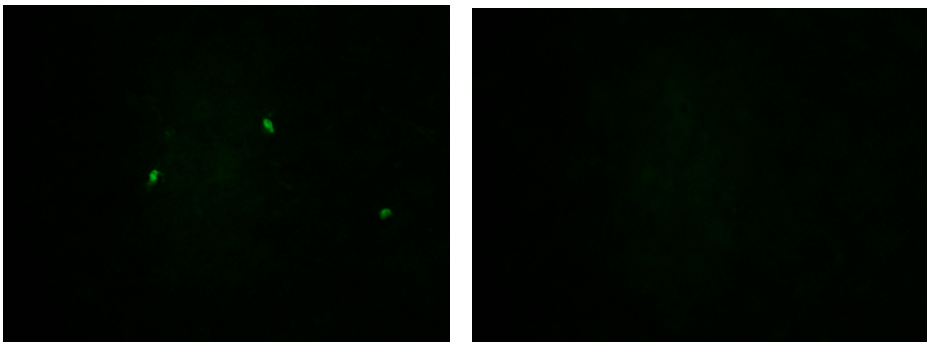

Figure 4.4. BCoV-Lun infected (panel A) and uninfected (panel B) HRT-18G cells 12 h post-infection.

epitopes, of particular interest for their ability to incite the production of antibody not dependent on protein secondary structure for recognition. This was deemed a vital feature since production of truncated and/or recombinant versions of the gp would likely not

share native conformation with wild-type S gp. For this reason, regions encompassing amino acids 20-400 and 400-700 within the S1 subunit were selected. In addition, the production of small recombinant proteins less than 450 amino acids was desirable since the Profinia system (Bio-Rad, Hercules, CA) would be used for purification. This system utilizes an automated two-step affinity chromatography procedure to immobilize recombinant GST or His-tagged proteins for protein purification. However, the system is restricted to purification of relatively small GST-tagged proteins. Thus, we restricted our selected regions within the S1 portion of the S gp to encompass fewer than 400 amino acids.

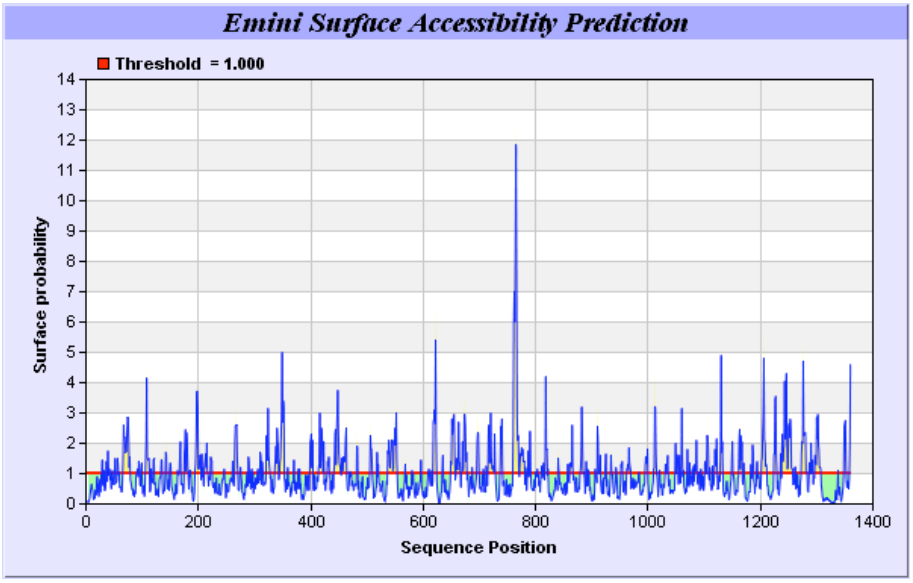

Figure 4.5. Emini surface accessibility prediction plot of the S1 region of the BRCoV Sopt gp. Regions most likely to be accessible when the protein is folded in native conformation are shown as spikes above a surface probability value equal to 1; an increase in surface probability value is proportional to an increase in the likelihood that the residue is accessible on the surface of the protein in native conformation.

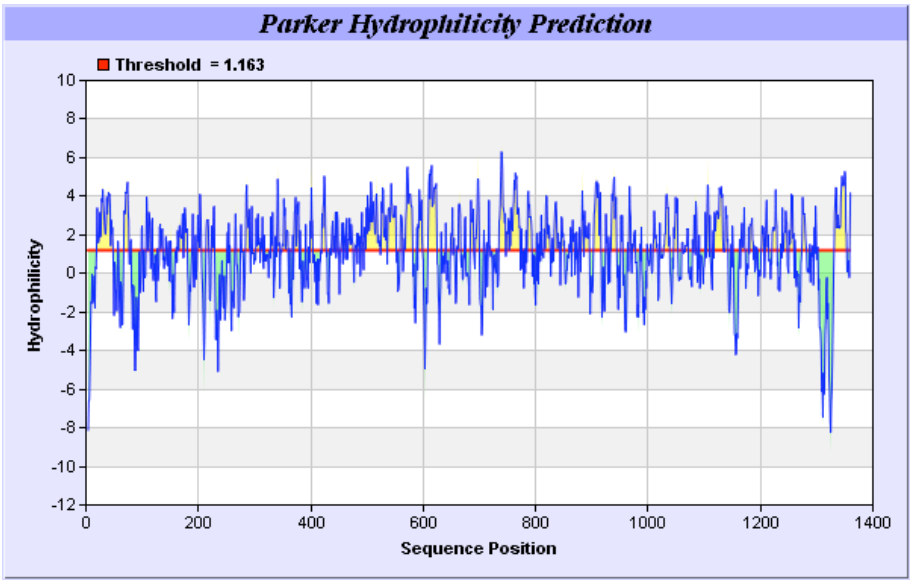

Figure 4.6. Parker hydrophilicity prediction plot. Regions of the BRCoV predicted to contain particularly large concentrations of hydrophilic residues are depicted as spikes above the threshold of 1.163. These regions are more likely to be exposed on the surface of the protein when folded in its native conformation.

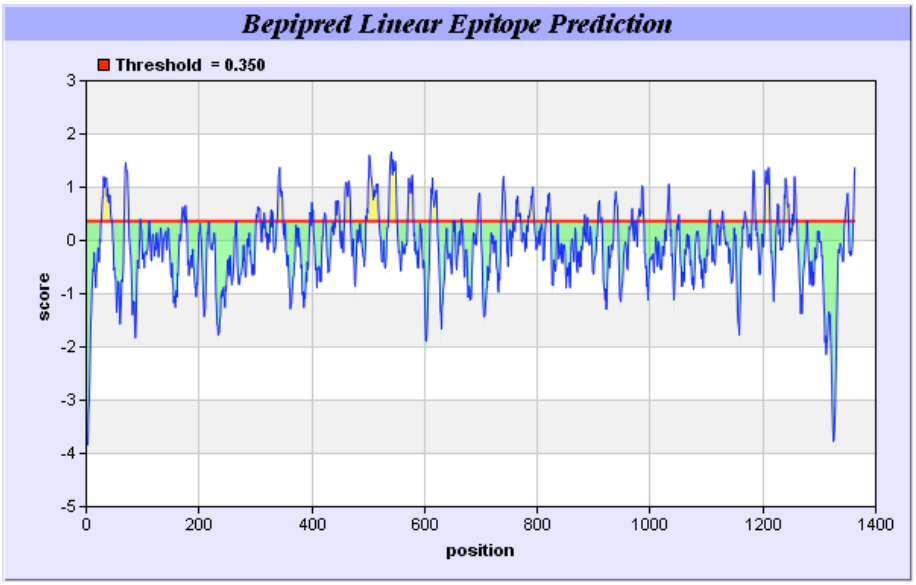

Figure 4.7. Bepipred linear epitope prediction plot. Regions of the BRCoV sopt gp more likely to contain potential linear epitopes are shown as spikes above the threshold value line, equal to 0.350, where an increase in spike distance from the threshold is proportional to the likelihood that the region my contain antigenic residues not reliant on native protein structure for recognition.

Recombinant Sopt-R1-GST and Sopt-R2 are expressed to high levels in BL21 *E. coli*

Because expression of recombinant proteins in bacterial systems generally generates large quantities of recombinant protein products, a BL21 *E. coli* (Invitrogen, Carlsbad, CA) expression system was selected for expression of the *pGEX-R1* and *pGEX-R2* plasmid constructs. The multiple cloning site of this plasmid places the inserted cassette under control of the inducible expression promoter/operator *tac*, which is inducible by IPTG. Expression from the *tac* promoter/operator is IPTG concentration dependent and proportional to the concentration of IPTG added. Addition of IPTG at a concentration of 1 mM resulted in high level expression of the Sopt-R1-GST and Sopt-R2-GST proteins, as shown by western immunoblot. As expected, bands representing the 71.5 kDa Sopt-R1-GST and the 60.5 kDa R2 proteins were visible, primarily in lanes containing the resuspended bacterial pellet following lysis treatment. The immunoblot was treated with anti-GST antibody (Invitrogen, Carlsbad, CA) for detection of the fusion proteins. Based on results of the immunoblot, it was concluded that a large amount of the fusion protein remained insoluble following lysis of the bacterial cells, as considerably more protein was evident in lanes corresponding to the bacterial pellet following lysis than in lanes corresponding to the lysate, necessitating optimization of the expression protocol.

Sopt-R1-GST and Sopt-R2-GST remain trapped within bacterial inclusion bodies following cell lysis

In an attempt to increase the solubility of recombinant Sopt-R1-GST and Sopt-R2-GST proteins expressed in *E. coli*, growth of *E. coli* cultures at two different temperatures

(Smith and Corcoran, 1990) in conjunction with induction via two different concentrations of IPTG were considered (Figure 4.8). Bacterial cell cultures were grown at either 32°C (lanes 3, 4, 7, and 8) or 37°C (lanes 1, 2, 5, and 6). Expression of the recombinant proteins was induced using concentrations of 0.1 mM IPTG (lanes 1-4) or 0.5 mM IPTG (lanes 5-8). These cultures were sampled at 0 and 1.5 h post-induction, and again at 3 h post-induction, when cells were harvested, pelleted via centrifugation, and frozen until analysis. Western immunoblot analysis of Sopt-R1-GST (panel A) and Sopt-R2-GST (panel B) cell lysates (lanes 1, 3, 5, and 7**)** and remaining pelleted cellular material (lanes 2, 4, 6, and 8) at 3 h post-induction revealed that both changing the culture incubation temperature and reducing the IPTG concentration failed to increase the amount of soluble protein that could be recovered from the cells. For that reason, adjustments were again made to the induction protocol. For this experiment, induction of Sopt-R1-GST expression was performed when at two different concentrations of bacteria in culture: when the OD_{600} = 0.6 and when the OD_{600} = 1.0 and two different concentrations of IPTG for induction, 0.5 mM and 1.0 mM. Again, samples were taken at 0 h, 1.5 h, and 3 h post-induction. Western immunoblot analysis (Figure 4.9) of both the cell lysates (lanes 1, 3, 5, and 7) and remaining pelleted material (lanes 2, 4, 6, and 8) sampled at 3 h post-induction revealed that, once again, the majority of protein remained insoluble within the remaining cell pellet. No differences were observed in protein solubility between either samples taken from cultures induced at OD600 = 0.6 or 1.0, or between samples taken from cultures induced using 0.5 or 1.0 mM IPTG. Based on the combination of these and previous results, it was concluded that the recombinant Sopt-

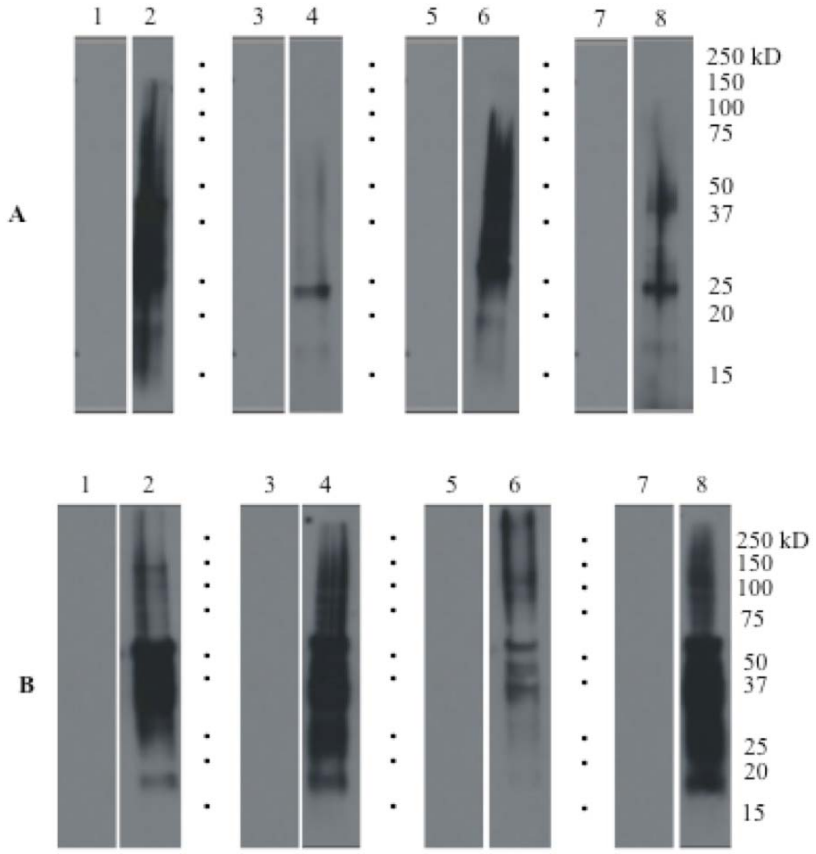

Figure 4.8. R1-Sopt (panel A) and R2-Sopt (panel B) expressed in BL21 *E. coli* under two different culture temperatures and induced using two different IPTG concentrations.

R1-GST and Sopt-R2-GST bacterial expression products were trapped within inclusion bodies within the bacteria.

Therefore, in an attempt to free the expressed recombinant proteins trapped within bacterial inclusion bodies, a new lysis technique was attempted utilizing high salt solution coupled with the addition of both lysozyme and sarkosyl in conjunction with mechanical shearing of the bacterial pellet. When the resulting lysates from bacteria expressing the Sopt-R1-GSTrecombinant protein were GST column-purified via the automated Profinia system (Bio-Rad. Hercules, CA) and analyzed via denaturing gel

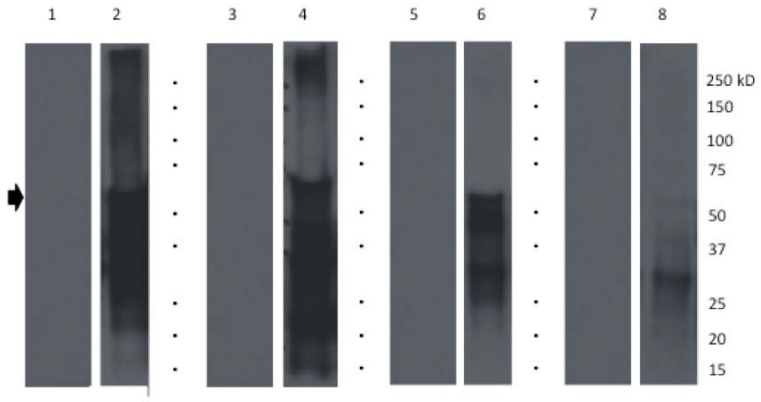

Figure 4.9. Western immunoblot analysis of Sopt-R1-GST expressed in BL21 *E. coli* at two different concentrations of IPTG and two different culture concentrations (OD_{600}) for induction. The 71 kDa band representing Sopt-R1-GST is denoted by an arrow.

electrophoresis and coomassie blue staining (Figure 4.10), Profinia-purified and eluted Sopt-R1-GST could be visualized only as a very faint band (lane 6), corresponding to the relatively small quantity of protein, only 0.08 mg/mL, that could be recovered via this method. The same gel showed that, as before, a considerable amount of the protein seemed to remain associated with the pelleted fraction following bacterial lysis (lane 2). In addition, a considerable amount of the solubilized protein escaped the GST-column and could be observed as bands corresponding to lanes in which the Profinia flow-through and wash were added (lanes 4 and 5). To corroborate these results, a western immunoblot was also performed (Figure 4.11), the results of which were in agreement with those from the Coomassie blue gel. When the new lysis procedures were performed on *E. coli* expressing the recombinant Sopt-R2-GST fusion protein followed by western immunoblot to check protein solubility (Figure 4.12), it was observed that, similar to the results obtained via the new lysis conditions of bacteria expressing the recombinant Sopt-R1-GST protein, the majority of the recombinant Sopt-R2-GST protein remained

associated with the cell pellet following lysis (lane 1), suggesting that this protein, too, may be insoluble, trapped inextricably within bacterial inclusion bodies.

Discussion

Production of rabbit-derived anti-spike serum

Given the observation in our laboratory as well as others that BRCoV, especially virus isolated from clinical samples, fails to produce *in vitro* plaques even though CPE including swollen, granular, detached cells may be evident (Benfield and Saif, 1990; Cho et al., 2000), coupled with the fact that our laboratory currently did not possess antibody specific for the respiratory strain of BCoV, there was considerable need for the

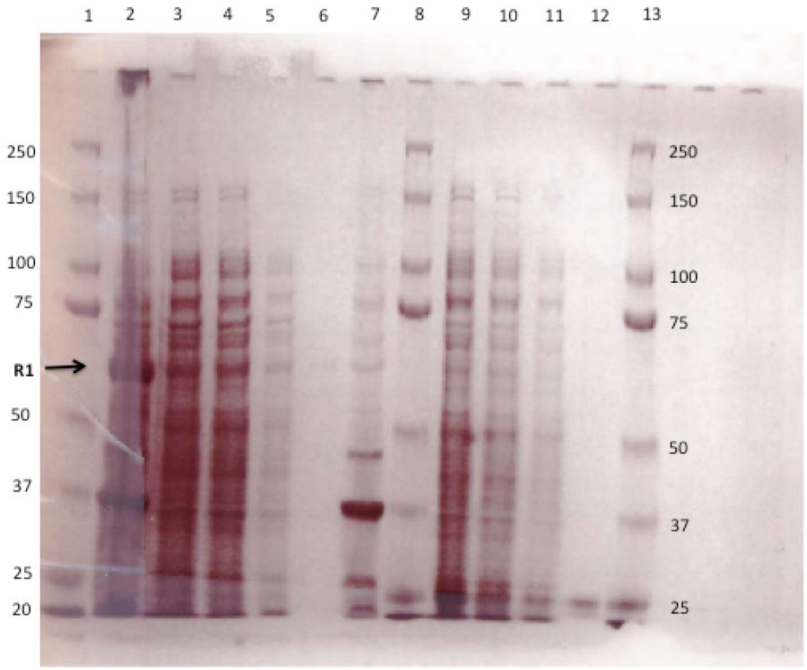

Figure 4.10. Coomassie stained 10% Polyacrylamide gel of Profinia purified Sopt-R1-GST recombinant protein (lanes 2-6) and GST expressed alone (lanes 8-12).

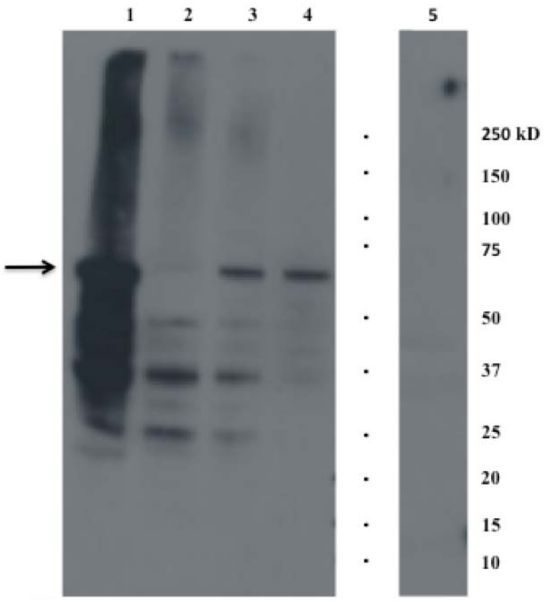

Figure 4.11. Western immunoblot confirmation of coomassie results of Sopt-R1-GST purification via the Profinia system. Lane 1 contains bacterial pellet following lysis.

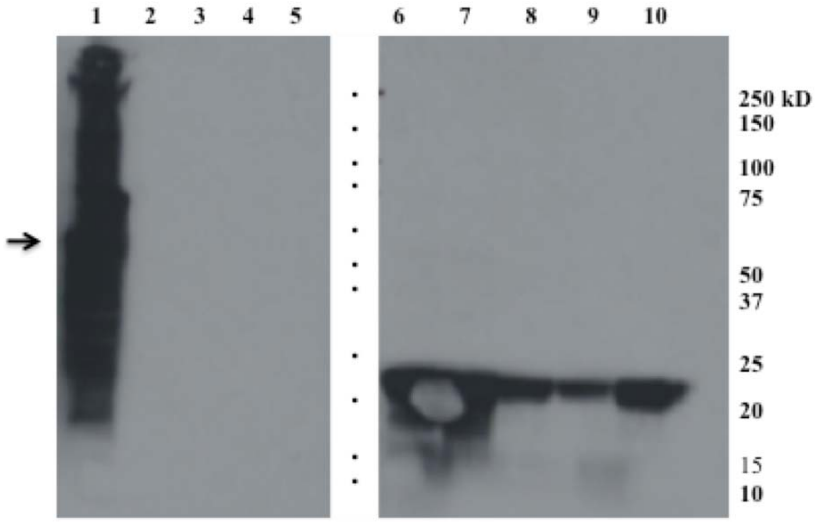

Figure 4.12. Sopt-R2-GST Profinia affinity chromatography protein purification. Sopt-R2-GST pellet (lane 1) contains completely insoluble protein, while lanes 2-5 represent the clear bacterial lysate, wash, flow-through, and eluate, respectively. A GST (24 kDa) control was also performed using pGEX-6-P-1 plasmid DNA containing no insert (lanes 6-10); this protein was also subjected to Profinia purification, with lanes set up in the same order as listed for Sopt-R2-GST.

development of a method with which to detect virus, for use in both immunohistochemical applications as well as western immunoblot detection. Production of the S gp via an insect cell culture system proved to be fairly robust, providing adequate protein for use in the vaccination of a naïve rabbit for the purpose of antibody production. The baculovirus/insect cell protein expression system is one of the most widely used systems for expression of heterologous proteins within a eukaryotic host, and previous studies have utilized the insect cell system for the production of recombinant proteins specifically for vaccine use. Thomas and associates used this system for the production of recombinant E2 protein from BVDV in a study comparing the efficacy of proteins derived from baculovirus/insect cell systems as vaccine candidates versus the same recombinant proteins expressed via a mammalian system. The group reported a considerably higher yield of the recombinant protein was obtained with the baculovirus/insect cell system as compared with expression in the mammalian MDBK cell line (Thomas et al., 2009). However, it was found that the insect cell-derived proteins were less effective as a vaccine when compared with the same recombinant proteins derived from mammalian protein expression, as evidenced by the observation that in order to obtain a comparable level of BVDV protection with the insect cell-derived protein, considerably higher concentrations were required than were needed when mammalian-derived proteins were used (Thomas et al., 2009). There are differences in the glycosylation pathways utilized by insect and mammalian cells, and these differences could potentially affect protein conformation and even biological function (Jarvis, 2003). Fortunately, we observed no difficulty in eliciting a robust antibody response against the recombinant S gp we used; the deficit in immune response to low concentrations of insect

cell-derived proteins described by Thomas et al (2009) may have been ameliorated in our study by the fact that, at 1 μg/mL total dose concentration, we used a relatively high concentration of protein for vaccination. Furthermore, we found that antibody present in the hyper immune antiserum from this rabbit was specific for the S gp, as evidenced by its ability to detect wild type virus S gp in both western immunoblot and IFA. Our results were in agreement with those reported by Shmaljohn and colleagues (1990), in which Hantaan virus proteins expressed in a baculovirus system were observed to be specific for Hantaan virus, effectively eliciting a functional antibody response. In addition, as in our study, antibody specific for the wild-type Hantaan virus proteins were able to effectively recognize the recombinant proteins resulting from expression in a baculovirus system.

Interestingly, but perhaps somewhat expected, was the observation that, in response immunization with the recombinant Sopt fusion protein possessing a truncated version of bovine CD154 at its carboxyl terminus, the antiserum appears to also have some degree of reactivity to bovine CD154, as evidenced by the appearance of an additional 24 kDa band in the lane corresponding to recombinant Sopt-CD154 purified from SF9 cell culture supernatants. It is likely that some amount of soluble CD154 may have been expressed or may have been a consequence of protein degradation either during the course of cell culture or during the purification process, resulting in soluble CD154 available for recognition by anti-CD154 antibody within the serum.

Production of recombinant Sopt-R1-GST and Sopt-R2-GST in *E. coli*

Based on our success in producing both the soluble portion of the S gp and a fusion protein containing bovine CD154 in a baculovirus protein production system followed by production of specific antibody against the S gp, we next wanted to design a

small subunit vaccine that could easily be purified via automated means using the Profinia purification system (Bio-Rad) for high-throughput, inexpensive production of proteins. Because of its ease, low cost, and high protein production capabilities, as well as the ready availability of a plasmid for production of GST-tagged proteins, we decided to use a bacterial system for production of these small recombinant proteins. The positive results obtained with the use of a recombinant S gp fusion protein in the production of anti-S antibodies in rabbit prompted us to again use the S gp for this purpose. As it is a vital structural protein of the coronavirus virion and the primary viral protein implicated in host cell binding and infectivity, the S gp is also the primary target of the host adaptive immune response (Collins et al. 1982; Stohlman, 1985; Williams et al., 1991; Compton et al., 1992). Accordingly, antibodies developed against this protein are associated with strong protection against viral infection (Buchmeier et al., 1984; Nakanaga, 1986). However, its considerable size presented a potential problem with regards to purification via the Profinia system. For this reason, the S gp was evaluated for small regions containing predicted linear epitopes, as well as for indication of regions that would not undergo extensive folding when solubilized, based on the hydrophilicity prediction plots of these regions. We chose to target the S1 subunit of the S gp, as this region has previously been shown to be a major target for the induction of neutralizing antibody (Gallagher et al., 1990).

The GST-tagged protein production system has previously been used for the production of protein subunit vaccines. The pGEX-6-p-1 expression plasmid was successfully used for the high output production of the recombinant S gp subunit proteins in *E. coli*. However, most of these proteins were trapped within cytoplasmic inclusion

bodies following expression, a phenomenon commonly observed in the production of heterologous eukaryotic proteins expressed to high levels in bacteria (Eaton et al., 1986). As a result, the recombinant proteins could not be extracted via typical bacterial lysis. Manoj et al reported that, in agreement with our experience using this system, the vast majority of the tagged proteins expressed were insoluble, preventing isolation and purification directly from cell lysates (2003). As a result, the recombinant proteins required denaturing of the protein via SDS-PAGE gel extraction and related purification techniques in order to be isolated for use as a subunit vaccine. Unfortunately, because use of the Profinia purification system was desired for high-throughput protein production, maintaining the native conformation of the GST tag was necessary, as it was possible that disrupting this conformation may interfere with its ability to bind the glutathione sepharose columns used by the Profinia system. Further attempts to increase protein solubility were made by adjusting culture incubation and induction conditions, but these changes made no difference in the availability of the recombinant proteins for purification directly from the cell lysate. As a result, it was decided that the use of GST-tagged proteins in this specific case would not be possible since they could not be extracted from the bacteria while maintaining native conformation.

Future directions

It would be interesting, and potentially informative, to utilize the Sopt-R1-GST and Sopt-R2-GST proteins, as well as other small subunit Sopt proteins, for delineation of immunogenic epitopes capable of generating BRCoV neutralizing antibodies. This work could lead to the efficient production of smaller immunogenic segments or synthetic peptides that can be incorporated into a “cocktail” vaccine containing multiple

proteins and peptides. In addition, a study of this nature may provide information on the effect, if any, of CD154 fusion on B and T cell recognition of conformational versus sequential epitopes.

The use of a bacterial expression system resulted in the entrapment of recombinant Sopt-R1-GST and Sopt-R2-GST within cytoplasmic inclusion bodies rendering difficult the further purification of these antigens by affinity chromatography. Typically, inclusion bodies contain more than 70% of the expressed protein. In this regard, inclusion bodies could be purified by simple centrifugation methods due to their high density and used as immunogens. These antigens could serve as vaccines for animal vaccination, although they are not suitable for human vaccine production. Alternatively, expression of these antigens in insect cells enables their subsequent purification by affinity chromatography, although in significant lower amounts than those that can be achieved in *E. coli*. Post-translational modification of the BRCoV S glycoprotein in insect cells may preserve conformational epitopes that generate neutralizing antibodies, In this regard; insect cell expression may provide a unique advantage in the generation of potentially protective humoral immune responses. Additional work is needed to further clarify the differential abilities of S-CD154 fusion proteins expressed in *E. coli* versus insect cells to generate anti-BRCoV humoral and cellular immune responses.

References

Aiyar, A., Xiang, Y. & Leis, J. 1996. Site-directed mutagenesis using overlap extension PCR. *Methods Mol. Biol.,* 57**,** 177-191.

Benfield, D. A. & Saif, L. J. 1990. Cell Culture Propagation of a Coronavirus Isolated from Cows with Winter Dysentery. *J. Clin. Microbio.,* 28**,** 1454-1457.

Buchmeier, M. J., Lewicki, H. A., Talbot, P. J. & Knobler, R. L. 1984. Murine hepatitis virus-4 (strain JHM)-induced neurologic disease is modulated in vivo by monoclonal antibody. *Virology,* 132**,** 261-270.

Cavanagh, D., Davis, P. J., Darbyshire, J. H. & Peters, R. W. 1986. Coronavirus IBV: Virus Retaining Spike Glycopolypeptide S2 but Not S1 Is Unable to Induce Virus-neutralizing or Haemagglutination-inhibiting Antibody, or Induce Chicken Tracheal Protection. *J. Gen. Virol.,* 67**,** 1435-1442.

Cho, K.-O., Halbur, P. G., Bruna, J. D., Sorden, S. D., Yoon, K.-J., Janke, B. H., Chang, K.-O. & L, J. S. 2000. Detection and isolation of coronavirus from feces of three herds of feedlot cattle during outbreaks of winter dysentery-like disease. *JAVMA,* 217**,** 1191-1194.

Chouljenko, V. N., Lin, X. Q., Storz, J., Kousoulas, K. G. & Gorbalenya, A. E. 2001. Comparison of genomic and predicted amino acid sequences of respiratory and enteric coronaviruses isolated from the same animal with fatal shipping pneumonia. *Journal of General Virology,* 82**,** 2927-2933.

Collins, A. R., Knobler, R. L., Powell, H. & Buchmeier, M. J. 1982. Monoclonal antibodies to murein hepatitis virus-4 strain (strain JHM) define the viral glycoprotein responsib'e for attachment and cell-cell fusion. *Virology,* 119**,** 358-371.

Compton, S. R., Stephensen, C. B., Snyder, S. W., Weismiller, D. G. & Holmes, K. V. 1992. Coronavirus species specificity: murine coronavirus binds to a mouse-specific epitope on its carcinoembryonic antigen-related receptor glycoprotein. *J. Virol.,* 66**,** 7420-7428.

deGroot, R. J., Luytjes, W., Horzinek, M. C., Zeijst, B. A. v. d., Spaan, W. J. & Lenstra, J. A. 1987. Evidence for a coiled-coil structure in the spike proteins of coronaviruses. *J. Mol. Biol.,* 196**,** 963-966.

Delmas, B. & Laude, H. 1990. Assembly of coronavirus spike protein into trimers and its role in epitope expression. *J. Virol.,* 64**,** 5367-5375.

Eaton, D., Rodriguez, H. & Vehar, G. A. 1986. Proteolytic processing of human factor VIII. Correlation of specific cleavages by thrombin, factor Xa, and activated protein C with activation and inactivation of factor VIII coagulant activity. *Biochemistry,* 25**,** 505-512.

Emini, E. A., Hughes, J. V., Perlow, D. S. & Boger, J. 1985. Induction of hepatitis A virus-neutralizing antibody by a virus-specific synthetic peptide. *J. Virol.,* 55**,** 836-839.

Frana, M. F., Behnke, J. N., Sturman, L. S. & Holmes, K. V. 1985. Proteolytic cleavage of the E2 glycoprotein of murine coronavirus: host-dependent differences in proteiolytic clevage and cell fusion. *J. Virol.,* 56**,** 912-920.

Gallagher, T. M., Escarmis, C. & Buchmeier, M. J. 1991. Alteration of the pH-dependence of coronavirus-induced cell fusion: Effect of mutations in the spike glycoprotein. *J. Virol.,* 65**,** 1916-1928.

Gallagher, T. M., Parker, S. E. & Buchmeier, M. J. 1990. Neutralization-resistant variants of a neurotropic coronavirus are generated by deletions within the amino-terminal half of the spike glycoprotein. *J. Virol.,* 64**,** 731-741.

Godet, M., Grosclaude, J., Delmas, B. & Laude, H. 1994. Major receptor-binding and neutralization determinants are located within the same domain of the transmissible gastroenteritis virus (coronavirus) spike protein. *J. Virol.,* 68**,** 8008-8016.

Goffard, A. & Dubuisson, J. 2003. Glycosylation of hepatitis C virus envelope proteins. *Biochemie.,* 85**,** 295-301.

Harrison, R. L. & Jarvis, D. L. 2006. Protein N-glycosylation in the baculovirus-insect cell expression system and engineering of insect cells to produce 'mammalianised' recombinant glycoproteins. *Adv. Virus Res.,* 68**,** 159-191.

Hogue, B. G. & Brian, D. A. 1986. Structural proteins of human respiratory coronavirus OC43. *Virus Res.,* 5**,** 131-144.

Holmes, K. V., Doller, E. W. & Sturman, L. S. 1981. Tunicamycin-resistant glycosylation of coronavirus glycoprotein: demonstration of a novel type of viral glycoprotein. *Virology,* 115**,** 334-344.

Hoover, D. M. & Lubkowski, J. 2002. DNAWorks: an automated method for designing oligonucleotides for PCR-based gene synthesis. *Nucleic Acids Res.,* 30**,** e43.

Jarvis, D. L. 2003. Developing baculovirus–insect cell expression systems for humanized recombinant glycoprotein production. *Virology,* 310**,** 1-7.

Kubo, H., Yamada, Y. K. & Taguchi, F. 1994. Localization of neutralizing epitopes and the receptor-binding site within the amino-terminal 330 amino acids of the murine coronavirus spike protein. *J. Virol.,* 68**,** 5403-5410.

Larsen, J. E., Lund, O. & Nielsen, M. 2006. Improved method for predicting linear B-cell epitopes. *Immunome. Res.,* 2**,** 2.

Manoj, S., Griebel, P. J., Babiuk, L. A. & Hurk, S. V. D. L.-V. D. 2003. Targeting with bovine CD154 enhances humoral immune responses induced by a DNA vaccine in sheep. *J. Immunol.,* 170**,** 989-996.

Mockett, A. P. A., Cavanagh, D. & Brown, T. D. K. 1984. Monoclonal antibodies to the S1 soike and membrane proteins of avian infectious bronchitis coronavirus strain Massachusetts M41. *J. Gen. Virol.,* 65**,** 2281-2286.

Nakanaga, K., Yamanouchi, K. & Fujiwara, K. 1986. Protective effect of monoclonal antibodies on lethal mouse hepatitis virus infection in mice. *J. Virol.,* 59**,** 168-171.

Navas, S., Seo, S.-H., Chua, M. M., Sarma, J. D., Lavi, E., Hingley, S. T. & Weiss, S. R. 2001. Murine Coronavirus Spike Protein Determines the Ability of the Virus To Replicate in the Liver and Cause Hepatitis. *J. Virol.,* 75**,** 2452-2457.

Navas, S. & Weiss*, S. R. 2003. Murine Coronavirus-Induced Hepatitis: JHM Genetic Background Eliminates A59 Spike-Determined Hepatotropism. *J. Virol.,* 77**,** 4972-4978.

Parker, J. M., Guo, D. & Hodges, R. S. 1986. New hydrophilicity scale derived from high-performance liquid chromatography peptide retention data: correlation of predicted surface residues with antigenicity and X-ray-derived accessible sites. *Biochemistry,* 25**,** 5425-5432.

Phillips, J. J., Chua, M. M., Seo, S.-h. & Weiss, S. R. 2001. Multiple regions of the murine coronavirus spike glycoprotein influence neurovirulence. *J. Neuro. Virol.,* 7**,** 421-431.

Qiu, Z., Hingley, S. T., Simmons, G., Yu, C., Sarma, J. D., Bates, P. & Weiss, S. R. 2006. Endosomal Proteolysis by Cathepsins Is Necessary for Murine Coronavirus Mouse Hepatitis Virus Type 2 Spike-Mediated Entry. *J. Virol.,* 80**,** 5768-5776.

Rottier, P. J., Horzinek, M. C. & Zeijst, B. A. M. v. d. 1981. Viral protein synthesis in mouse hepatitis virus strain A59-infected cells: effect of tuicamyacin. *J. Virol.,* 40**,** 350-357.

Schmaljohn, C. S., Y.-K. Chu, Schmaljohn, A. L. & Dalrymple, J. M. 1990. Antigenic Subunits of Hantaan Virus Expressed by Baculovirus and Vaccinia Virus Recombinants. *J. Virol.,* 64**,** 3162-3170.

Smith, D. B. & Corcoran, L. M. 1990. Current Protocols in Molecular Biology. In: Ausubel, F. M., Brent, R., R. E. Kingston, Moore, D. D., Seidman, J. G., Smith, J. A. & Struhl, K. (eds.) *Current Protocols in Molecular Biology.* Wiley, New York.

Stohlman, S. A., Matsushima, G. K., Casteel, N. & Weiner, L. P. 1985. In vivo effects of coronavirus-specific T cell clones: DTH inducer cells prevent a lethal infection but do not inhibit virus replication. *J. Immunol.,* 136**,** 3052-3056.

Sturman, L. S., Ricard, C. S. & Holmes, K. V. 1985. Proteolytic clevage of the E2 glycoprotein of murine coronavirus: activation of cell-fusing activity of virions by trypsin and separation if two different 90K clevage fragments. *J. Virol.*, 56**,** 904-911.

Thomas, C., Young, N. J., Heaney, J., Collins, M. E. & Brownlie, J. 2009. Evaluation of efficacy of mammalian and baculovirus expressed E2 subunit vaccine candidates to bovine viral diarrhoea virus. *Vaccine,* 27**,** 2387-2393.

Wang, W., Singh, S., Zeng, D. L., King, K. & Nema, S. 2007. Antibody Structure, Instability, and Formulation. *J. Pharm. Sci.,* 96**,** 1-26.

Warr, G. W., Magor, K. E. & Higgins, D. A. 1995. IgY: clues to the origins of modern antibodies. *Immunol. Today,* 16**,** 392-398.

Williams, R. K., Jiang, G. S. & Holmes, K. V. 1991. Receptor for mouse hepatitis virus is a member of the carcinoembryonic antigen family of glycoproteins. *Proc. Natl. Acad. Sci. USA,* 88**,** 5533-5536.

APPENDIX: PROTOCOLS

TALON RESIN PURIFICATION OF NATIVE HIS-TAGGED PROTEINS FROM CELL SUPERNATANTS (IMAC PROCEDURE)

1. Centrifuge detached cells in 50 mL centrifuge tube, 10 min, 2500 rcf.
2. Decant supernatant into new 50 mL centrifuge tube
3. Add 20% Igepal solution to supernatant for a final Igepal concentration of 1%
4. Mix well via inversion (avoid vortexing, as it will result in bubbles since Igepal is a detergent)
5. Centrifuge at 10,000 rcf, 4°C for 30 min to remove any remaining cell debris
6. Decant supernatant into new 50 mL centrifuge tube. Place on ice.
7. Add Talon Metal Affinity resin to supernatant; beads to supernatant ratio should be 1:100
8. Mix well, and incubate with rocking at 4°C overnight
9. Centrifuge supernatant/resin solution 4,000 rcf, for 10 min at 4°C
10. Decant and discard supernatant carefully, ensuring that the resin pellet is not disturbed
11. Wash beads/resin 4 times:
    - Add 8 mL native wash buffer to each sample
    - Incubate with rocking 5 min
    - Centrifuge 4,000 rcf for 5 min, at room temperature
    - Carefully discard supernatant, ensuring that resin pellet at bottom of tube is not disturbed
    - Repeat 3 additional times

- On last wash, *all* remaining wash buffer must be removed; following inital decanting of liquid, centrifuge an additional 2-5 min at 4,000 rcf, room temperature
- Pipette off remaining liquid

12. Elute protein with native elution buffer, using at least an equal amount of elution buffer to resin (slightly more is better, ie, if using 200 uL beads, use 250 uL elution buffer)
    - Add elution buffer to resin carefully, tapping gently to mix. Incubate with gentle agitation (ie tapping) for 5 minutes
13. Repeat elution step with same volume elution buffer as first elution

TALON RESIN PURIFICATION OF HIS-TAGGED PROTEINS FROM CELL PELLET (IMAC PROCEDURE)

1. For attached cells, detach cells from culture flask via scraping; Decant detached cells and centrifuge cells in 50 mL centrifuge tube, 10 min, 2500 rcf
2. Decant supernatant
3. Prepare Native lysis buffer
4. Resuspend pellet in lysis buffer (5mL lysis buffer/pellet from 25 mL culture) by gently pipetting up and down 5 to 10 times

10. Incubate cells in lysis buffer on ice approximately 30 min with occasional agitation
11. Centrifuge 20 min, 10,000 rcf @ 4°C
12. Decant supernatant into new 15 mL corning tube
    - Aliquot 75 μL of sample into microcentrifuge tube for western analysis of lysate.
13. Add Talon Metal Affinity Resin (ClonTech) beads to lyates; the minimal resin to lysate ratio is 1:50, often use 1:25
14. Thoroughly mix lysate and resin by tapping tube; incubate with rocking 1 to 1.5 h, or overnight for large samples
15. Centrifuge samples at 4500 rcf for 5 min (18-20°C)
16. Discard supernatant
17. Wash beads in resin 4 times:
    - Add 8 mL wash buffer to each sample
    - Incubate with rocking 5 min
    - Centrifuge 4,000 rcf 5 min, at room temperature

- Carefully discard supernatant, ensuring that resin pellet at bottom of tube is not disturbed
- Repeat 3 additional times
- On last wash, *all* remaining wash buffer must be removed; following decanting of liquid, centrifuge an additional 2-5 min at 4,000 rcf, room temperature
- Pipette off remaining liquid

18. Elute protein with native elution buffer, using at least an equal amount of elution buffer to resin (slightly more is better, ie, if using 200 uL beads, use 250 uL elution buffer).
    - Add elution buffer to resin carefully, tapping gently to mix. Incubate with gentle agitation (ie tapping) for 5 minutes.
19. Repeat elution step with same volume elution buffer as first elution.

SDS-PAGE GEL, NITROCELULOSE TRANFER, AND WESTERN IMMUNOBLOT PROCEDURE

**Samples must be mixed with Lammeli Sample Buffer (1:1) that has had β-mecaptoethanol already added (50 μL BME, 950 μL lammeli sample buffer). Sample should then be boiled at 100°C for 5 minutes for denaturing.

Polyacrylamide Gel:

1. Set gel (either 12% or 4-20% gradient, appropriate well number) into running cell, opening of lanes facing inward. Ensure that gel is centered and pushed down to bottom of cell, so as to both ensure the gel is *straight* in the assembly, and limit leaking of running buffer. If running only 1 gel, will need to add dummy to opposite side of the cell.
2. Add running buffer to the top of the gel(s), between the gels. Add running buffer to the outside of the gel unit, but only until it covers the very bottom of the gels
3. Flush all urea out of each lane using 200 μL pipette and running buffer.
4. Load samples. Marker must also be added to a lane, and it is important NOT to add it to the middle of the lanes containing sample; add marker so that sample arrangement is asymmetrical (for identification/orientation purposes). Typically load 32 μL of sample in buffer, adding 16 μL at a time. Any volume over 20 μL should be added in two volumes. ** It is typically advisable to avoid loading the first and last.
5. Run gel at 77 V (low voltage allows for increased resolution over time, especially for proteins close in MW) for approximately 1 h. Gel may be run longer (up to 1.5 h), but only if protein MW is relatively high; otherwise bands may run off of gel.

6. Remove gel from cell; gently crack open protective casing and remove gel, cleaning up rough edges. Gently lift gel and place into container with small amount of transfer buffer.

Nitrocellulose Transfer:

** Will need to prepare ahead of time:

- Small container containing transfer buffer
- Pre-cut sheet(s) or nitrocellulose, labeled with name of antibody (Ab) and direction of lanes
- 4 pre-cut sheets of immunoblotting paper, pre-soaked in transfer buffer

1. Pre-soak 4 transfer sponges with ddH_2O, ringing out excess. Place transfer sponges into container containing enough transfer buffer to saturate all four sponges.
2. Place pre-soaked sponge into transfer assembly first. Use 1 sponge if performing transfer on two gels, or two sponges of only performing one transfer.
3. Place pre-soaked immunoblotting paper (soaked in transfer buffer; cut to approximately sponge-size) down next. Again, if performing two gel transfers use one immunoblotting paper, but if performing only one transfer place two papers down.
4. Pour small amount of transfer buffer onto immunoblotting paper.
5. Place gel onto immunoblotting paper, in *reverse* orientation (so, numbered backwards from right to left, ie, 10 to 1 or 12 to 1). Ensure that no bubbles form between the gel and the immunoblotting paper.

6. Pour small amount of transfer buffer onto gel, just enough to dampen, to keep air bubbles from forming between gel and nitrocellulose.
7. Place pre-soaked nitrocellulose paper onto gel (try to use forceps for this part; avoid touching nitrocellulose as much as possible), lining up edges and ensuring that no bubbles form between the gel and the paper. Protein bands will not transfer through bubbles!
8. Place pre-soaked immunoblotting paper on top of nitrocellulose. Again, if running two gels place one sheet, if running one gel place two sheets.
9. Place sponge(s) on top of assembly last.

** If transferring two gels, repeat steps 1-9 on top of first gel "sandwich".

10. Place cover onto assembly. Lift gently over container with transfer buffer, and squeeze excess buffer from assembly. Place entire assembly into transfer cell. Tighten, again pouring off any excess running buffer.
11. Add running buffer to top of white nodes *in between* the transfer assembly only. Ice-cold tap water will be added to the outside of the assembly.
12. Add ice to the cell, *outside* of the transfer assembly. Pour cold tap water to almost the top of the assembly and place lid onto assembly in proper orientation. Run at 30 V for 1 h.
13. After running 1 h, remove transfer assembly from cell. Remove nitrocellulose membrane from assembly, ensuring that as little gel as possible remains associated with nitrocellulose.

Western Immunoblotting:

1. Block nitrocellulose membrane in 6 mL milk, rocking 1 hr.

2. 5 to 10 minutes before h is up (so after 50 to 55 minutes) prepare primary Ab treatment:
3. After 1 h, discard blocking milk and add primary Ab preparation. Incubate on rocker 1 h.
4. While waiting, prepare TBS wash buffer (~200 mL per immunoblot/membrane):
5. After 1 h, wash membrane 4 times: 1 initial 2-3 min wash in 15 mL TBS, followed by 3 subsequent 10 min washes (on rocker) in 15 mL TBS.
6. During final wash, prepare secondary Ab (anti-mouse Ab conjugated to HRP):
7. After final wash, discard TBS and add secondary Ab preparation. Incubate on rocker 1 h.
8. After 1 h, wash membrane 4 times: 1 initial 2-3 min wash in 15 mL TBS, followed by 3 subsequent 10 min washes (on rocker) in 15 mL TBS.
9. Develop immunoblot according to developing substrate instructions.

QIAGEN DNA EXTRACTION PROTOCOL FOR MODERATE VOLUME DNA EXTRACTION

1. Pour contents of culture into 50 mL centrifuge tube. Centrifuge for 10 to 15 min at max speed (4,000 to 6,000 rpm).
2. Discard resulting supernatant.
3. Resuspend pellet with 5 mL Qiagen Buffer P1 (stored at 4°C). Resuspend cells by vortexing vigorously.
4. Add 5 mL Qiagen Buffer P2 (stored at room temp). Mix gently by inversion (vigorous mixing or shaking will shear genomic DNA). *Proceed to next step within 5 minutes of adding Buffer P2!*
5. Add 5 mL Qiagen Buffer P3 (stored at 4°C). Mix well via gentle inversion.
6. Place on ice for 10 to 15 minutes. Longer incubation time on ice will result in less genomic DNA, so increasing incubation time may be beneficial.
7. Centrifuge for 15 min @ 4°C, 4,000 rpm.
8. Using a coffee filter, filter resulting supernatant into new 50 mL centrifuge tube.
9. Add an equal volume of isopropanol (or two volumes of EtOH) to filtered supernatant.
10. Mix by gentle inversion, and allow to stand 10 to 15 minutes at room temperature (or, if working with EtOH, incubate *on ice*) to allow DNA to precipitate.
11. After 10 to 15 minutes, centrifuge at 4°C, 4,000 rpm for 10 to 15 minutes. The DNA will be contained in the resulting pellet.
12. Discard supernatant and place 50 mL tube containing pellet upside down on paper towel/chem wipe to drain. Watch to ensure that pellet does not slide onto paper towel.

13. Resuspend pellet in 0.5 mL TE buffer or DEPC-treated dH_2O. Place on ice.
14. Centrifuge DNA sample at 13,000 rpm for 5 minutes at 4°C.
15. Equilibrate Qiagen-tip 100 by applying 4 mL Buffer QBT, and allow column to empty via gravity flow. Allow tip to drain completely.
16. Apply 500 μL DNA sample supernatant from step 1 to 4 mL QBT buffer. Apply 4.5 mL buffer+sample to Qiagen-tip and allow it to enter the resin by gravity-flow.
17. Wash the Qiagen-tip with 2 × 10 mL Buffer QC. Allow buffer QC to move through the Qiagen-tip by gravity-flow. The first wash is generally sufficient to remove all contaminants in the majority of plasmid DNA preps. The second wash is especially necessary when large culture volumes or bacterial strains producing large amounts of carbohydrates are used.
18. Elute DNA with 5 mL buffer QF into a 15 mL conical tube.
19. Precipitate DNA by adding 3.5 mL room-temperature isopropanol to the eluted DNA. Mix and centrifuge immediately at ≥ 15,000 x g for 30 min at 4°C. All solutions should be at room temperature to minimize salt precipitation, but centrifugation is carried out at 4°C to avoid overheating of the sample. Larger, conical-bottom centrifuge tubes may be used for centrifugation at 5,000 x g for 60 min at 4°C. Carefully decant supernatant; isopropanol pellets are loosely associated with the centrifugation tube, so care should be taken during decanting not to lose the pellet.

20. Dry the pellet and resuspend in 500 μL DEPC-treated H_2O. Transfer to a microcentrifuge tube and centrifuge at 13,000 rpm (or max speed) at 4°C for 10 to 15 minutes.
21. Pipette supernatant into new 1.5 mL microcentrifuge tube and reprecipitate with equal volume of isopropanol plus potassium acetate added at 1/10 volume (so 50 μL KAc added to 500 μL DNA in DEPC-treated H_2O).
22. Centrifuge at maximum speed at 4°C for 10 to 15 minutes.
23. Carefully decant the supernatant and add 1 to 1.5 mL room temperature 70% EtOH and centrifuge at max speed and 4°C for 20 minutes. Carefully decant the supernatant without disturbing the pellet.
24. Air-dry the pellet for 5 to 10 min, and dissolve the DNA in 500 μL TE buffer or DEPC-treated H_2O. Rinse walls with suspension liquid to recover all DNA, but avoid pipetting DNA up and down to facilitate resuspension, as this may result in shearing of the DNA. Overdrying the pellet will make it very difficult to resuspend the DNA, too.

CORONAVIRUS ISOLATION FROM FECAL SAMPLES

** ideally, HRT-18G cells should have been plated and confluent 12 hours prior to infection**

1. Collect samples in sterile specimen collection cups or 50 mL corning tubes
2. Store on ice or at 4°C until prep
3. Prepare 10-20% (w/v) suspension of fecal material in PBS containing antimicrobials (pen-strep and amphoceterin B). Store remaining undiluted sample at -70°C.
4. Homogenize suspension by vortexing gently.
5. Clarify suspension (~ 1 mL) via low-speed centrifugation at 1000 x g for 10 minutes
6. Dilute resulting supernatant 1:10 in DMEM containing appropriate antimicrobials (pen-strep and amphoceterin B)
7. Prepare a 0.45 μm filter by wetting with 1 mL DMEM to keep virions from adsorbing onto the filter
8. Filter resulting supernatant through a 0.45 μm filter into a clean microcentrifuge tube.
9. At this point, sample may be stored overnight (or short-term) at 4°C or may be stored long-term at -70°C until analysis
10. Wash HRT-18G cells twice in PBS containing antimicrobials
11. Remove media, and add diluted fecal sample filtrate supernatant to HRT-18G cells (~ 500 μL diluted fecal sample filtrate supernatant per well of 6-well plate). Rock 1 h at 37° C to allow for adsorption.

12. Add DMEM containing antimicrobials and 2% γ-irradiated FBS to wells and return to incubator at 37° C. Observe daily for CPE.
13. Perform a minimum of 3 blind passages before attempting to harvest virus from infected cells.
14. After third passage, observe cells for CPE. Lyse cells via 3 cycles of freeze-thaw at -80°C.
15. Free any remaining attached cells via pipetting. Aliquot 1.5 mL per well into pre-labeled microcentrifuge tubes and store at -80°C until analysis.

CORONAVIRUS ISOLATION FROM NASAL SWAB SAMPLES

** ideally, HRT-18G cells should have been plated and confluent 12 hours prior to infection**

1. Swabs should be placed in either DMEM or RPMI containing antibiotic and antimycotic
2. If not using immediately, place on ice or at 4° C for transport
3. Allow samples to incubate at room temperature for 30 min
4. Homogenize swabs in DMEM/RPMI containing antimicrobials by vortexing vigorously for approximately10 seconds.
5. Centrifuge low-speed (1000 x g) for 10 min. Remove and discard swabs following centrifugation.
6. Remove a small aliquot (~ 1 mL) and store at -70° C.
7. Centrifuge 1500 x g, 15 minutes
8. Filter resulting supernatant via 0.45 μm filter into clean 15 mL corning tube (at this point, sample may be stored short-term at 4° C or frozen at -70° C).
9. Wash HRT-18G cells twice in PBS containing antimicrobials
10. Remove media, and add nasal swab supernatant to HRT-18G cells (~ 500 μL swab supernatant per well of 6-well plate). Rock 1 h at 37° C to allow for adsorption.
11. Add DMEM containing antimicrobials and 2% γ-irradiated FBS to wells and return to incubator at 37° C. Observe daily for CPE.
12. Perform a minimum of 3 blind passages before attempting to harvest virus from infected cells.

13. After third passage, observe cells for CPE. Lyse cells via 3 cycles of freeze-thaw at -80°C.
14. Free any remaining attached cells via pipetting. Aliquot 1.5 mL per well into pre-labeled microcentrifuge tubes and store at -80°C until analysis.

INDIRECT ENZYME-LINKED IMMUNOSORBENT ASSAY FOR DETECTION OF ANTI-CORONAVIRUS ANTIBODIES

1. Prepare antigen for coating by diluting appropriately in coating buffer, pH 9.6.
2. Coat well of a PVC microtiterplate by pipetting 100 μL of diluted antigen into each well.
3. Cover the plate with adhesive plastic or wrap in foil and incubate for 2 h at room temperature or 4°C overnight.
4. Remove the coating solution and wash wells 4 times with 1X TBS solution. Solution between washes is removed by flicking the plate over a sink; residual solution in wells may be removed by firmly patting plate onto a clean paper towel between washes.
5. Block remaining protein binding sites in coated wells by adding 200 μL blocking solution (PBS containing 5% goat serum) to each well. Cover plate with adhesive plastic or wrap in foil. Incubate with rocking for 2 h at room temperature. Alternatively, plate may be blocked at 4°C overnight.
6. Wash the plate twice with 1X TBS solution.
7. Add 100 μL primary antibody in blocking solution to each well.
8. Cover the plate with adhesive plastic or wrap in foil and incubate 1 h with rocking at room temperature. Alternatively, if a stronger signal is desired, plate may be incubated at 4°C overnight.
9. Wash the plate 4 times with 1X TBS.
10. Add conjugated secondary antibody diluted appropriately in blocking solution,100 μL per well.

11. Cover plate with adhesive plastic or wrap with foil and incubate with rocking 1 to 2 h at room temperature.
12. Wash the plate 4 times with 1 X TBS.
13. Apply appropriate detection solution to wells for detection of conjugated protein signal.

CORONAVIRUS NEUTRALIZATION ASSAY

1. Seed wells of a 24-well plate with HRT-18G cells to be confluent the following morning.
2. Prepare 5-fold serial dilution of sample and control sera, 4 dilutions (1:5, 1:25, 1:125, and 1:625) per sample.
    - 1:5 → 70 μL undiluted serum + 280 μL DMEM containing 0.2% Primocin but no FBS
    - 1:25 → 70 μL 1:5 diluted serum + 280 μL DMEM containing 0.2% Primocin but no FBS
    - 1:125 → 70 μL 1:25 diluted serum + 280 μL DMEM containing 0.2% Primocin but no FBS
    - 1:625 → 70 μL 1:125 diluted serum + 280 μL DMEM containing 0.2% Primocin but no FBS
3. For each dilution, combine 250 μL BCoV-Lun p8 stock virus with 250 μL dilute serum for a final volume of 500 μL. Incubate for 30 min at room temperature on nutator.
4. Infect tightly confluent HRT-18G cells in 24-well culture plate with 150 μL per well of serum-treated BCoV-Lun, infecting wells in triplicate per dilution. Rock cells with serum-treated virus at room temperature for 1 h to allow virus adsorption onto the monolayer.
5. Remove supernatant from each well and wash once with 1 mL PBS per well.
6. Add 0.5 mL fresh DMEM containing 0.2% Primocin but no FBS to each washed well. Return plate to 37°C incubator with 5% atmospheric CO_2. Incubate 16 h.

7. After 16 h incubation, wash wells once with 1 mL PBS per well. Add 200 μL TrypLE to each well and incubate at 37°C for 10 to 15 min, or until majority of cells have detached from bottom of each well.
8. Add 50 μL goat serum to each well to quench TrypLE.
9. Dislodge remaining attached cells via gentle pipetting and transfer the entire 250 μL volume to well of a 96-well U-bottom plate.
10. Centrifuge 96-well plate containing transferred cells at 400 rcf, 4°C, for 7 min.
11. Flick plate over sink to remove resulting supernatant from wells, being careful not to dislodge cell pellet.
12. Wash cells with 100 μL cold FACS wash buffer, gently pipetting each well to resuspend cells. Centrifuge 96-well plate at 400 rcf, 4°C, for 7 min.
13. Add primary antibody diluted appropriately in PBS containing 5% goat serum, 100 μL per well. Incubate with rocking for 30 min at 4°C.
14. Centrifuge 96-well plate at 400 rcf, 4°C, for 7 min. Flick plate over sink to remove resulting supernatant from wells, being careful not to dislodge cell pellet.
15. Wash cells once with 200 μL cold FACS wash buffer, pipetting to completely resuspend cells. Centrifuge 96-well plate at 400 rcf, 4°C, for 7 min. Flick plate over sink to remove resulting supernatant from wells, being careful not to dislodge cell pellet.
16. Add secondary, fluorophore-conjugated antibody diluted appropriately in PBS containing 5% goat serum to each well, 100 μL per well. Incubate with rocking for 30 min at 4°C.

17. Centrifuge 96-well plate at 400 rcf, 4°C, for 7 min. Flick plate over sink to remove resulting supernatant from wells, being careful not to dislodge cell pellet.
18. Wash cells once with 200 μL cold FACS wash buffer, pipetting to completely resuspend cells. Centrifuge 96-well plate at 400 rcf, 4°C, for 7 min. Flick plate over sink to remove resulting supernatant from wells, being careful not to dislodge cell pellet.
19. Resuspend cell pellet in 150 μL cold FACS wash buffer.

OVERNIGHT BACTERIAL LYSIS/RELEASE OF FUSION PROTEINS FROM INCLUSION BODIES

1. Thaw bacterial pellet to room temperature.
2. Wash pellet with 1 mL Lysis Buffer, completely resuspending pellet.
3. Transfer contents to 2 mL microcentrifuge tube.
4. Centrifuge at 18,000 rcf (~14,000 rpm) for 5 min at 4° C
5. Discard supernatant; tap tube onto a paper towel to remove remaining liquid from pellet
6. Resuspend with 1 mL Lysis Buffer
7. Using a 21 gauge needle, resuspend pellet completely in Lysis Buffer
8. Transfer solution to 15 mL conical tube using syringe and needle
9. Bring volume in tube to 5 mL with Lysis Buffer and vortex briefly to mix
10. Add 50 μL of 500 mM EDTA to each 5 mL solution (cells in buffer) for a final concentration of 5 mM EDTA
11. Vortex solution briefly to mix
12. Add 200 μL of 25 mg/mL Lysozyme to each 15 mL tube for a final concentration of 1 mg/mL lysozyme
13. Place tube onto gentle inversion shaker for 30 minutes
14. Add Benzonase at 5 units/mL (so, 25 μL for 5 mL)
15. Return tube to shaker for an additional 30 min
16. Pipette 1.75 mL into each of three 2 mL microcentrifuge tubes
17. Centrifuge at 18,000 rcf for 20 min at 4° C
18. Discard supernatant
19. Add 1 mL Lysis Buffer to resulting pellet
20. Add 50 μL EDTA to each tube

21. Using a 21 gauge needle, resuspend pellet and transfer resulting solution to a 15 mL conical tube

22. Bring volume in 15 mL tube to 5 mL with Lysis Buffer. Vortex briefly.

23. Add 25 μL of 1M DTT for a final concentration of 5 mM DTT. Vortex briefly

24. Add 200 μL of 10% Sarkosyl solution to tube. Vortex briefly.

25. Place tube onto shaker, incubate with gentle inversion shaking at room temperature for 30 min.

26. Place tubes at 4° C and incubate overnight with gentle inversion shaking.

27. If original cell pellet was large, add an additional 3 mL of lysis buffer to sample mid-lysis.

28. At the end of lysis-incubation period, sonicate samples 3 to 4 times (or as many as 10 times) *on ice*, 12 to 15 seconds each time, with a 1 min rest period between each sonication:
    a. Pulse
    b. Output control = 7
    c. 20% duty cycle
29. Pipette ~1.7 to 1.75 mL of sample into each of five 2 mL microcentrifuge tubes

30. Centrifuge samples @ 18,000 rcf, 4° C for 25 to 30 min

31. Decant supernatant into a new 15 mL conical tube. Return remaining pellets to ice.

32. Add 750 μL 10% Triton X in ddH2O to supernatant. Keep at room temp if planning to purify via Profinia. Otherwise, clear lysate should be stored at 4° C for no longer than 1 d.

33. Resuspend pellets in 1.5 mL lysis buffer (total, for all pellets. Combine pellets.) Store resuspended pellet at 4° C until gel analysis can be performed.

VITA

Genevieve Elizabeth Lum was the first child born to Donald Kelly and Genevieve Schoeffler Lum of Clinton, Louisiana. Genevieve has two younger siblings, Lauren Meagan and Daniel Jacob. Lauren is currently pursuing a degree in economics at Louisiana State University, and Daniel is pursuing his doctorate in Physics at The University of Rochester in Rochester, NY. Genevieve was raised in Clinton, Louisiana, until moving to Baton Rouge, Louisiana, to attend high school. She attended high school at Christian Life Academy in Baton Rouge, Louisiana, where Genevieve graduated valedictorian of her high school class.

After graduating high school in May 2001, Genevieve attended Louisiana State University, where she obtained her Bachelor of Science Degree in animal, dairy, and poultry Sciences in December of 2005. In the spring of 2005, Genevieve took part in undergraduate research under the supervision of Dr. John Chandler at the D.E. Patrick Dairy Herd Improvement Center in Baton Rouge, Louisiana.

Genevieve entered graduate school in January of 2006 under the direction of Dr. Jason Rowntree. She obtained her Master of Science degree in the School of Animal Sciences at Louisiana State University in Baton Rouge, Louisiana. After graduation, Genevieve joined the doctoral program in the School of Animal Sciences at Louisiana State University under the direction of Dr. Kenneth Bondioli and in the BioMMed laboratory in Pathobiological Sciences under the direction of Dr. Gus Kousoulas.

Genevieve is currently a candidate for the doctoral degree in The School of Animal Sciences at Louisiana State University in Baton Rouge, Louisiana. Upon graduation, Genevieve intends to accept a post-doctoral research position in the

Endocrinology laboratory at the Tulane School of Medicine in New Orleans, Louisiana, under the direction of Dr. Hongi Wu, where she will pursue research regarding the underlying molecular changes involved in the development of type I and II diabetes.